Development of Coarse Recycled Hardmetal Reinforced Hardfacings

TAAVI SIMSON

TALLINN UNIVERSITY OF TECHNOLOGY
School of Engineering
Department of Mechanical and Industrial Engineering

This dissertation was accepted for the defence of the degree of Doctor of Philosophy in Engineering on 02/05/2018

Supervisor: Prof. Priit Kulu
                           School of Engineering
                           Tallinn University of Technology
                           Tallinn, Estonia

Co-supervisor: Teach. Ass. Andrei Surženkov
                           School of Engineering
                           Tallinn University of Technology
                           Tallinn, Estonia

Opponents: Assoc. Prof. Regita Bendikiene
                           Department of Production Engineering
                           Kaunas University of Technology

                           Assoc. Prof. Alexander Ryabchikov
                           Institute of Forestry and Rural Engineering
                           Estonian University of Life Sciences

Defence of the thesis: 12/06/2018, Tallinn

Declaration:
Hereby I declare that this doctoral thesis, my original investigation and achievement, submitted for the doctoral degree at Tallinn University of Technology, has not been previously submitted for doctoral or equivalent academic degree.

Taavi Simson

_____
                                                      signature

Taaskasutatava jämekõvasulamarmatuuriga kõvapinnete arendus

TAAVI SIMSON

Contents

LIST OF PUBLICATIONS

The list of author's publications, on the basis of which the thesis has been prepared:

Paper 1 <u>T. Simson</u>, P. Kulu, A. Suržénkov, D. Goljandin, R. Tarbe, M. Tarraste, M. Viljus, Optimization of structure of hardmetal reinforced iron-based PM hardfacings for abrasive wear conditions, *Key Engineering Materials*, 2017, **721**, 351 – 355

Paper 2 <u>T. Simson</u>, P. Kulu, A. Suržénkov, R. Tarbe, D. Goljandin, M. Tarraste, M. Viljus, R. Traksmaa, Wear resistance of sintered composite hardfacings under different abrasive wear conditions. *Materials Science (Medžiagotyra)*, 2017, **23**(3), 249 – 253

Paper 3 <u>T. Simson</u>, P. Kulu, A. Suržénkov, A. Ciuplys, M. Viljus ,G. Zaldarys, Comparison of plasma transferred arc and submerged arc welded abrasive wear resistant composite hardfacings, *Materials Science (Medžiagotyra)*, 2018, **24**(2), 172 – 176

Paper 4 A. Surzhenkov, M. Viljus, <u>**T. Simson**</u>, R. Tarbe, M. Saarna, F. Casesnoves, Wear resistance and mechanisms of composite hardfacings at abrasive impact erosion wear, *Journal of Physics: Conference Series*, 2017, **843**, 012060

Paper 5 <u>T. Simson</u>, R. Tarbe, M. Tarraste, M. Viljus, Abrasive impact erosion of composite Fe-based hardfacings with coarse WC-Co reinforcement, *Proceedings of the 24th IFHTSE Congress*, 26th – 29th of June 2017, Nizza, France

Paper 6 P. Kulu, F. Casesnoves, <u>**T. Simson**</u>, R. Tarbe. Prediction of abrasive erosion impact wear, *Solid State Phenomena*, 2017, **267,** 201 – 206

Author`s Contribution to the Publications

Contribution to the papers in this thesis are:

Paper 1 preparation of specimens (preparation of microsections), performing ARWW tests, hardness measurements, microstructure analysis, writing of paper

Paper 2 preparation of specimens (preparation of microsections), performing AWW test, hardness measurements, microstructure analysis, writing of paper

Paper 3 performing AWW tests, Vickers hardness measurements, microstructure analysis, writing of paper

Paper 4 measurements of hardness, writing of paper

Paper 5 measurements of hardness, modulus of elasticity and fracture toughness, writing of paper

Paper 6 measurements of hardness, wear tests

INTRODUCTION

Motivation for the research

In industry applications, wear results in high cost if not dealt with. Thus, to achieve greater efficiency, components with higher wear resistance are needed. These can be made using materials with higher wear resistance, or applying corresponding heat treatment (if applicable), surface treatment (e.g., shot peening, case hardening, etc., depending on the treated material), or surfacing process (e.g., physical vapour deposition (PVD), thermal spraying (TS), etc.). Wear resistant materials are not always acceptable to produce a whole component. The reasons are uncompetitive price of the received component or other properties required will be influenced in a way that is undesired (e.g ductility). Neither is heat treatment is possible in many situations due to price, size of a component or other reasons. Therefore, wear resistant overlays, otherwise called hardfacings, are in many cases the best or the only possible solution for improving component lifetime [1].

Besides wear resistance of hardfacings, another point of interest is the materials used to create these hardfacings. For example, due to their high hardness and ductility, WC-Co hardmetals are useful in the production of hardfacings. At the same time, many materials that are used in the production of hardmetals (e.g tungsten) are either expensive or scarce [2].

Excavation of tungsten that is always present in hardmetals is on the rise. At this rate, tungsten resources will be depleted in 35 years. Currently, 60% of excavated tungsten is used to produce hardmetals. End-of-life recycling rate (EOL-RR; fraction of metal in discarded products that is reused in such a way as to retain its functional properties) in the case of common materials, such as iron, cobalt, nickel, copper and zinc, is over 50%. In the case of tungsten, it is approximately 25%. Therefore, it is required to find a way to recycle tungsten and tungsten containing materials at a larger extent. One method for that is to use crushed hardmetal scrap as reinforcement in hardfacings. That is a motivation for this thesis research to study ways of using recycled hardmetal for production of hardfacings and finding suitable technologies for production of these hardfacings [3 – 7].

The limits of using recycled hardmetal powders in hardfacings obtained by thermal spray or welding result from the shape, size and purity of powders produced by mechanical milling. Thermal spray (HVOF etc.), for example, allows use of powders with fraction size under 300 μm, also spherical powder shape is preferred to allow better powder flow in powder supply tubing of a spraying device.

In conclusion, the main objective of this thesis is to develop metal matrix composite (MMC) hardfacings based on recycled hardmetal reinforcement and low cost iron based metal matrix with suitable technologies (Plasma transferred arc welding (PTAW), etc.) [8].

Scientific novelty and practical impact

Scientific novelty of this work lies in the development of plasma transferred arc welding (PTAW) and submerged arc welding (SAW) technologies for the deposition of coarse hardmetal reinforced hardfacings, and in the comprehensive study of the influence of the coarse hardmetal reinforcement`s size, shape and volume fraction on the wear performance of hardfacings under different abrasive wear conditions.

The thesis research focused on the influence of particle shape, size and volume fraction on the structure and wear resistance of hardfacings under different abrasive wear conditions.

Three different hardfacing methods, powder metallurgy (PM), submerged arc welding (SAW) and plasma transferred arc welding (PTAW), were used to produce coarse hardmetal containing composite hardfacings. PM technology produced hardfacings were used for the analysis of

forming structures (influence of reinforcement parameters) and wear testing. Based on the results of PM hardfacings, PTAW and SAW technologies were used to produce hardfacings with optimal structure, comparative wear tests of PTAW and SAW hardfacings were performed and recommendations given for the selection of hardfacings.

Results presented in this thesis have been published in six peer-reviewed articles in journals and conference proceedings, and were also presented at four international scientific conferences.

ABBREVIATIONS

AEMW	Abrasive Emery Wear
AEW	Abrasive Erosion Wear
AIW	Abrasive Impact Wear
ARWW	Abrasive Rubber Wheel Wear
AWW	Abrasive Wheel Wear
DFB	Diffusion Brazing
EDS	Energy-Dispersive (X-Ray) Spectroscopy
EOL-RR	End-Of-Life Recycling Rate
HVAF	High Velocity Air Fuel (spraying)
HVOF	High Velocity Oxy-Fuel (spraying)
KTU	Kaunas University of Technology
LCW	Low Carbon Wire
LPS	Liquid Phase Sintering
MMC	Metal Matrix Composite
PM	Powder Metallurgy
PTAW	Plasma Transferred Arc Welding
PVD	Physical Vapour Deposition
SAW	Submerged Arc Welding
SEM	Scanning Electron Microscope
TS	Thermal Spray
TTÜ	Tallinn University of Technology
XRD	X-Ray Diffraction

1. REVIEW OF LITERATURE

1.1 Wear in engineering

Wear is generally defined as a progressive loss of displacement of material from a surface as a result of relative motion between that surface and another. Loss due to the mechanical wear of machine parts accounts for 1.3 – 1.6% size loss of the gross domestic product (GDP) of a country. Another survey of wear problems and costs in UK industry in 1997 indicated that a typical average cost of wear was about 0.25 percent of company turnover. The estimated cost of wear to Canadian industry is $ 2.5 billion a year [9 – 11]. Different types of wear occur with different frequency. Frequency of encounter with different types of wear in industry are as follows: abrasive wear 50%, adhesive wear 15%, erosive wear 8%, fretting wear 8%, chemical wear 5% and other types of wear 14% [12]. Therefore, combating abrasive wear singly is of the utmost importance.

1.1.1 Classification of wear

There are two ways to approach the wear classification. One method is to divide wear into three larger categories: sliding wear, impact wear and rolling contact wear. Sliding wear itself can be divided into smaller categories: abrasive wear, adhesive wear, fatigue wear, fretting wear, and polishing wear [13].

The other method is to divide wear into four larger categories: abrasion, erosion, adhesion and surface fatigue (Fig. 1). By this method, abrasion is divided into low stress abrasion, high stress abrasion, gouging, and polishing [13]. As both abrasion and erosion involve cutting of surface by harder particles, they are viewed as part of abrasive wear in this thesis.

High stress abrasion occurs where the abrasive is crushed in the process, as in ball mill grinding, while low stress abrasion occurs when abrasive particles do not fracture during the wear process [12].
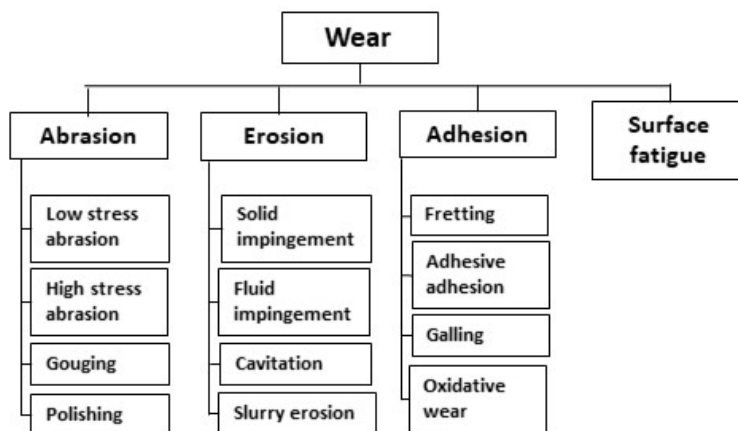

Figure 1. Wear modes classification [13].

Abrasive wear is traditionally classified as two-body abrasion and multibody (three-body) abrasion. Two-body abrasion is a situation where harder particles that are fixed firmly in another body (e.g., sandpaper) scratch against a softer surface. In three-body abrasion, harder particles

are free to move, but pressed against a softer surface by another object (e.g., sand between gears, sand and gravel between road and snowplow).

Abrasion is a problem in most wear environments at one point or another, even though it may not be the primary wear mechanism initially. In any tribosystem where dust and wear debris are not controlled and excluded, abrasive wear will be a problem [14].

Abrasive wear is a major problem for the excavation, earth moving, mining, and minerals processing industries and occurs in a wide variety of equipment, such as bulldozer blades, excavator teeth, rock drill bits, crushers, slushers, ball mills and rod drills, chutes, slurry pumps, and cyclones [14].

1.1.2 Abrasive wear resistance of materials

The abrasive wear resistance of a material is a function of its structure, mechanical properties, such as hardness [12, 15 – 17], modulus of elasticity [16 – 17] and fracture toughness [15], and, on the other hand, type of wear and its parameters, such as abrasive hardness and size [12].

If impact loads are insignificant or not present (e.g., two-body abrasion or three-body abrasion), ceramics are the best choice [18 – 24].

Under impact loads (i.e., toughness is required) and/or at high impact angles (in erosion), high toughness materials such as low carbon steels and tool steels are preferable over composite (cermet) and ceramic coatings because toughness requirements dominate over hardness in these conditions (Fig. 2). At erosive wear in mixed conditions, i.e. if the impact angle varies in the range from 0° to 90°, composite hardfacings are likely to perform better than tool steels because of higher importance of hardness in these conditions (Fig. 3).
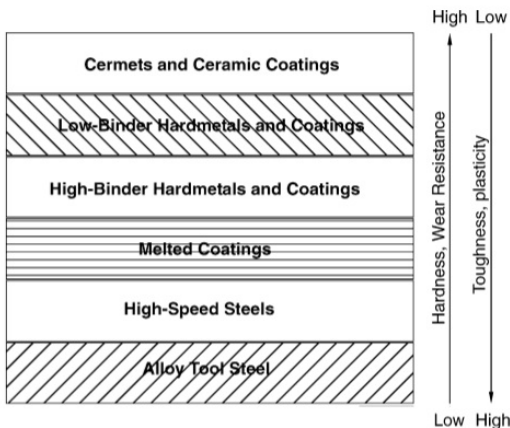

1- ceramics, 2 – white cast iron, 3 – cermets,
4 – tool steels, 5 – low carbon steels

Figure 2. Properties of different materials [24].   *Figure 3. Matching materials and wear conditions* [24].
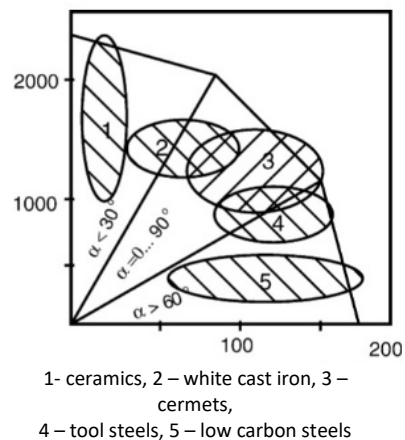
Materials with double-cemented structure (e.g., hardmetal particles in Ni-based self-fluxing alloy) give an optimal combination of ductility and abrasive wear resistance in mixed abrasive-impact wear conditions, being capable of withstanding abrasive wear by hard particles as well as impact loads. Depending on reinforcement and matrix content, double-cemented hardfacings are applicable in both high and low angle (angle between stream of eroding particles and surface) abrasive-impact wear conditions [24 – 26].

1.2 Wear resistant carbide based hardfacings and surfacing technologies

1.2.1 Composition and structure

Hardfacing is an overlay deposited either by thermal spraying or welding on a surface of a material in order to improve its wear and/or corrosion resistance [27]. By their structure, hardfacings may be classified as one-phase and multiphase, or composite hardfacings. One-phase hardfacing materials are manufactured, for example, from stainless steels, Stellites, self-fluxing alloys, but also intermetallides, such as Ni_3Al and ceramics, such as Al_2O_3.

Hardfacings manufactured from cermets (such as WC-Co, Cr_3C_2-NiCr, $NiCrAlY$-Al_2O_3) fall into the composite hardfacing category. So do reinforced metal alloys (NiCrSiB-WC) and reinforced plastics. Reinforcement in hardfacings can have monolithic or composite (so called double-cemented) structure [28]. Beside this, reinforcement may be monosized (reinforcement particles with the same size) or multisized (have reinforcement in different sizes) (Fig. 4).
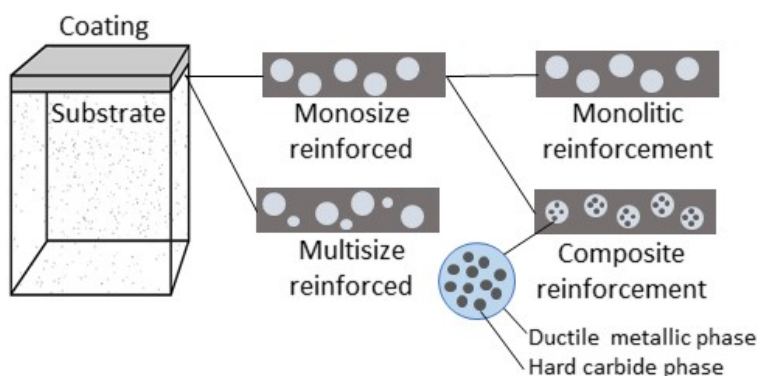

Figure 4. Structure of particle reinforced coating.

Double-cemented structure means that the composition comprises a plurality of first regions and a ductile second phase that separates the first regions from each other (Fig. 4). Each first region comprises a composite of grains and a second ductile phase bonding the grains. The grains are selected from the group of carbides consisting of W, Ti, Mo, Nb, V, Hf, Ta, and Cr carbides. The second ductile phase is selected from the group consisting of Co, Ni, Fe, alloys thereof, and alloys with materials selected from the group consisting of C, B, Cr, Si, and Mn [29]. The following hardfacing compositions (one-phase and composite) are recommended for use in abrasive wear conditions: Cr_2O_3, Cr_3C_2, WC, NiCrBSiC-WC, NiCrBSi. In erosive wear conditions, the following hardfacing compositions can be used: WC, Cr_3C_2, Cr_2O_3 and NiCrBSiC-WC [28].

One-phase hardfacings are most often manufactured from Fe-, Ni- or Co-based alloys [30]. One of the most common groups of alloys used for hardfacings is self-fluxing alloys (designated as MCrSiB, where M = Ni, Fe or Co). Self-fluxing alloys are iron, nickel or cobalt based alloys that contain boron and silicon not less than 1.5 wt%. Boron and silicon form oxides during melting. These oxides form boronsiliconfluxes that have lower melting temperature than the other constituents in the alloy. This flux provides protection from oxidation to the rest of the hardfacing under the flux [12]. Chromium and boron are effective in increasing the hardness, boron and silicon enhance wettability. As a result, coatings have no pores and adhere well to the substrate after the fusing process and are widely used for components requiring wear and

corrosion resistance [31]. Self-fluxing alloys have low melting temperature (1000 – 1200 °C in the case of Ni-based alloys) while having high heat resistance and high hot strength; in addition, they have good wear resistance and high hardness (40 – 60 HRC in the case of Ni-based alloys) [32]. NiCrSiB is used when resistance to wear, corrosion and heat is required. FeCrSiB is used when high performance to price ratio is required, i.e., it exhibits price advantage compared to Ni-based and Co-based alloys [33 – 37].

Fe-based self-fluxing coatings can also be used in applications where Ni-based and Co-based coatings are not recommended or not allowed to be used at all, for example, in the food industry. In addition, Fe-based self-fluxing alloys are a good alternative to Ni-based coatings under sliding wear conditions at room temperature as they exhibit lower wear than the latter. They are also a good substitute to hazardous electrolytic hard chromium plating [38].

To increase wear resistance of self-fluxing alloy based hardfacings, they are reinforced with tungsten carbide or hardmetal particles [39 – 40].

Among Co-based hardfacing materials, Stellites (Co-Cr-W alloys [41]) are most widely used. Out of the different existing Stellite alloys, Stellite 6 is widely used in industrial applications where a high degree of wear and corrosion strength is required at high temperatures, such as valves, turbine blades, exhaust pipes and similar industrial applications. Stellite 6 has an approximate composition of Co-28Cr-4.5W-1.1C. Stellite surface-hardfacing alloys are more expensive than other surface-hardfacing alloys. Despite their high cost, they are preferred because of their superior properties (wear and corrosion resistance at high temperatures) when compared with other hardfacing alloys [42 – 43].

Stellite alloys are highly resistant to nitric and acetic acid at room temperature and tend to passivate in a manner similar to stainless steels. Stellite alloys maintain reasonably good corrosion resistance in formic acids regardless of temperature. The corrosion resistance of Stellite alloys in hydrochloric acid is poor, regardless of temperature. Stellite alloys are quite tough in comparison with other materials at equivalent hardness or at equivalent volume fractions of hard particles. Stellite alloys can be welded by virtually any known fusion welding process and are particularly well suited for hardfacing applications, because welded Stellite hardfacings have finer structure than those of casted [44].

Another good example of wear resistant hardfacing materials is high chromium Fe-Cr-C alloys that have moderate impact resistance and excellent abrasion resistance. Fe-Cr-C alloys are used in mining, minerals and cement industry and to further improve (abrasive) wear resistance, reinforcement (or modification of structure by additives) is used. The reinforcement in these alloys can be a composite by itself, such as hardmetal (therefore, a double-cemented hardfacing forms) [45 – 47].

High hardness and good abrasive wear resistance of Fe-Cr-C alloys comes from high chromium content which results in the formation of chromium carbides. To be more precise, the wear resistance of these alloys is due to their microstructure, which comprises hard rod like carbides dispersed in a matrix of austenite or martensite. Similar to Stellites, welded Fe-Cr-C hardfacings have finer microstructure, and therefore higher wear resistance than casted Fe-Cr-C bulk materials [48 – 49].

Composite hardfacings are manufactured of metal-matrix composite (MMCs) materials (as MMC is a composite material itself) or a combination of MMC particles and the above-described one-phase (unreinforced) materials. The principle of incorporating a high-performance second phase into a conventional engineering material to produce a combination with features not obtainable from the individual constituents is well known. In a MMC, the continuous, or matrix phase is a monolithic alloy, and the reinforcement consists of high-performance carbide, metallic or ceramic additions [50]. Cermets are subclass of MMC materials.

Cermet is an acronym used worldwide to designate a heterogeneous combination of metal(s) or alloy(s) with one or more ceramic phases in which the latter constitutes approximately 15 to 85 % by volume and in which there is relatively little solubility between metallic and ceramic phases at the preparation temperature [50].

Various transition metal carbides (TiC [51 – 53], Cr_3C_2 [54 – 55], carbonitrides [56 – 57]), borides [58 – 59], as well as metal oxides [60 – 61], have been applied as a reinforcement in cermets.

Cemented carbides (further referred to as hardmetals) are a subtype of cermets. Hardmetal uses tungsten carbide (WC) as a reinforcement and cobalt (Co) as a binder. The performance of hardmetal tool lies between that of tool steels and other cermets. While having higher hardness and wear resistance than tool steels, they have lower ductility and thermal conductivity than the latter. Compared to ceramics, hardmetals (with the same ceramic material particles) have lower hardness, but at the same time higher ductility and fracture toughness. Hardmetals are used in mining, construction, oil and gas drilling and metalforming applications [50]. For example, thermal sprayed hardmetal coatings offer good protection against abrasive and sliding wear. Recent developments in coatings microstructure and properties allow consideration of new applications as well, such as fatigue-relevant applications. Thermal sprayed WC-Co coatings can be applied on boiler elements because they offer good abrasion and erosion resistance up to the temperatures of 773 K. WC-Co-Cr, in addition, has good corrosion resistance in aqueous solutions and good cavitation wear resistance. WC-CrC-Ni coatings can be applied up to the temperature of 933 K [62 – 63].

Self-fluxing alloy hardfacings with ceramic or cermet reinforcement can be viewed as MMCs as well. Most common reinforcements in self-fluxing alloy based MMC hardfacings are WC, TiC and hardmetal, but other types of reinforcement, such as TiN or Cr_3C_2, are used as well [64 – 67].

Composite hardfacings with double-cemented structure have been produced with many different compositions. Zikin et al. have used WC-Co, TiC-NiMo, ZrC-Ni and Cr_3C_2-Ni as reinforcement. Sarjas et al. have used WC-Co and Cr_3C_2-Ni as reinforcement. Both have used FeCrSiB or NiCrSiB as matrix material [26, 47, 68 – 69].

1.2.2 Coatings technologies

Hardfacings may be divided into thin (< 0.1 mm) and thick ones (> 0.1 mm) (Fig. 5). Thick hardfacings provide a longer protection and thus a longer lifetime of a coated part. Technologies used for manufacture of thick hardfacings may be classified as thermal spray, fusion and bulk melting technologies.

Thermal spray (TS) is a generic term for a group of processes in which metallic, ceramic, cermet, and some polymeric materials in the form of powder, wire, or rod are fed to a torch or a gun with which they are heated to near or somewhat above their melting point. The resulting molten or nearly molten droplets of material are accelerated in a gas stream and projected against the surface to be coated (i.e., the substrate). On impact, the droplets flow into thin lamellar particles adhering to the surface, overlapping and interlocking as they solidify. The total coat thickness is usually generated in multiple passes of the hardfacing device [70].

One of the best methods for the production of high quality thermal spray hardfacings is high velocity oxy-fuel (HVOF) spraying. The process is called high velocity air-fuel (HVAF) spraying if air is used as fuel oxidizer. Usual thickness of HVOF hardfacings is in the range of 0.05 to 0.5 mm. HVOF hardfacings are noted for high bond strength, exceeding 69 MPa [28, 70 – 72].
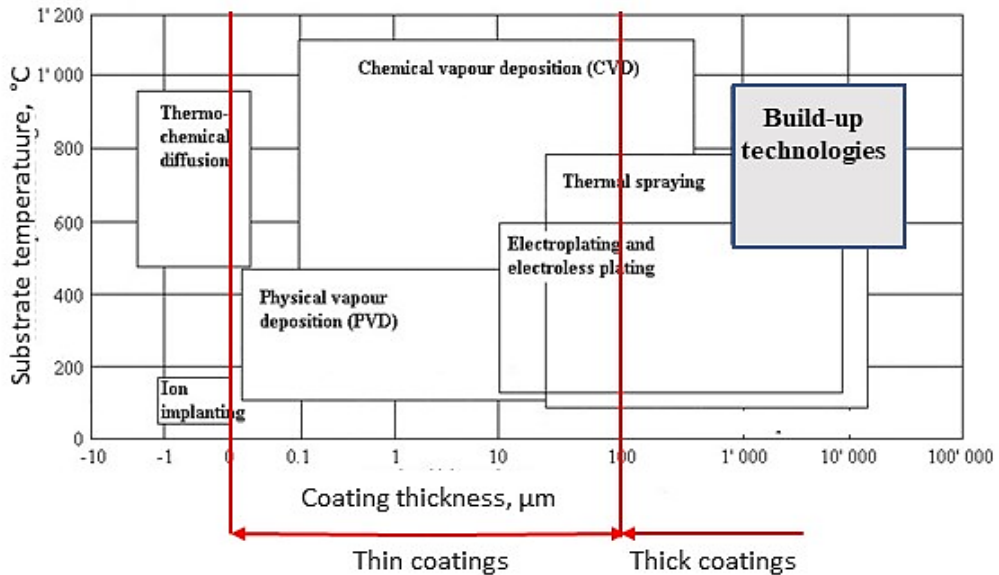

Figure 5. Classification of coating technologies.

The addition of a cermet as a reinforcing component to a HVOF sprayed coating generally leads to an increase in its wear resistance. For example, Sarjas et al. [69] showed that addition of 40 vol.% WC-Co to a self-fluxing alloy improved the wear resistance of the HVOF sprayed coating up to 2.7 times compared with the reference steel C45 under the three-body abrasion and the wear resistance under the room-temperature low impact angle erosion up to 1.2 times. Under the elevated temperature erosion wear conditions, reinforcing a HVOF sprayed coating with 10 vol.% of WC-Co particles led to 2.6 times lower wear at the low impact angle and 1.3 times lower wear at the normal impact angle [73]. In [74] it was demonstrated that HVOF and HVAF sprayed coatings containing 40 wt.% of WC-Co exhibited up to 3 and 3.5 times higher resistance to wear under the three-body abrasion and sliding wear conditions, respectively.

Surzhenkov et al. [75] showed that the addition of 15 vol.% TiC-NiMo and 20 vol.% Cr_3C_2-Ni reinforcement to an iron-based self-fluxing alloy HVOF sprayed coating allowed an increase of its wear resistance by 1.8 and 2.8 times, respectively. Analogously, Terajima et al. [76] reported an 8-fold improvement in the wear resistance of HVOF sprayed Fe-based metallic glass coatings with the addition of 8 vol.% WC-Co. However, reinforcing of nickel-based self-fluxing alloy HVOF sprayed coating by TiC-NiMo and Cr_3C_2-Ni particles had a detrimental effect, causing a 4.2 – 4.5 times increase in wear [77] under the conditions identical to those described in [76].

Fusion technologies may be regarded as welding technologies, which are applied not for joining two dissimilar parts, but for applying an overlay to a metal surface. Here feedstock materials are delivered towards the substrate separately from the heat source (depending on the technology, either instantly fed to the melting zone, or preliminarily deposited onto the substrate manually or by means of thermal spraying), and subsequently melt by a concentrated heat source (e.g., gas flame, electric arc, plasma arc).

In the case of fused and welded hardfacings, different methods are used for their deposition (thermal spray fusion, build-up welding, etc.). Fused hardfacings have many advantages compared to sprayed hardfacingss. First of all, they have better adhesion to the substrate, in sprayed hardfacings mostly only mechanical bond is created while in the case of fused hardfacings, metallurgical bond is created. This gives them better resistance to impact loading [78].

Disadvantages of thermal spray fusion methods are: use of relatively fine (reinforcement) spray powders and the fact that the fusion process (namely heat input during spraying) cannot be precisely controlled. To avoid these disadvantages, fused coatings produced by welding technologies should be preferred.

Many different welding technologies can be used (Fig. 6) to produce fused hardfacings. For example, Fe-based hardfacings reinforced by TiC particles produced by submerged metal arc welding (SMAW) show better wear resistance and lower coefficient of friction compared to AISI 1045 steel. The difference in wear is about three times [79]. However, among other welding technologies, plasma transferred arc welding (PTAW) and submerged arc welding (SAW) are among the most advantageous [1].

Plasma transferred arc welding (PTAW) can be defined as a gas shielded arc welding process where the coalescence of metals is achieved via the heat transferred by an arc that is created between a tungsten electrode and a workpiece. The arc is constricted by a copper alloy nozzle to form a highly collimated arc column. The plasma is formed through the ionization of a portion of the plasma gas (mostly Ar) [80].

The plasma gas is used to generate the arc, whereas the shielding gas is used to provide the weld pool with supplementary shielding from atmospheric contamination while it solidifies and cools. The temperature of plasma gases used in PTAW can reach 15 000 K. This means that materials with high melting point can be used for hardfacings. Materials in PTAW are mostly in powder form [28, 80].

PTAW has been reported to be suitable for hardfacing applications as it can produce hardfacings with dilution levels much lower than conventional welding processes. The reason is that despite a high temperature of plasma, heat input into the substrate is smaller during the process and the material is deposited in precise quantities [81].

Zikin et al. showed that PTAW produced NiCrBSi hardfacings with Cr_3C_2-Ni cermet reinforcement had better wear resistance than pure NiCrBSi hardfacing in impact-abrasive wear conditions. Still with Cr_3C_2 carbide reinforcement, the wear resistance was lower compared to unreinforced hardfacing [82]. In [26] Zikin et al. demonstrated that a Ni-based PTAW welded hardfacing with 40 vol% recycled hardmetal content had about 10% better wear resistance than a Ni-based reference material containing 40 vol% W_2C/WC (Sulzer WOKA 50005) in three-body

abrasion (ARWW) conditions. 40 vol% is the amount required to guarantee homogeneous distribution of hardmetal particles; from that content on, there is some certainty that every part of a hardfacing has a similar amount of reinforcement in it. In [47] it was demonstrated by Zikin et al. that in high temperature impact abrasion conditions, PTAW welded Ni-based hardfacings with cermet TiC-NiMo reinforcement showed better wear resistance than a hardfacing with commercial W_2C/WC reinforcement, the difference was about 20%.

In Canada, in the excavation of oil sands, PTAW hardfacings of Ni-WC and chromium carbide overlays (CCO) are used. Ni-WC offers much higher wear resistance while CCOs are 10 − 15 times cheaper [10]. PTAW welding can be applied to produce composite hardfacings with a wide variety of fine and also coarse reinforcement and with different matrix materials, such as self-fluxing alloys and Stellites. Different carbides can be used as reinforcement, or other ceramics or cermets.

Submerged arc welding (SAW) is an arc welding process in which the arc is concealed by a blanket of granular and fusible flux. Heat for SAW is generated by an arc between a bare, solid-metal (or cored) consumable-wire or strip electrode and the workpiece. The arc is maintained in a cavity of molten flux or slag, which refines the weld metal and protects it from atmospheric contamination. Alloy ingredients in the flux may be present to enhance the mechanical properties and crack resistance of the weld deposit [80].

To produce a submerged arc weld, both a flux and an electrode are consumed. Each flux and electrode combination, along with the variation of base material and process parameters will produce a unique weld deposit. Because the integrity of the weld deposit depends on these parameters, specific fluxes and electrodes must be used in combination to optimize the weld metal properties [80].
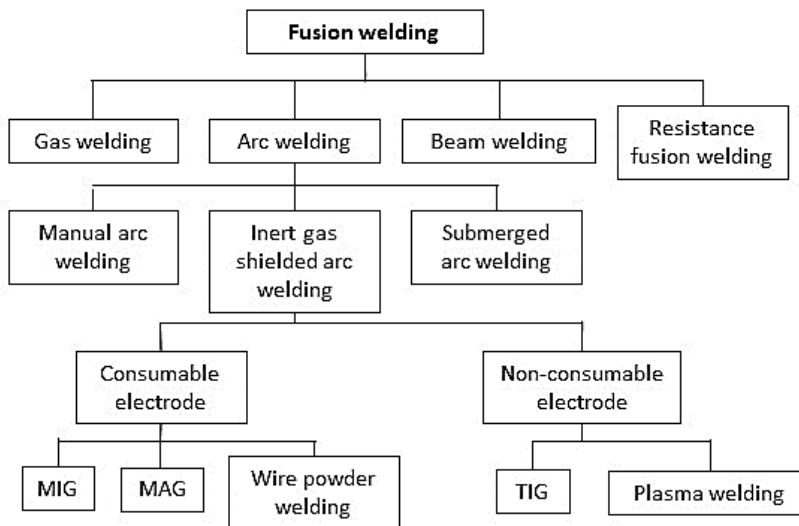

Figure 6. Classification of fusion welding technologies [1].

Weld hardfacing is mainly applied to the surface of the base metal using wire, rods or compact powder mixtures, which are automatically fed to the welding zone. As an alternative, powders mixture can be easily mixed and placed on a surface for flat applications. In such a case, the SAW welding technique makes a good economical choice in which the powder mixture as the main source of alloying is melt to form a hard hardfacing under a flux coverage [83].

SAW is known for its high deposition capabilities and surfacing or overlaying for improving

the surface properties such as hardness, wear and corrosion resistance of base material. SAW is also a cost effective process for restoration of worn parts in different industries [84].

Previous research has shown that PTAW and SAW can be used for the production of composite hardfacings as well, including double-cemented composite hardfacings [68, 85].

SAW hardfacings with composite structure show higher wear resistance and other mechanical properties (hardness) compared to unreinforced ones. Improvement in (abrasive) wear resistance seems to be in correlation with the amount of reinforcement, increased amount of reinforcement (in the form of carbides, ceramics or other) seems to increase wear resistance of SAW hardfacings. [85 – 88].

Wear resistance of WC-8Co containing SAW hardfacing on steel turning tools is comparable to SAW welded high-speed tool hardfacing, as was demonstrated by Bendikiene et al. [85]. The wear resistance improves up to 20% compared to high speed steel when up to 13% graphite is inserted into the flux during SAW surfacing. However, in [89] wood cutting tools produced by SAW welding containing 9 – 27 wt% WC-8Co showed a slightly higher wear rate compared to tool surfaced with SSH18 tool steel, the difference was 10 – 20%.

If in the case of build-up welding, heating is localized and only a part of substrate and hardfacing material is heated at a time, then in bulk melting technology, the whole substrate and hardfacing material is heated together. One example of bulk melting technologies is diffusion brazing (DFB).

It is a process that coalesces or joins metals by heating them to a suitable brazing temperature at which either a preplaced filler metal will melt and flow by capillary attraction or a liquid phase will form *in situ* between one laying surface and another. In either case, the filler metal diffuses into the base metal until the physical and mechanical properties of the joint become almost identical to those of the base metal. Pressure may or may not be applied to accomplish this [80].

The wear resistance of brazed WC-Co reinforced NiCrBSi coating grows with increasing reinforcement content. Differences in the wear resistance between 52 wt% and 70 wt% of WC-17Co containing hardfacings at high speed slurry erosive wear are about 1.5 times. At the same time, brazed hardfacings with similar composition are more wear resistant than thermal spray fused ones [90].

Another technology similar to DFB is surfacing by powder metallurgy (PM) technology based on liquid phase sintering (LPS) (hereinafter: PM hardfacings). In the PM technology, matrix material in the powder form is layed onto a substrate and heated in vacuum up to the melting temperature of the matrix material and a hardfacing with a metallurgical bond to the substrate forms. Hardfacings produced by PM can be several millimetres thick, making this technology suitable for the production of very thick hardfacings. PM hardfacings can be produced not only from powder materials, but from polymer-bound mats of filler and hard material as well [1, 91 – 92].

PM allows using reinforcement with high melting point in matrixes with a lower melting temperature. Using reinforcement in carbide (or cermet or hardmetal) form increases the wear resistance of these hardfacings compared to unreinforced counterparts. Density of PM hardfacings is affected little by the sintering temperature (in given operating range), but other characteristics, such as hardness and fracture toughness, are more affected by the sintering temperature and time [93 – 96].

PM technology allows using coarse reinforcement (> 1 mm) without additional steps (i.e., without adding it separately by hand during the hardfacing production process), which is a benefit compared to HVOF spraying and PTAW technology. PM technology also allows most precise control of temperature, and oxidation can be avoided because it takes place in vacuum. Hardfacings with double-cemented structure can also be produced by casting in the form of

wear plates. Casting technologies allow using of reinforcement with large particle sizes. Hardfacings with double cemented structure and large reinforcement particles are suitable for wear in high stress abrasive wear conditions [97].

In [8] it was demonstrated by Kulu et al. that PM produced self-fluxing alloy hardfacings containing approximately 40 vol% recycled hardmetal have about 5 -10 times higher wear resistance than Hardox 400 steel in the three-body abrasion. In abrasive erosive wear, the same hardfacings showed equal performance to Hardox 400 at 30-degree angle and higher wear at normal impact angle when coarse reinforcement was used [8].

1.3 Summary of literature review

As reported in the review, metal matrix composite (MMC) hardfacings have many benefits. Most importantly, MMC hardfacings can offer us an optimal combination of hardness and toughness properties that the (ceramic or metallic) materials separately could not provide. In addition, good abrasive wear resistance, especially in impact wear conditions can be achieved using reinforcement with large particle sizes (>1 mm) [8].

At the same time, coarse reinforcement leads to technological problems, because widely used hardfacing production technologies, such as HVOF/HVAF, PTAW and SAW, directly allow using powders with small particle sizes (e.g., at PTAW <300 μm). Coarse reinforcement is usually applicable only by casting and PM technology. Therefore, the aim is to find ways of using coarse reinforcement in spraying and welding surfacing technologies to produce hardfacings with controlled composition and structure.

Tungsten carbide based (WC-Co hardmetal) materials used in the production of wear resistant hardfacings are rare. Therefore, it is required to find ways of replacing or recycling wear resistant materials for the production of new materials and hardfacings without the risk of resource depletion and also reduce the cost of hardfacings and make them more attractive commercially.

Table 1 compares most promising hardfacing technologies. As can be seen, welding technologies provide the best combination of desired properties.

Table 1. Comparison of production technologies

Technology	Using coarse reinforcement	Heat input to substrate	Productivity	Thick hardfacings	Complex shapes
HVOF	No	Low	Medium	Yes	Yes
PM	Yes	High	Low	Yes	No
PTAW	Yes	Average	High	Yes	Yes
SAW	Yes	Average	High	Yes	Yes / No

1.4 Objectives of the study

The objectives of the PhD thesis research are as follows:
- Development of PTAW and SAW surfacing technologies for the production of MMC hardfacings based on recycled hardmetal reinforcement and Fe-based self-fluxing alloy.
- Optimization of reinforcement parameters of MMC hardfacings for different abrasive wear applications.

Hypothesis:
- Using coarse or multisized (mixture of small and large particles) reinforcement improves abrasive wear resistance of PTAW hardfacings. The higher the reinforcement content (up to 50 vol%), the higher the abrasive wear resistance.
- Hardfacings with composite spherical reinforcement have higher wear resistance than hardfacing containing composite angular reinforcement.

To achieve these objectives, focus is on the following studies:
- Structure formation of bulk melted hardfacings using PM technology for the production of hardfacings in controlled conditions.
- Optimization of PTAW and SAW technologies for the production of double-cemented composite hardfacings with coarse and multisized hardmetal reinforcement.
- Wear resistance and wear mechanisms and optimization of composition of MMC hardfacings at different abrasive wear conditions (two-body abrasion, three-body abrasion, impact abrasion wear (low and high kinetic energy)). Comparative wear resistance studies of PTAW and SAW hardfacings.

2. EXPERIMENTAL AND MATERIALS

2.1 Used materials

Hardfacing materials were selected according to the objectives of the study and planned activities. As stated, composite hardfacings provide best performance in mixed abrasive-impact wear conditions, making this kind of composition suitable for a large variety of applications.

Reinforcement chosen was mostly recycled disintegrator milled hardmetal powder (except for S3 and S5 hardfacings), as it is cheap, easily accessible and producible in different particle sizes. The advantage of WC-Co hardmetal as reinforcement is high hardness as well as relatively high fracture toughness compared to other cermets.

Self-fluxing alloy was used as a matrix material due to its low melting temperature (~1050 °C [98]), low cost, relatively high hardness and ductility, in addition, high iron content of disintegrator milled hardmetal powder (up to 13% depending on the fineness of powder [99]). This iron comes from the wear of internal parts of the disintegrator mill.

Table 2. Used materials

Material	Composition, wt%	Use
FeCrSiB[a]	13.7 Cr; 2.7 Si; 3.4 B, 6.0 Ni; 2.1 C; bal Fe	Matrix
LCW[b]	C < 0.1; Si < 0.03; Mn 0.35 – 0.6; Cr < 0.15; Ni 0.3; bal Fe	Matrix
WC-Co[c]	85-67 WC; 12-20 Co; 3-13 Fe	Reinforcement
Steel S235	0.17 C; 0.55 Cu; 0.025 P; 0.12 N; bal Fe	Substrate
Hardox 400[d]	0.32 C; 0.70 Si; 1.60 Mn; 0.025 P; 0.010 S; 1.40 Cr; 0.60 Mo; 0.004 B; bal Fe	Reference
CDP 112[e]	35 WC; 65 NiCrSiB (0.3 C; 15.0 Cr; 3.0 Fe; 5.8 Co; 6.5 BSi; bal Ni)	Reference

[a] Powder 6 AB from Höganäs AB, particle size 15 – 53 μm

[b] LCW – low carbon wire, wire diameter Ø 1.2 mm

[c] disintegrator milled in TTÜ, particle sizes 0.16 – 0.31 mm (fine – F, Fe content ≈13 %) and 1.6 – 2.0 mm (coarse – C, Fe content ≈3%)

[d] Uddeholm AB as reference steel, 425 ± 25 HV30

[e] Composite wear plate CDP 112, Castolin Eutectic® Ltd., as reference hardfacing (710 HV30) [100].

Table 3. Composition of powder mixtures

Designation	Composition, vol.%	Reinforcement particle size, mm	Comments	Technology
P1	100 FeCrSiB	-	-	PM
C3	30 WC-Co + 70 FeCrSiB	1.6 – 2.0	C, A, DM	PM
C4	40 WC-Co + 60 FeCrSiB	1.6 – 2.0	C, A, DM	PM
C5	50 WC-Co + 50 FeCrSiB	1.6 – 2.0	C, A, DM	PM, PTAW
S3	30 WC-Co[a] + 70 FeCrSiB	Ø 2.8	C, S	PM
S5	50 WC-Co[a] + 50 FeCrSiB	Ø 2.8	C, S	PM
M5	50 WC-Co + 50 FeCrSiB	0.16 – 0.32 & 1.6 – 2.0	M, A, DM	PM, PTAW
F5	50 WC-Co + 50 FeCrSiB	0.16 – 0.31	F, A, DM	PM
B1	50 WC-Co + 50 LCW	1.6 – 2.0	C, A, DM	SAW
B2	25 WC-Co + 25 FeCrSiB + 50 LCW	1.6 – 2.0	C, A, DM	SAW
D	50 WC-Co + 50 LCW	0.16 – 0.32 & 1.6 – 2.0	M, A, DM	SAW

[a] Commercial WC-Co spherical powder, Wansheng Cemented Carbide Ltd. WC-15Co (wt%)

C – coarse, M – multisized, F – fine. A – angular, S – spherical, DM – disintegrator milled

2.2 Surfacing technologies

Powder metallurgy technology

Powder metallurgy (PM) technology based on liquid phase sintering (LPS) was used to produce WC-Co containing hardfacings on steel S235 (Table 1) substrate molds that were welded together. Sintering of hardfacings was performed in vacuum. LPS parameters were chosen based on preliminary experiments and the melting temperature (~1050 °C)) of used FeCrSiB self-fluxing alloy (see Table 3) [94]. WC-Co powder was cleaned in ethanol and dried before mixing with FeCrSiB powder. Powder mixtures were prepared with the help of a scale (to have specific wt% of reinforcement) and then mechanically mixed for several hours. These mixtures where then placed into molds and sintered at 1100 °C during 30 minutes.

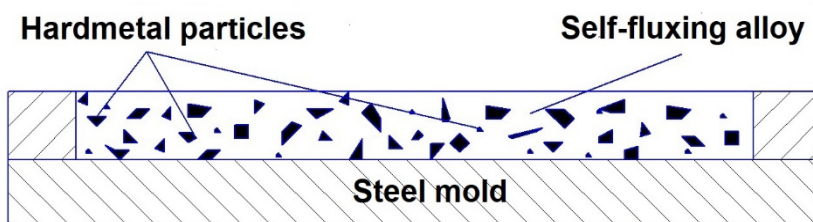Coating thickness as sintered was about 5 – 6 mm and 3 – 4 mm after grinding.

Figure 7. Mold used for production of PM hardfacings.

Plasma transferred arc welding technology

Plasma Transferred Arc Welding (PTAW) was performed on Gastolin Eutectic EuTronic® GAP 3001 device in Tallinn University of Technology (TTÜ). Principal scheme of the PTAW device is shown in Fig. 8.

Before surfacing, surface of the substrate was treated by gritblasting. Fe-based self-fluxing alloy matrix powder was fed directly from powder feeder to the torch by carrier gas. Reinforcement powders were layed manually. First, a layer of matrix with a thickness of approximately 2 mm was deposited on top of the substrate. During deposition of the first (bond) layer, current 65 A and powder deposition rate 50 mm^3/s were used. Torch movement speed perpendicular to hardfacing direction (Y) was approximately 10 mm/s. (weld width A = 30 mm, frequency 0.16 – 0.18 Hz). Torch forward movement (X) speed was 0.8 mm/s (Fig. 8).

After the deposition of the first layer of the self-fluxing alloy, the hardfacing was cleaned with gritblasting before the next step. Then a layer of reinforcement powder(s) was layed on top of the first layer. Finally, the top layer of the self-fluxing alloy matrix was deposited on top of the reinforcement layer, resulting in a composite hardfacing with very good bonding to the substrate. The dissolution of the hardmetal reinforcement was insignificant. Top layer was welded using a weld current of 55 A, and powder deposition rate was 40 mm^3/s. Torch movement parameters were the same as during the deposition of the first layer.

Gas usage for both welded hardfacing layers was the same: plasma gas (argon) – 1.5 l/min, shielding gas (argon) – 6.5 l/min and carrier gas (Varigon®; 95% Ar+ 5% H$_2$) – 6.5 l/min. Hardfacing total thickness (all layers combined) as welded was about 3.5 – 4 mm and about 2 mm after grinding. Substrate material thickness was 5 mm (Table 2).

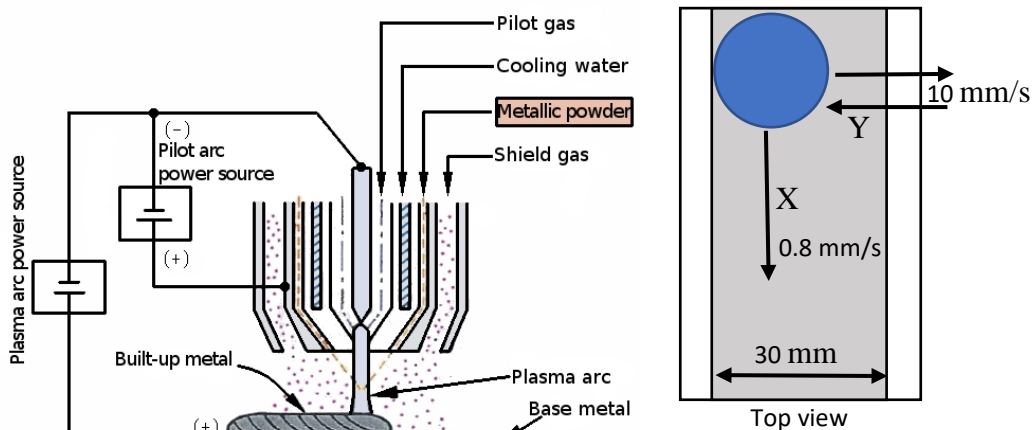Technological parameters of PTAW are presented in Table 4.

Figure 8. PTAW schematics (left) [101] *and torch movement (right).*

Submerged arc welding technology

Submerged Arc Welding (SAW) of composite hardmetal reinforced hardfacings was done in Kaunas University of Technology (KTU). Principal scheme of the SAW device is depicted in Fig. 9. Low carbon steel wire (LCW) and standard flux AMS1 (composition described in Paper 3) were used during welding (see Table 2).

During SAW welding, hardmetal reinforcement powder or the mixture of hardmetal reinforcement and Fe-based self-fluxing alloy matrix powder were placed on a steel substrate. This layer was then covered with a flux layer. After that, an arc was ignited and low carbon steel wire deposited, forming the hardfacing. During welding, self-fluxing alloy in the mixture and low carbon wire melted, surrounding hardmetal particles and forming a metallurgical bond to the substrate, thus forming a hardmetal reinforced composite hardfacing. Hardmetal particles melt only partially during welding.

Thickness of the welded hardfacing was about 5 – 6 mm and about 2 mm after grinding. Substrate material thickness was 10 mm (Table 2).

Technological parameters of SAW are presented in Table 4.

Table 4. Parameters of surfacing technologies

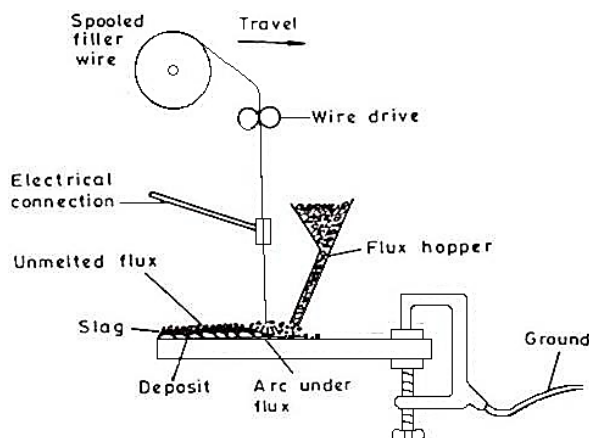| Technology	Parameters
PM (LPS)	Sintering temperature 1100 °C, sintering time 30 min, in vacuum
PTAW	Current 55 – 65 A, voltage 22 – 24 V, deposition rate 40 – 50 mm^3/s
SAW	Current 180 – 200 A, voltage 22 – 24 V, wire diameter 1.2 mm, Flux AMS1, feed rate 25.2 m/h (7 mm/s), torch speed 14.4 m/h (4 mm/s), wire deposition rate – 7.9 mm^3/s

Figure 9. SAW schematics [102].

2.3 Methods of characterization of hardfacings

Microstructure

Microstructure of the produced hardfacings was studied with the help of scanning electron microscope (SEM). Porosity of the hardfacings was estimated according to the standard ISO/TR 26946:2011, using the optical microscope Axiovert 25 (Carl Zeiss, Germany) and Buehler® Omnimet® software. Phases in the structure and dissolution of materials in hardfacings were analysed using energy-dispersive X-ray spectroscopy (EDS) and X-ray diffraction (XRD). XRD was used to determine phase composition of hardfacings and EDS to analyse dissolution of hardmetal and distribution of chemical elements in the hardfacing.

EDS analysis was performed on INCA Energy System (Oxford Instruments, Great Britain, extra module on EVO MA-15 SEM device) device. XRD device was AXS D005 X-ray diffractometer (Bruker, Germany), measurements were done using CuK$_\alpha$ radiation source, measurement step was 0.04°.

X-ray diffraction analysis was performed on C5 (hardfacing with best results in wear testing) produced by PM technology (Paper 2).

Determination of mechanical properties

Macrohardness of the produced hardfacings was measured by the Vickers hardness method in the case of PM and PTAW produced hardfacings, load 30 kgf (298 N) was used (measuring device Indentec 5030SKV). In the case of SAW hardfacings, Rockwell C-scale (HRC) hardness was measured on a device Verzus 750CCD (as this is the method typically used in KTU for hardness measurements of SAW hardfacings). In the matrix and reinforcement microhardness measurements, Vickers hardness with loads 0.3 kgf (2.98 N) and 1 kgf (9.8 N) was used (measuring device Buehler Micromet 2001).

Hardness HV1 distribution of matrix and hardphase of hardfacings with a step of 0.25 mm was measured on two hardfacings (C3 and S3), 100 measurements were made in both cases.

Modulus of elasticity and fracture toughness [103] were determined based on the universal hardness test (method described in Paper 5). Universal hardness (HU) and modulus of elasticity (E) were simultaneously determined according to the standard EN/ISO 14577-02 using the universal hardness tester 2.5/TS (Zwick, Germany). The applied load was 50 N. The average values of HU and E were calculated on the basis of five measurements.

Fracture toughness was determined as [103]:

$$K_{IC} = \frac{(HV \cdot P)^{0.5}}{3 \cdot (1-v^2) \cdot (2^{0.5} \cdot \pi \cdot \tan\varphi)^{1/3} \cdot (4 \cdot \alpha)^{0.5}}$$ (1)

where:
K_{IC} – fracture toughness, MPa·m$^{-0.5}$
HV – Vickers hardness, kgf/mm^2
P – load, N; P = 50 N
v – Poisson`s ratio, v = 0.23
φ – half aperture angle, 2ɸ = 136°
α – median crack length, μm

2.4 Wear testing

With regard to the potential application areas of composite hardmetal reinforced hardfacings, wear resistance in different abrasive wear conditions was tested.

Four different wear testing methods (see Table 5) were used to find out the performance of hardfacings in the two-body abrasion (AWW, AEMW), three-body abrasion (ARWW), abrasive erosive wear (AEW), and abrasive impact erosion (AIW) conditions. Reference materials were a pure self-fluxing alloy based hardfacing (P1), steel Hardox 400 and CDP 112 wear plate.

Abrasive Rubber Wheel Wear
Abrasive Rubber Wheel Wear (ARWW) tests, simulating low-stress three-body abrasion (free abrasive is fed to the contact zone of hardfacing and rubber wheel) conditions, were carried out according to ASTM G65 standard at TTÜ.

Testbodies used in testing had a length of 50 mm, a width of 25 mm and a total testbody thickness of 6 – 7 mm, of which 2 – 3 mm is hardfacing (after grinding).

Parameters of the ARWW wear test are presented in Table 5.

Abrasive Wheel Wear and Abrasive Emery Wear
Abrasive Wheel Wear (AWW) test is similar to ARWW but it simulates two-body abrasion. This means that abrasive particles are firmly fixed in the abrasive wheel.

Testbodies used in AWW testing had a length of 50 mm and a width of 25 mm (PM) or 6 mm (PTAW and SAW). Total thickness of testbodies was 6 – 7 mm (PM) or about 12 mm (PTAW and SAW).

AWW tests were conducted at TTÜ. Parameters of the AWW wear test are presented in Table 5.

Abrasive Emery Wear (AEMW) (test method similar to AWW) tests were carried out in Kaunas University of Technology (KTU), where this test method has been developed and used. AEMW tests were performed to find out two-body abrasion resistance of composite hardfacings.

Testbodies used had a length of 20 mm and a width of 6 mm, with a total thickness of 10 mm. Parameters of the AEMW wear test are presented in Table 5.

Abrasive Erosion Wear
Abrasive Erosion Wear (AEW) tests were carried out with a CUK device developed at TTÜ [98, 104] according to standard GOST 23.201-78 (referred to as a low-energy impact test).

Testbodies used had a length of 25 mm and a width of 15 mm, coating thickness was 2 mm and total thickness was 4 mm.
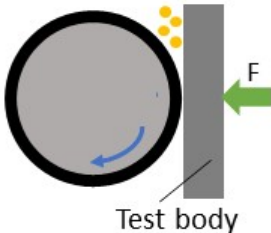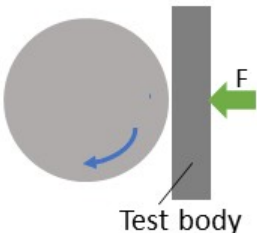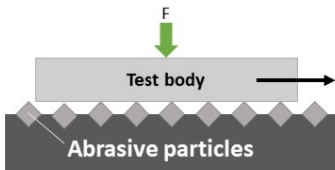
Parameters of AEW are presented in Table 5.

Abrasive Impact Wear

Abrasive Impact Wear testing (AIW) was carried out with a disintegrator based device DESI at TTÜ [105] (referred to as high-energy impact test). Testbodies used had a length of 20 mm and a width of 15 mm, coating thickness was 2 mm and total thickness was 4 mm.
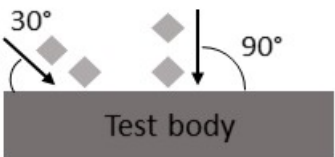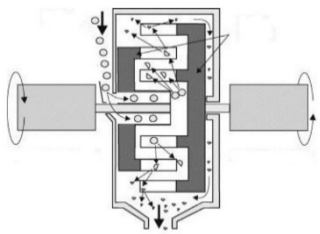
Parameters of AIW are presented in Table 5.

Table 5. Wear testing methods and parameters

Test method	Wear schematics	Wear parameters
ARWW Abrasive Rubber Wheel Wear ASTM G65	 Test body	Velocity – 2.4 m/s, Duration – 10 minutes Distance – 1440 m Abrasive – silica sand Force F = 130 N Abrasive particle size – 0.2 – 0.3 mm Abrasive hardness – 1000 – 1100 HV Abrasive flow – 375 g/min Wheel dimensions – Ø228 x 12.7 mm
AWW Abrasive Wheel Wear	 Test body	Velocity – 2.4 m/s Duration – 10 minutes Distance – 1440 m Abrasive – SiC Abrasive particles size – 0.6 – 0.8 mm Abrasive hardness – 2200 – 2500 HV Wheel dimensions – Ø245 x 35 mm Force F = 50 N
AEMW Abrasive Emery Wear	 Test body Abrasive particles	Velocity – 0.4 m/s Duration – 60 minutes (6 x 10 minutes) Distance – 1440 m Abrasive – electrocorundum Abrasive particle size – 0.08 – 0.10 mm Force F = 5 N
AEW Abrasive Erosion Wear (low-energy)	 30° 90° Test body	Impact velocities – 40 m/s and 80 m/s Abrasive quantity – 6 kg Abrasive – silica sand Abrasive particles size – 0.2 – 0.3 mm Abrasive hardness – 1000 – 1100 HV Impact angles – 30° and 90° Energy of impacting particle – $3.0 \cdot 10^{-4}$ J
AIW Abrasive Impact Wear (high-energy)		Impact velocity – 80 m/s Abrasive quantity – 15 kg Abrasive – granite gravel Abrasive particle size ~5 mm Abrasive hardness – 900 – 950 HV Impact angle – 90° Eenergy of impacting particle – $1.4 \cdot 10^{-2}$ J

3. RESULTS AND DISCUSSION

3.1 Study of structure formation during fusion processes

Formation of the structure of a double-cemented reinforced hardfacing depends to great extent both on the melting temperature of the matrix material and on the melting temperature of the binder metal (Co) of hardmetal reinforcement. Excessively high process temperature can lead to melting of the reinforcement binder and dissolution of this in the matrix metal, causing undesirable structure of hardfacings.

For this purpose, the study focused on the formation of hardfacing microstructure – wetting of substrate, distribution of higher density hardmetal, influence of hardmetal and matrix shrinkage during cooling on porosity and cracking. Macrostructure was studied visually, microstructure – with the help of SEM images of cross-sections of the produced PM hardfacings.

3.1.1 Study of microstructure

Analysis of microstructure showed a correlation between porosity and reinforcement size. The hardfacings containing finer reinforcement had higher porosity than those containing coarser reinforcement (Fig. 10).

Figure 10. Microstructure of hardfacings.
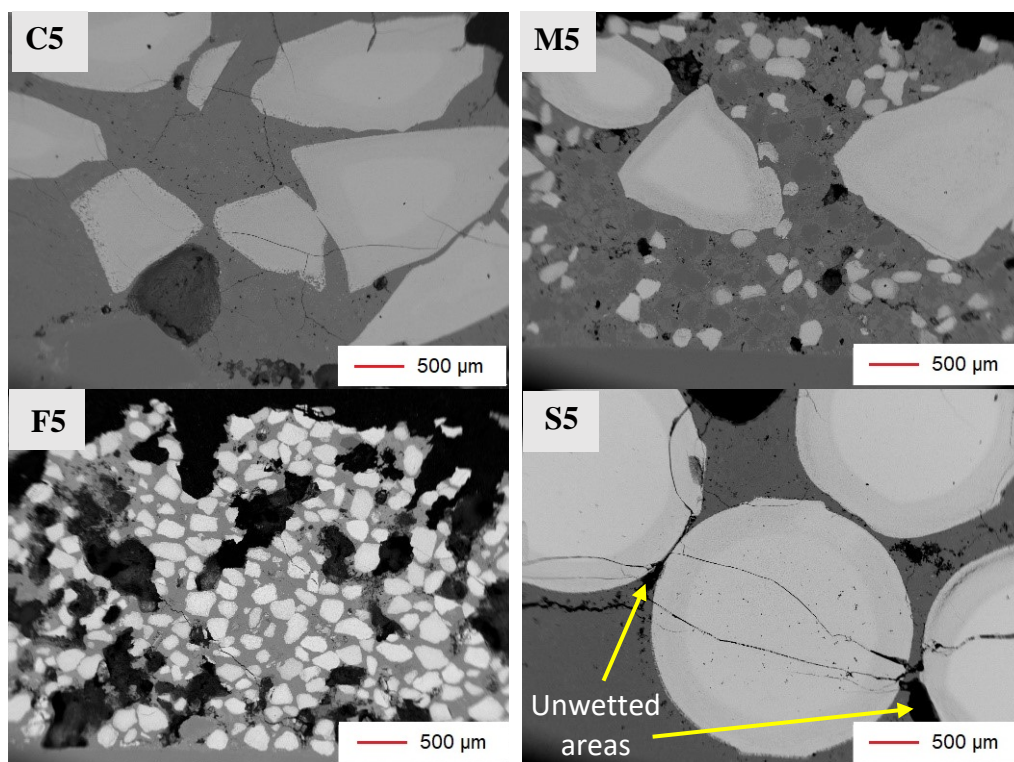
Good wetting of the disintegrator milled angular WC-Co reinforcement (C5) by the molten matrix is shown in Fig. 10 (C5, M5, F5); however, in the case of the sintered spherical WC-Co reinforcement (S5), some unwetted areas can be seen. The most apparent reason for a poorer wettability of the spherical WC-Co is the formation of sinter skin on the surface of the hardmetal balls (Paper 5).

All produced hardfacings, with different reinforcement particle sizes and shapes exhibited three zones in the structure near the matrix-reinforcement interface: dissolution-reprecipitation zone, diffusion zone and core zone (Fig. 11). The first zone, reprecipitation-dissolution zone, contained micrometer sized grains of primary WC, which became loose during the sintering process due to the dissolution and partial melting of the cobalt binder. These grains are embedded in the reprecipitated iron, chromium and tungsten carbides. In the second zone, dissolution zone, cobalt binder is partially replaced by iron, and on a smaller scale, by nickel and chromium due to interdiffusion between the matrix and reinforcement. In the third zone, core zone, the initial typical hardmetal structure is preserved. This was also confirmed by microhardness distribution measurements (Fig. 13), where interdiffuson zone can be seen from the hardness results, which were found to be between the hardness of the matrix and hardmetal.

Cracks that are clearly seen on the SEM images of the microstructures of C5 and S5 are caused by tensions the reason of which are the differences (~3 times) in the thermal expansion coefficients of hardmetal ($5 \cdot 10^{-6}$ 1/K) and self-fluxing alloy ($16 \cdot 10^{-6}$ 1/K). This thermal shrinkage takes place at cooling during sintering and may occur also while cutting samples for cross-sections [97], where samples heat up significantly even when watercooling is used. At cutting due to the heating, the matrix expands more, causing pulling stresses and cracking in hardmetal particles.

Phases and distribution of elements in the structure (Fig. 12) were analysed using EDS and XRD. XRD analysis showed formation of new $((W,Fe,Co)_xC_y)$ carbides during the sintering process, WC already exists inside initial hardmetal. Most notable were Fe_5C_2 and $Fe_{23}C_6$. Phases formed due to the dissolution of hardmetal were: Fe(Cr) (zone I), WCoB (zone II), $Cr_{12}W_3B_4$ (zone II), and CrB (zone I) (Paper 2).
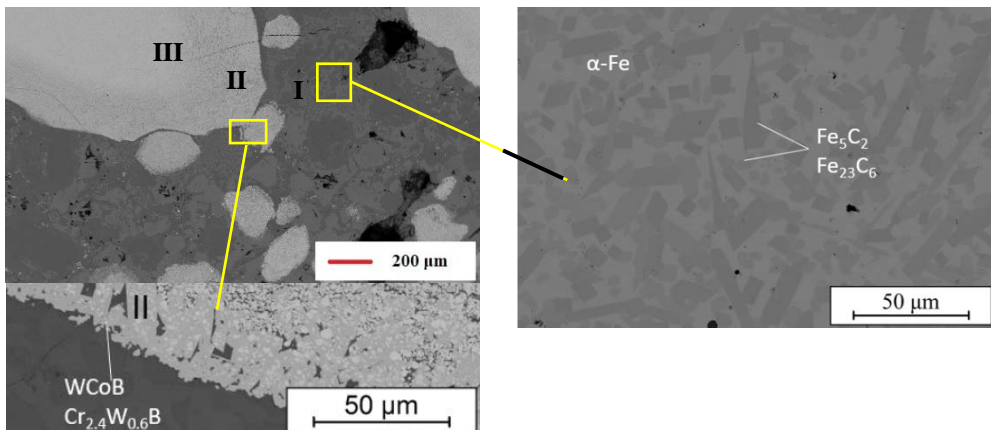

Figure 11. Zones in the microstructure of hardfacing M5: I – reprecipitation-dissolution zone, II – diffusion zone, III – core zone.
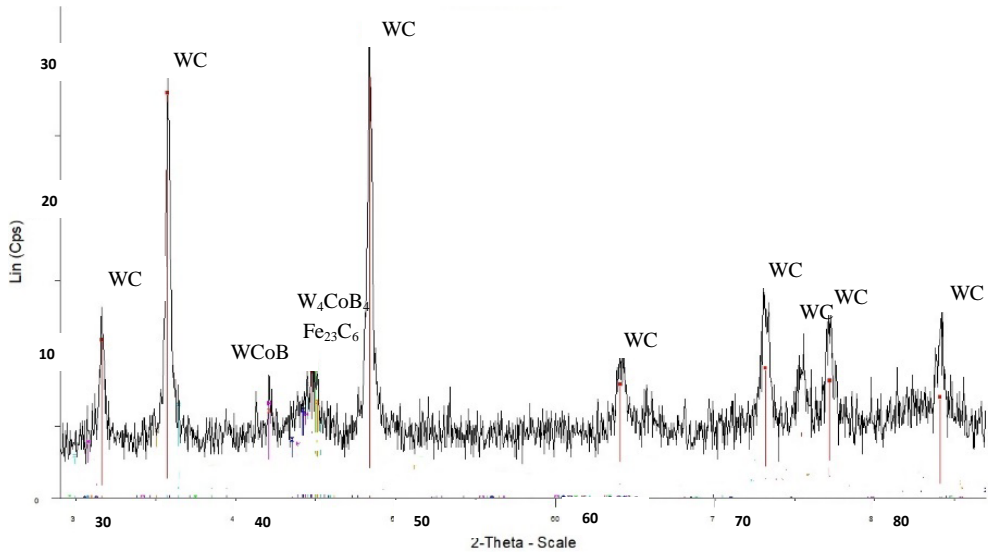
Figure 12. XRD graph of PM produced C5 hardfacing.

Results of the study of porosity show that addition of hardmetal reinforcement increases porosity of composite hardfacings. Modulus of elasticity of the matrix (FeCrSiB) material decreases with the increase of hardmetal reinforcement content. Decrease in the modulus of elasticity is higher in the case of angular reinforcement (C3, C5). Fracture toughness of the matrix material also decreases with the increase of hardmetal reinforcement content. This means that matrix material becomes less ductile with the addition of hardmetal reinforcement. Though the exact reason remains undetermined, tensile stresses in the matrix mentioned earlier are supposed to be the reason for such a decrease of mechanical properties (Paper 5).

Table 7. Porosity, modulus of elasticity and fracture toughness of hardfacings (Paper 5)

Designation	Porosity, %	E, GPa	Fracture toughness, MPa·m$^{-0.5}$ Load 50N
P1	1.9	290.9 ± 26.7	14.5 ± 3.3
C3 Matrix Reinforcement	4.6	243.5 ± 18.0 449.7 ± 30.3	12.6 ± 1.4
S3 Matrix Reinforcement	3.0	256.4 ± 15.5 547.4 ± 64.3	12.0 ± 1.2
C5 Matrix Reinforcement	4.8	215.3 ± 42.9 483.4 ± 156.4	11.2 ± 0.3
S5 Matrix Reinforcement	1.8	221.4 ± 20.5 433.5 ± 46.0	11.7 ± 3.3

3.1.2 Mechanical properties of hardfacings

As it follows from Table 6, maximum macrohardness was demonstrated by hardfacing with multimodal reinforcement (M5), which should have positive influence on the wear resistance at abrasion, but it was not confirmed later by our tests.

Microhardness of the metal matrix of composite hardfacings should be influenced by hardmetal content (C3, C4, C5). However, the results showed no increase in matrix microhardness as compared to unreinforced hardfacing (P1). This is probably caused by stresses in the matrix caused by differences in the thermal expansion coefficents of the matrix material and hardmetal reinforcement, these tensions weaken the matrix and therefore influence hardness, which should otherwise increase due to the partial dissolution of hardmetal particles [107]. Microhardness of the matrix grows with increasing hardmetal content when reinforced hardfacings (C3, C4, C5) are compared between themselves.

Table 6. Hardness of PM hardfacings (Paper 1, Paper 2)

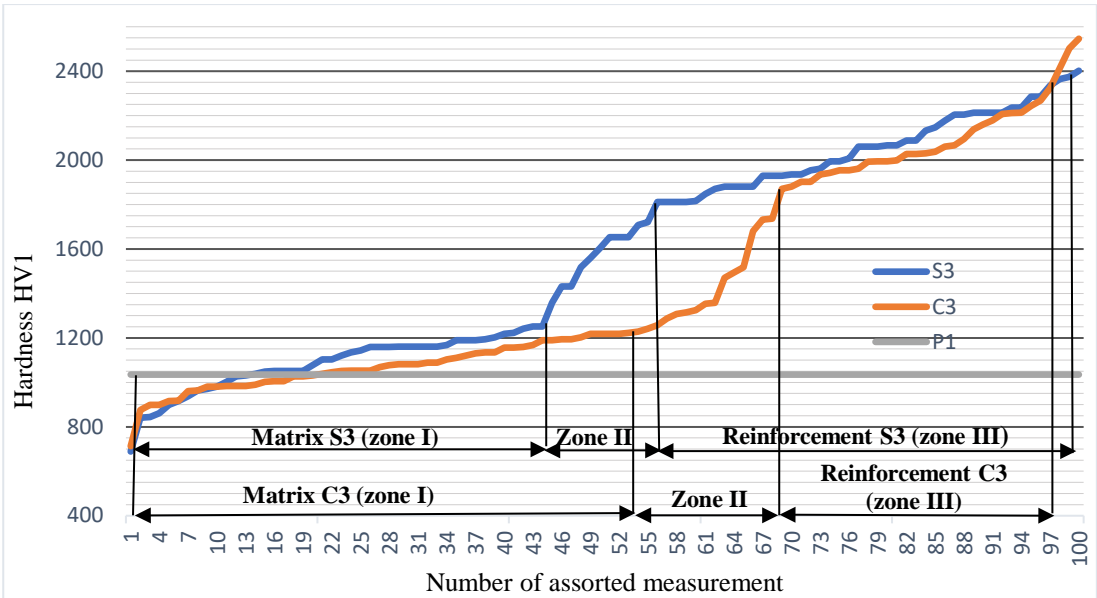| Designation	Macrohardness HV30	Microhardness HV0.3	
		Matrix	Reinforcement
P1	868 ± 28	1035 ± 70	-
C3	1098 ± 308	978 ± 54	1912 ± 97
C4	1154 ± 351	1047 ± 68	1911 ± 135
C5	1260 ± 436	1005 ± 41	1856 ± 67
S5	1161 ± 420	950 ± 107	1637 ± 117
M5	1714 ± 296	817 ± 63	1482 ± 126
F5	830 ± 161	900 ± 90	1444 ± 136
CDP*	548 ± 50	524 ± 111	1730 ± 318

* NiCrSiB matrix

Figure 13. Hardness distribution of C3 and S3 hardfacings (zones described on Fig. 11).

Results of hardness distribution are displayed in Fig. 13. Results from the measurements of spherical reinforcement containing a hardfacing (S3) show that the number of measurements corresponding to hardphase hardness exceeds the amount of hardmetal in the initial powder

mixture (about 40 measurements and 30 vol% hardmetal in the initial powder mixture). In the case of the hardfacing (C3) containing angular hardmetal, the number of hardness measurements corresponding to hardphase hardness corresponds to the amount of hardmetal in the initial powder mixture (about 30 measurements and 30 vol% hardmetal in initial powder mixture)). In both cases, average matrix hardness changes little compared to a pure self-fluxing alloy hardfacing (P1). Hardness results are considered to be matrix in the range of 800 – 1200 HV1 and hardmetal/hardphase in the range of 1800 – 2400 HV1.

The following conclusions were drawn from the study of microstructure and mechanical properties of PM hardfacings:

- Noticeable dissolution (melting) of reinforcement takes place by using angular or spherical hardmetal as reinforcement,.
- Macrohardness of the hardfacing depends on the reinforcement type:
  hardfacing with multisized reinforcement (M5) showed the highest hardness due to the dense and equal distribution of both fine and coarse hardmetal particles in the matrix, whereas hardfacing with fine reinforcement (F5) in fact exhibited lower hardness, mostly due to its porosity.
- The average macrohardness of the hardfacing increased with an increasing hardmetal content when coarse angular hardmetal was used (C3 – C5). Microhardness of the matrix was higher also with the increase of coarse hardmetal content (when comparing C3, C4 and C5 between themselves), which can probably be explained by the higher amount of hardmetal dissoluted in the matrix.
- Matrix microhardness of reinforced hardfacings compared to hardfacings consisting only of a self-fluxing alloy (P1) decreased. The reason is that tensions caused by differences in the thermal expansion coeffecents of the hardmetal and the self-fluxing alloy weaken the matrix.

3.2 Development of PTAW and SAW surfacing technologies

Two welding technologies (PTAW – plasma transferred arc welding and SAW – submerged arc welding) were applied for the production of composite Fe-based metal matrix hardfacings with WC-Co reinforcement.

3.2.1 Development of PTAW technology

Due to the limitations of the PTAW technology in thepowder fractions use (up to 300 μm), the ways to introduce coarse powder (reinforcement) into hardfacings during welding were studied. During the first test series, hardmetal powder was layed by hand on the steel substrate, which was girtblasted before that. Then a Fe-based self-fluxing alloy matrix layer was welded on top of it. At first, higher currents were used, beginning from 95 A and decreasing. This proved to be unsuccessful because high currents resulted in high oxidation of the surface (matrix material). After multiple attempts it was found that currents in the range of 55 – 65 A are most suitable. The other parameters were also optimized and it was found that higher torch movement speed also increases the quality (because heat input decreases). Optimal torch movement speed was found to be in the range of 10 mm/s. Results from the first test series can be seen in Fig. 14.

Composition of PTAW hardfacings (C5 and M5) is similar (50 vol% coarse or multisized reinforcement) to PM hardfacings (see powders mixtures used for production in Table 3).
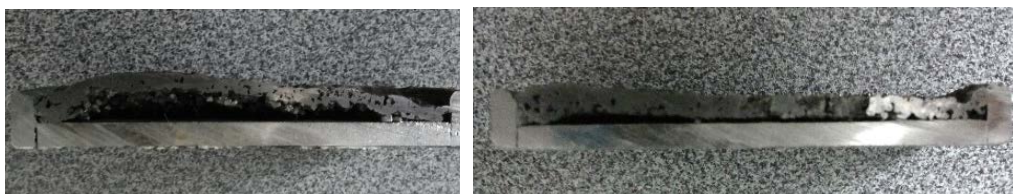

Figure 14. Cross-sections of PTAW surfacings (left 75A current, right 65A current) with the one-pass method.

Results from the first test series showed that this method proved to be unsuccessful, due to the absence of bonding between the hardfacing and the substrate (Fig. 14). During the second test series, a two-pass method was used where at first a bond layer of metal-matrix self-fluxing alloy was welded on top of the substrate. After that a layer of hardmetal particles was layed on top of the bond layer of the self-fluxing alloy weld. Finally, a top layer of the self-fluxing alloy was welded on top of the placed hardmetal particles layer. By this method, a hardfacing with good metallurgical bond to the substrate was achieved. Though the surface showed a high amount of cracks and pores after grinding (which was necessary for wear tests), some of them were visible already after welding. This indicates that preheating of the hardmetal before depositing it to the surface should be used, which would mean that thermal shrinking in the composite hardfacing would be more equal (Fig. 15).

Figure 15. Cross-section of PTAW surfacing (current 65A) by the two-pass method.

Microstructure of the PTAW welded hardfacing C5 produced by the two-pass method is depicted in Fig. 16

As can be seen from the SEM image of the microstructure of the hardfacing C5 (Fig. 16), double reinforced composite structure is formed during welding – coarse WC-Co hardmetal in FeCrSiB matrix reinforced with micrometrical WC particles (Table 8).
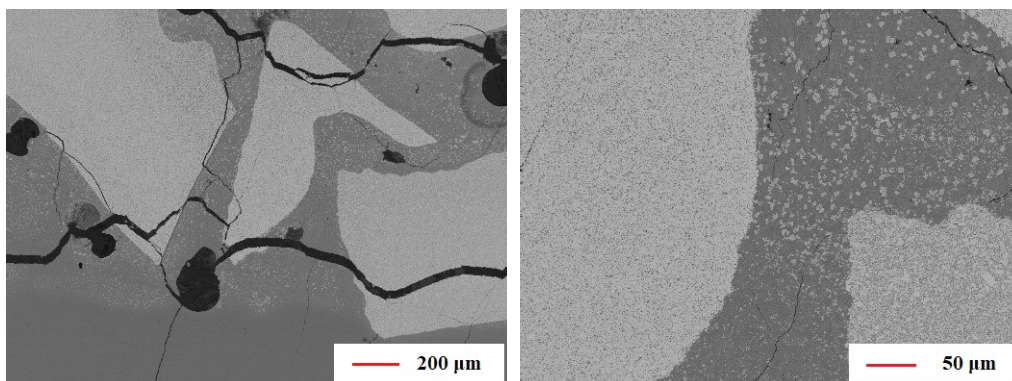

Figure 16. SEM images of PTAW welded hardfacing C5

Table 8. Hardness of PTAW hardfacings

Designation	Macrohardness HV30	Low-force hardness HV1	
		Matrix	Reinforcement
C5	1045 ± 196	975 ± 125	1485 ± 60
M5	1101 ± 244	975 ± 83	1670 ± 156

3.2.2. Improving the SAW hardfacing technology

Similar to the PTAW technology, in SAW, the one-pass method was used at first, where the hardmetal powder or the mixture of hardmetal and self-fluxing alloy was layed on top of the substrate and then low carbon wire (LCW, see Table 2) was welded on top of it. Unlike PTAW, however, in SAW no intermediate layer was needed, as good metallurgical bonding between the hardfacing and the substrate was achieved without it. Therefore, in SAW the one-pass technology is sufficient to achieve quality hardfacings, while in PTAW the two-pass technology is needed (Fig. 17).

Three different compositions of hardfacings produced by SAW (B1, B2 and D) were studied (see Table 3). Hardfacing B1 consists of 50 vol% coarse hardmetal reinforcement similar to hardfacing C5, but the matrix material is only low carbon steel (LCW) instead of a self-fluxing alloy. This is the main difference between PTAW/PM and SAW hardfacings, SAW hardfacings always contain low carbon steel (LCW) due to the nature of the technology. In the case of hardfacing B2, the composition contained coarse hardmetal reinforcement, self-fluxing alloy and LCW. This composition was chosen to obtain a composition as similar to PTAW/PM hardfacings as possible. Hardfacing D contained 25 vol% coarse hardmetal, 25 vol% fine hardmetal and 50 vol% LCW to imitate the structure and composition of the M5 hardfacing.

Examples of the microstructures of SAW hardfacings are presented in Fig. 17. Similar to PM and PTAW hardfacings, cracks can be seen in the structure. These are caused by differences of thermal expansion coefficients of the hardmetal and the self-fluxing alloy matrix [107]. The biggest difference between SAW and PM/PTAW lies in the size of diffusion zone in hardmetal particles, which is the largest in the case of SAW due to the highest heat input during welding (welding currents during SAW are much higher compared to PTAW). In SAW in the case of

smaller particles, diffusion zone includes almost the whole hardmetal particle. Noticeable dissolution of both small and large hardmetal particles in SAW hardfacing was observerd (core zone, similar to Fig. 11, cannot be detected visually).
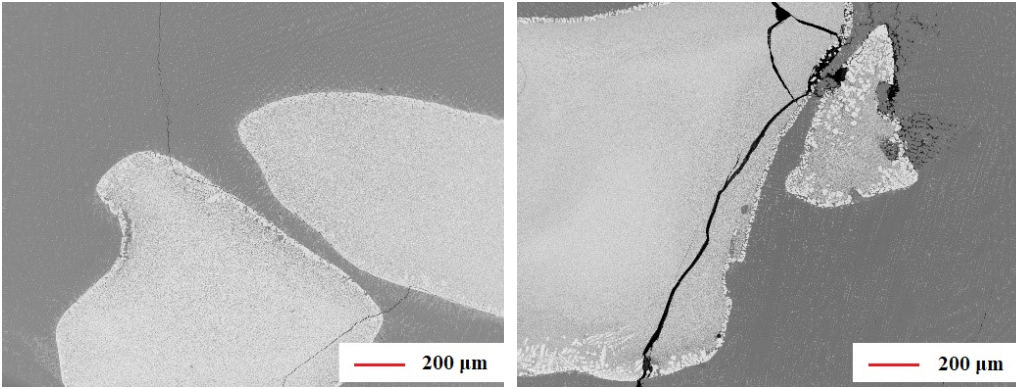

Figure 17 Microstructure of SAW hardfacings B1 (left) and B2 (right).

Heat treatment (tempering) of SAW hardfacings after surfacing was performed. This was done to reduce stresses and initiate transformation of possibly retained austenite in the structure. Macrohardness of SAW hardfacings as-welded and after tempering at 550 °C for 1 h and 600 °C for 1 h (between tempering cycles, hardfacings were air cooled to room temperature) and microhardness of the matrix and reinforcement is given in Table 9.

Table 9. Hardness of SAW hardfacings (Paper 3)

Designation	Macrohardness HRC[a] (HV)[b]			Low-force hardness HV1[a] (after tempering)	
	As welded	After tempering		Matrix	Reinforce-ment
		550 °C / I cycle	600 °C / II cycle		
B1	55 (610)	55 (610)	54 (590)	807	1441
B2	54 (590)	53 (560)	50 (500)	932	1557
D	39 (370)	58 (690)	54 (590)	710	1436

[a] average hardness
[b] according to conversion table [106]

3.2.3 Comparison of hardfacings produced by different surfacing technologies

To analyse the influence of surfacing technology on the properties (wear rate and hardness) of hardfacings with coarse hardmetal reinforcement (C5 / B1), different production technologies (PM, PTAW and SAW) were compared. Hardness results of different technologies for similar composition are given in Table 10. Wear rate results for these hardfacings are shown in Fig. 11.

Table 10. Comparison of different hardfacing technologies

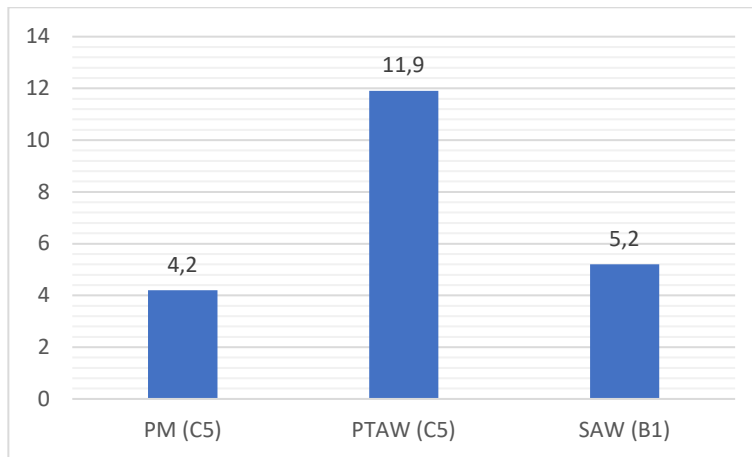| Technology and designation of hardfacing	Macrohardness HV30	Low-force hardness HV1	
		Matrix	Reinforcement
PM, C5	1260	1005	1856
PTAW, C5	1045	975	1425
SAW, B1	610 (55*)	807	1438

* Initially measured in HRC

Figure 18. Wear rate in mg at AWW of hardfacings with 50 vol% hardmetal content produced by different technologies. PM C5 is most wear resistant. (Paper 2, Paper 3)

Conclusions from the PTAW and SAW studies:

- Based on the results of two-pass surfacing, it was found that the PTAW technology offers a possible approach to produce double-cemented hardfacings based on the Fe-based self-fluxing alloy matrix and coarse recycled disintegrator milled hardmetal reinforcement intended for combating abrasive wear.
- Similar sequence of actions, but with one-pass surfacing, could be proposed for hardfacings produced by SAW. Double cemented structure of hardfacings in SAW can be achieved using hardmetal powder as reinforcement and low carbon wire (and FeCrSiB) as matrix.
- To avoid tensions in the hardfacings, hardmetal reinforcement and/or substrate pre-heating, as well as slow cooling after welding or post-welding treatment (tempering) are recommended.

4. WEAR RESISTANCE OF HARDFACINGS

To study wear resistance and mechanisms of wear, mainly PM produced hardfacings were used for wear testing. Hardfacings produced by PTAW and SAW technologies were tested only in two-body abrasion conditions, because studies showed that composite hardfacings give best performance in these conditons.

4.1 Wear resistance at ARWW test

ARWW testing was performed to find out the wear resistance of hardfacings in three-body abrasion conditions. In ARWW testing, hardfacings containing commercial spherical reinforcement (S5) showed the highest wear resistance. Hardfacings containing coarse angular disintegrator milled hardfacings (with the exception of C4) also showed slightly better wear resistance than the unreinforced hardfacing (P1), though their wear resistance in the three-body abrasion was lower compared to the spherical reinforcement containing hardfacing. Results of ARWW testing are presented in Table 11.

Table 11. ARWW test results (Paper 1, Paper 2)

Designation	Wear rate*, mm³/kg	Relative wear resistance to P1
P1	1.50	1.0
C3	1.30	1.13
C4	1.84	0.84
C5	1.28	1.28
S5	0.78	1.70
M5	2.31	0.58
F5	2.90	0.46

* Average of two test series (one test series is three tests)
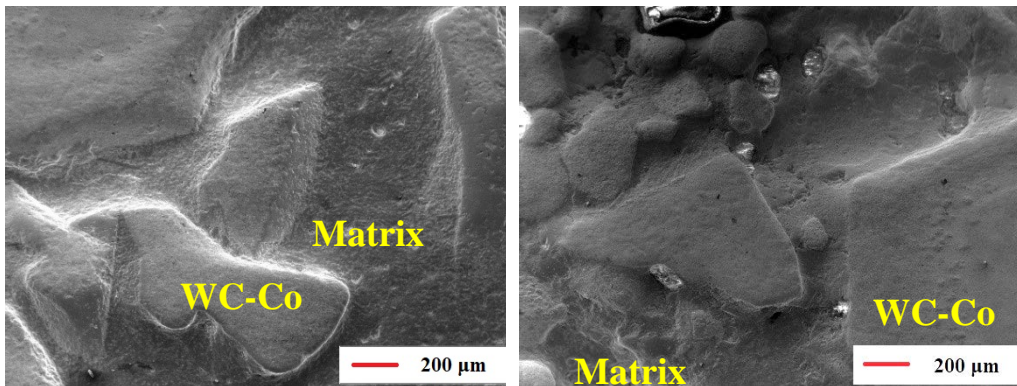

Figure 19. Worn surfaces of PM hardfacings at ARWW, C5 left, M5 right.

The main wear mechanism (Fig. 19) at ARWW is the wear of matrix material (FeCrSiB) as a result of microcutting as the hardness of abrasive (silica sand) is higher than that of the matrix material. Wear of the matrix is higher around hardmetal particles (where the porosity of the matrix is higher) as abrasive in the three-body abrasion is free to move and therefore matrix is cut by the abrasive particles from the weakest (with the least hardness) part of hardfacing. This results in hardmetal particles becoming loose during the wear process and, finally, their dropout, which contributes to the overall wear rate. Wear mechanism of hardmetal particles is

low-cycle fatigue as the hardness of hardmetal particles (1400 – 1900 HV in this thesis) is higher than the hardness of the abrasive (silica sand, $\approx$ 1050 HV) [108].

From the ARWW test results, the following conclusions can be made:
- Increase in the wear resistance of hardfacings with coarse angular reinforcement (C3 and C5) at three-body abrasion compared to unreinforced hardfacing (P1) was very small (~20 %).
- Reinforcing of a hardfacing with fine or multisized reinforcement decreases wear resistance about 2 times compared to a hardfacing made of a pure self-fluxing alloy (P1).
- Hardfacing containing coarse spherical hardmetal reinforcement (S5) demonstrated higher wear resistance than that with coarse angular hardmetal reinforcement.

4.2 Wear resistance at AWW and AEMW tests

AWW and AEMW testing was performed to find out the performance of hardfacings in two-body abrasion conditions. Results of AWW testing of PM hardfacings (Table 12) had some similarities compared to ARWW testing; however, some major differences were found in the results. Similar to ARWW testing, in AWW testing there is a correlation between the wear resistance and the hardmetal content in the case of hardfacings with coarse reinforcement. The higher the hardmetal content, the better the wear resistance (Fig. 20).

Like in ARWW testing, in AWW testing, hardfacings with coarse reinforcement (C3, C4, C5 and S5) showed better wear resistance than those with fine and multimodal reinforcement (F5 and M5). Unlike ARWW testing, however, in AWW testing hardfacings with fine and multimodal reinforcement showed better wear resistance than an unreinforced hardfacing (P1). This can be attributed to the fact that in AWW testing abrasive particles are fixed and therefore matrix is not depleted at a higher rate than reinforcement.

When in ARWW testing, hardfacings with spherical reinforcement showed better wear resistance than hardfacings with angular reinforcement, then in AWW testing, the situation was *vice versa*, and hardfacings with angular reinforcement showed better performance with the same hardmetal content.

Results of AWW testing of PTAW and SAW hardfacings are given in Fig. 22.
Test results show that PTAW produced hardfacing C5 has lower wear resistance than SAW produced hardfacings (B1, B2 and D). At the first stage of testing, hardfacings showed much higher wear rate compared to the following test series, indicating a work-in period (Fig. 21). This means that it takes time for the hardfacing to achieve stabilized wear rate. At stabilized wear, hardfacings C5 (PTAW) and B1, B2 and D (SAW) have up to 10 times higher wear resistance than unreinforced hardfacing P1.

In AWW, the main wear mechanism for that matrix material (FeCrSiB) is microcutting, as the abrasive particles in the abrasive wheel have much higher hardness than that of the matrix material. Wear mechanism at hardmetal reinforcement is micro-cutting [109]. Unlike three-body abrasion, in the two-body abrasion matrix and hardmetal particles on the hardfacings surface wear equally as abrasive particles are fixed in the abrasive wheel and cannot reach deeper than other parts of the hardfacings surface.

Table 12. AWW test results (Paper 2)

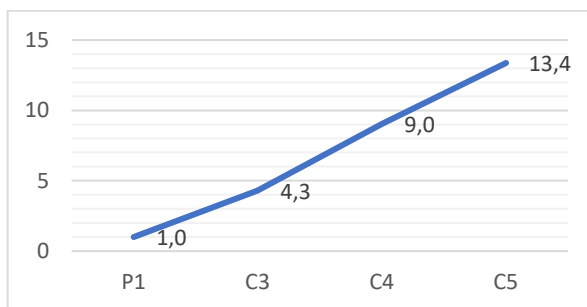| Designation	Wear rate, mm³
P1	6.15
C3	1.43
C4	0.68
C5	0.46
S5	1.02
M5	3.18
F5	2.98

Figure 20. Relative wear resistance compared to P1 at AWW (Paper 2).
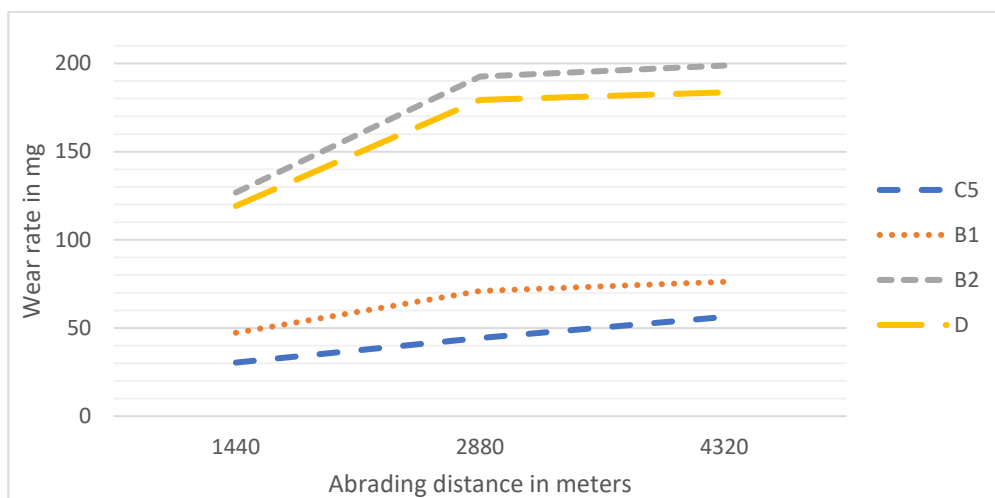
Figure 21. Influence of abrading distance on the wear rate (mass loss in mg) at AWW of SAW and PTAW hardfacings.
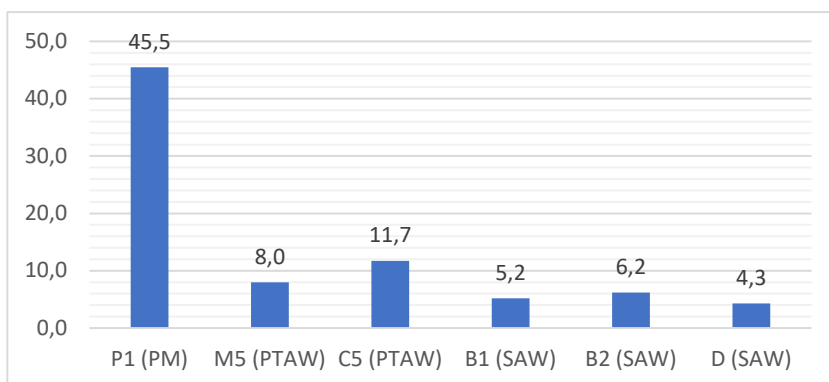
Figure 22. AWW test results (mass loss in mg) of SAW and PTAW hardfacings. Results of 3rd test series

Similar to AWW test, AEMW test is a two-body abrasion wear method. AEMW test was used to evaluate the wear resistance of PTAW and SAW produced hardfacings.

Results of AEMW tests are presented in Fig. 23 (Results of the 3rd test series is used for the reasons depicted in Fig. 21; at first, the wear rate is higher, but later on it stabilizes). As it follows

from Fig. 23, PTAW produced hardfacing (C5) showed better wear resistance than SAW produced hardfacings (B1) with the same composition. The results also show that similar to the AWW testing, the wear rate in the initial stage of the experiment is much higher than in the final stage of the experiment. This indicates that both SAW and PTAW produced hardfacings have a work-in stage before achieving maximum wear resistance. The reason is that heavy hardmetal particles sink in the molten matrix during the deposition process [26]. Higher wear rate of B2 compared to other hardfacings can be explained by lower initial hardmetal content.

Wear mechanisms in AEMW are similar to those described in AWW as both are (low-stress) two-body abrasion methods. Low-stress means no abrading particles (and if impacting particles are used, they do not fracture) and small used loads during testing.

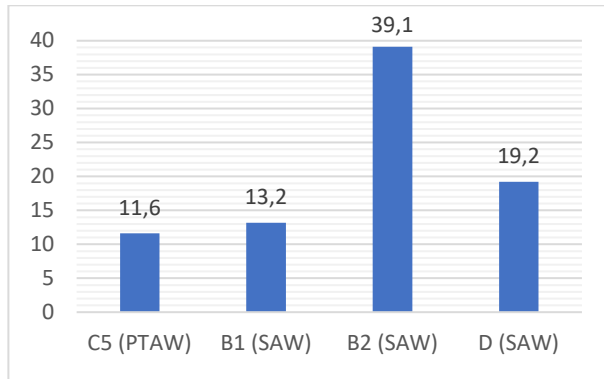*Figure 23. AEMW test results (mass loss in mg) of SAW and PTAW hardfacings. Results of 3rd test series*

The following conclusions can be made from the AWW and AEMW test results:
- Hardfacings with coarse hardmetal reinforcement (up to 50 vol%) show good wear resistance in two-body abrasion conditions – increase in wear resistance is up to 13 times compared to unreinforced hardfacings.
- SAW hardfacings performed better in the AWW test, PTAW hardfacing in the AEMW test.
- Both SAW and PTAW hardfacings exhibited "working-in" period in two-body abrasion conditions.

4.3 Wear resistance at AEW and AIW tests

AEW and AIW testing was performed to find out the wear resistance of hardfacings in impact erosion conditions. When in ARWW, AWW and AEMW hardness plays a key role in wear resistance, then in AEW and AIW toughness plays an important role in addition to hardness. Effects of abrasive hardness, impact velocity and impact angle were also studied.

Results of AEW with abrasive with lower hardness (granite sand) (Table 13) show that addition of hardmetal reinforcement has no or negative influence on the wear resistance of hardfacings. With coarse hardmetal reinforcement, hardfacing (C5) has basically the same wear resistance as unreinforced hardfacing (P1). Hardfacings with fine and multimodal reinforcement (F5 and M5) have lower wear resistance than an unreinforced hardfacing (P1).

Results of AEW tests with abrasive at higher hardness (quartz sand) (Table 13) show that the influence of reinforcement on the wear resistance of hardfacings is negative with all reinforcements. Hardfacing with coarse hardmetal reinforcement (C5) has almost the same

wear resistance as unreinforced hardfacing (P1).

Relatively higher wear resistance of hardfacings in AEW with lower hardness abrasive (granite sand) can be explained by the fact that abrasive (granite sand) has lower hardness than silica sand, which is similar to the hardness of the self-fluxing alloy matrix.

Table 13. Influence of abrasive hardness on the wear in AEW (Paper 4)

Designation	Wear rate[a], mm³/kg		Relative wear resistance to P1	
	Granite sand	Quartz sand	Granite sand	Quartz sand
P1	12.0	26.9	1.0	1.0
C5	11.7	30.2	1.0	0.9
F5	30.2	90.3	0.4	0.3
M5	21.9	76.3	0.5	0.4

[a] abrasive particle size 0.2 – 0.3 mm, impact angle of abrasive particle 30°, abrasive velocity – 80 m/s

Wear resistance of hardfacings in AEW depends on the impact angle as well. As can be seen from the results in Table 14, reinforcing with coarse hardmetal reinforcement increases the wear resistance about 40% at 90° impact angle compared to an unreinforced hardfacing. At the same time, wear resistance of hardfacings with fine and multimodal reinforcement is lower compared to the unreinforced hardfacing (P1) at both angles.

Table 14. Influence of impact angle in AEW test (Paper 4)

Designation	Wear rate[a], mm³/kg		Relative wear resistance to P1	
	$\alpha = 30°$	$\alpha = 90°$	$\alpha = 30°$	$\alpha = 90°$
P1	12.0	21.5	1.0	1.0
C5	11.7	15.5	1.0	1.4
F5	30.2	41.0	0.4	0.5
M5	21.9	40.0	0.5	0.5

[a] abrasive – granite sand, abrasive particle size 0.2 – 0.3 mm, abrasive velocity – 80 m/s

Study of the influence of impact velocity (Table 15) showed that with increasing velocity, the wear rate increases. Relative wear resistance of a hardfacing with coarse reinforcement (C5) is 2.1, i.e., 1.4 times higher compared to the unreinforced hardfacing (P1) at the impact velocities of 40 m/s and 80 m/s, respectively. Suprisingly, hardfacing with multimodal reinforcement (M5) showed good wear resistance at low impacting velocities (40 m/s) compared to the unreinforced hardfacing (P1). In other cases, hardfacings with fine (F5) and multimodal (M5) reinforcement had lower wear resistance than the unreinforced hardfacing (P1).

Table 15. Influence of impact velocity in AEW (Paper 4)

Designation	Wear rate[a], mm³/kg		Relative wear resistance to P1	
	v = 40 m/s	v = 80 m/s	v = 40 m/s	v = 80 m/s
P1	10.0	21.5	1.0	1.0
C5	4.8	15.5	2.1	1.4
F5	13.8	41.0	0.7	0.5
M5	5.6	40.4	1.8	0.5

[a] abrasive – granite sand, abrasive particle size – 0.2 – 0.3 mm, impact angle of abrasive particle – 90°

Besides the velocity, the kinetic energy of impacting particles is influenced by the mass (i.e., size) of the particles as well. For that reason, AIW tests were carried out and compared with AEW test results. At AIW tests, granite gravel (3.0 – 5.6 mm) was used as abrasive. Test results of AEW and AIW are given in Table 16.

At AEW tests, the differences between materials were smaller. At AIW tests, most wear

resistant materials proved to be the self-fluxing alloy based hardfacing (P1).

Wear resistance of composite hardfacings (F5, C5 and M5) at AIW testing was very low and at multimodal reinforcement containing hardfacings (M5), the wear resistance was more than 37 times lower than that of the unreinforced hardfacing (P1). Comparison of composite hardfacings between themselves revealed that the hardfacing containing coarse reinforcement (C5) showed higher wear resistance compared to fine and multimodal reinforcement, two times better compared to F5 and three times better compared to M5.

Table 16. Influence of impact energy at AIW (Paper 4)

Designation	Wear rate[a], mm³/kg		Relative wear resistance to P1	
	Low energy[a] ($E_k = 3.0 \cdot 10^{-4}$ J)	High energy[b] ($E_k = 1.4 \cdot 10^{-2}$ J)	Low energy[a] ($E_k = 3.0 \cdot 10^{-4}$ J)	High energy[b] ($E_k = 1.4 \cdot 10^{-2}$ J)
P1	10.0	9.3	1.0	1.0
C5	4.8	108.6	2.1	0.08
F5	13.8	215.2	0.7	0.04
M5	5.6	348.6	1.8	0.03

[a] abrasive – granite sand, abrasive particle size – 0.2 – 0.3 mm, impact angle of abrasive particles – 90°, abrasive velocity – 40 m/s

[b] abrasive – granite gravel, abrasive particle size – 3.0 – 5.6 mm, impact angle - 90°, abrasive velocity – 80 m/s

Wear mechanisms in AEW and AIW depend on the hardness ratio between the hardfacing (matrix) material and the abrasive hardness (H_m/H_a) and on the impact angle (low or high). Other properties that affect wear mechanisms are kinetic energies of impacting particles (depending on the velocity and particle size), toughness of the material and fracture toughness of the material.

If $H_m < H_a$, microcutting or plastic deformation with surface fatigue occurs. If $H_m \approx H_a$, then deformation with microcutting and/or surface fatigue occurs. If $H_m > H_a$, then elastic and small plastic deformation with surface fatigue and with high probability for direct fracture occurs.

This can be deducted from Table 7 as with increasing hardmetal content, fracture toughness of matrix material decreased, which lead to higher probability of direct fracture.

Depending on the fracture toughness, the following mechanisms of wear may occur: in the case of brittle materials like reinforcement (low K_{IC}), surface fatigue is dominating and a direct fracture is highly possible, and in the case of ductile materials like matrix (high K_{IC}), plastic deformation with microcutting and/or surface fatigue is dominating.

Wear mechanisms were analysed in the case of P1 and C5 hardfacings. Results showed that both under low-energy (AEW) and high-energy (AIW) conditions, the general wear process took place in two stages: firstly, destruction of the matrix and secondly, loss of loose WC-Co particles (Paper 4).

Under low-energy (AEW) conditions, the wear of FeCrSiB matrix is caused by microcutting at the low impact angle. The wear of WC-Co reinforcement occurred by the low-cycle fatigue mechanism both at low and high impact angles. In the case of unreinforced hardfacing (P1), wear included the stages of work hardening by the impacting particles, resulting in the formation and development of lateral cracks and, finally, spalling of flat fragments. One interesting observation was that the wear rate of the FeCrSiB matrix was more extensive in the composite hardfacings, and especially in the proximity of the reinforcing particles. The most likely reason is the thermally induced tensile stresses at the matrix-reinforcement interface, which favours the removal of the material (Paper 4).
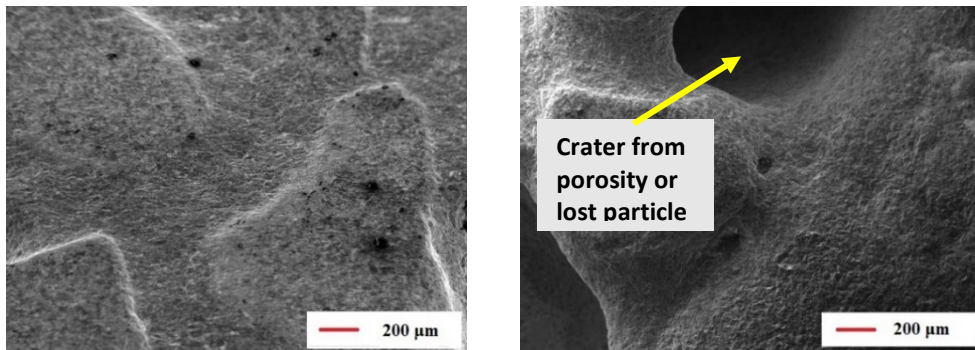
Figure 24. Worn surfaces of PM C5 hardfacing at AEW test, left image 30°, right image 90°.

Under high-energy (AIW) conditions, the wear mechanisms of the reinforcement were identical to those under the low-energy (AEW) conditions. However, the wear mechanism of FeCrSiB alloy was slightly different. In addition to the lateral cracks, median ones were seen (Paper 4). Therefore, the wear mechanism of the FeCrSiB matrix may be described as a combination of low-cycle fatigue and direct fracture. Similar to the abrasive erosive wear (AEW), the wear of the FeCrSiB matrix was higher in the case of the composite hardfacing for the same reasons (Paper 4).
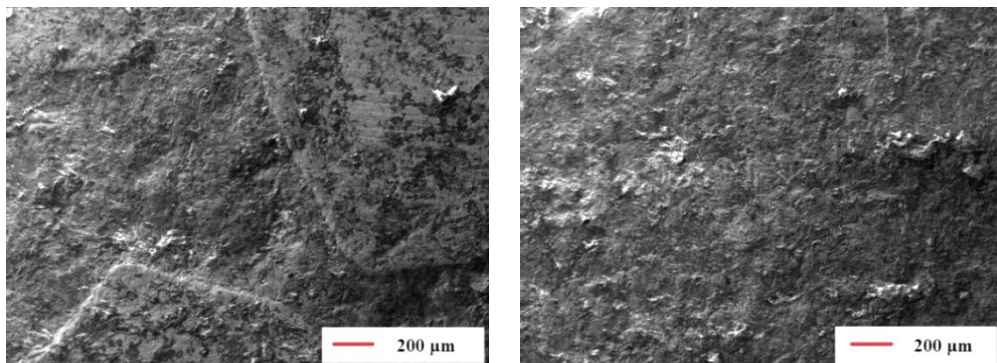

Figure 25. Worn surfaces of PM hardfacings at AIW test, C5 left, P1 right.

In AEW conditions, no instant correlation was found between porosity and fracture toughness on the wear rates of the hardfacings. Neither could any clear dependence of the wear rates on other parameters be found. Despite that, a higher elastic modulus should lead to lower wear by providing better resistance to penetration by the erodent particles, no such tendency was observed here.

In AIW conditions, impacting particles have higher kinetic energy. The latter causes a higher deformation rate, probably exceeding the elastic strain limit, especially in the case of the matrix FeCrBSi alloy. Therefore, the fracture toughness should become more important here than the hardness and modulus of elasticity.

Conclusions to section 4.3:
- The best wear behaviour in AEW was demonstrated by the composite coarse hardmetal containing hardfacing (C5), compared to the unreinforced hardfacing (P1), but an increase in the wear resistance is only about 2 times.
- In low energy (AEW) conditions, unreinforced hardfacings with high ductility are preferred and composite hardfacings should not be used in these conditions. In high

energy (AIW) conditions, composite hardfacings demonstrated very low wear resistance. Relative wear resistance decreased more than 10 times compared to unreinforced.

4.4 Recommendations for selection of hardfacings for specific wear conditions

Results of the abrasive wear resistance studies showed that hardfacings with coarse reinforcement have the best wear resistance compared to all other composite hardfacings in all wear conditions. Maximal effect of reinforcing of hardfacings with recycled coarse WC-Co hardmetal reinforcement was noticed at AWW conditions (increase in the wear resistance about 12-13 times, see Figs. 20 and 22). At the same time, as a result of reinforcing at ARWW and AEW, increase in the wear resistance was minimal (only 20 – 40%). Wear resistance of WC-Co hardmetal reinforced hardfacings at AIW was low.

For three-body abrasion conditions (ARWW), the pure self-fluxing alloy (FeCrSiB) based hardfacings are recommended because reinforcing with recycled hardmetal increases wear resistance only 20%. To compare with steel Hardox 400, relative wear resistance of self-fluxing alloy hardfacing (P1) is about 10 times higher. Compared to commercial wear plate CDP 112, the wear resistance of P1 is about 2 times higher. The best results were shown by hardfacings with spherical reinforcement, but from the economical point of view, they are not recommended.

In the following parts, wear resistance of Hardox 400 steel is compared with hardfacings because steel is the material we want to substitute in the wear applications with hardfacings. CDP 112 wear plate is compared to show differences between experimental hardfacings and commercial products.

Table 17. Relative wear resistance compared to Hardox 400 at ARWW

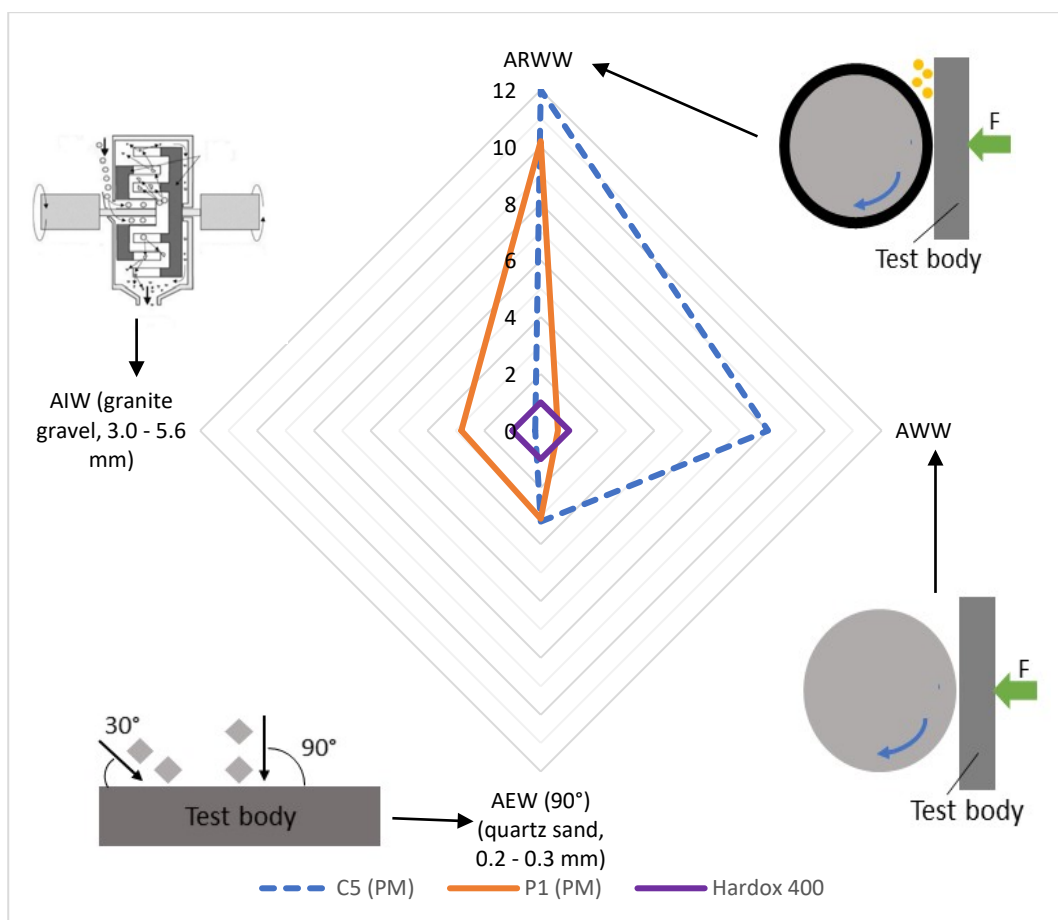| Designation	Wear rate, mm³/kg	Relative wear resistance to H400
P1	1.50	10.2
S5	0.78	19.6
C5	1.28	12.0
CDP	3.15	4.9
H400	15.33	1.0

Figure 22. Relative wear resistance of P1 and C5 compared to Hardox 400 in different wear conditions.

For two-body abrasion conditions, composite hardfacings reinforced with 50 vol% coarse angular hardmetal powder are recommended. Compared with steel Hardox 400, relative wear resistance of hardfacing C5 is about 8 times higher. Compared with commercial wear plate CDP 112, hardfacing C5 is about 1.5 times more wear resistant (Table 18). Commercial wear plate CDP 112 showed much better wear resistance in AWW testing conditions and was outmatched only by C4 and C5 hardfacings (Paper 2). Wear rate in AWW is given in volumetric units (mm^3) not in volume per kg abrasive (mm^3/kg) because no free abrasive exists in AWW test conditions.

Table 18. Relative wear resistance compared to Hardox 400 at AWW

Designation	Wear rate, mm^3	Relative wear resistance to H400
P1	6.15	0.6
C5	0.46	8.0
CDP	0.67	5.5
H400	3.66	1.0

For abrasive erosion wear at conditions where quartz sand is used ($H_{abrasive} > H_{matrix}$), hardfacings based on FeCrSiB self-fluxing alloy and recycled hardmetal reinforced hardfacings do not work (relative wear resistance is on the same level as steel Hardox 400) (Table 19). In conditions where softer abrasive is used ($H_{abrasive} < H_{matrix}$), self-fluxing alloy based hardfacings are recommended.

In AEW wear resistance of pure self-fluxing alloy hardfacing (P1) is about 3 times better than Hardox 400 steel when an abrasive with lower hardness is used.

Table 19. Relative wear resistance to Hardox 400 at AEW with different abrasives

Designation	Granite sand (900 – 950 HV)				Quartz sand (1000 – 1100 HV)	
	Wear rate, mm³/kg		Relative wear resistance to H400		Wear rate, mm³/kg	Relative wear resistance to H400
	30°	90°	30°	90°	30°	30°
P1	12.0	21.5	3.1	1.4	26.9	1.2
C5	11.7	15.5	3.2	1.9	30.2	1.1
CDP	-	-	-	-	27.6	1.2
H400	37.0	30.0	1.0	1.0	32.8	1.0

Abrasive velocity – 80 m/s

At high energy abrasive impact wear (AIW) wear conditions, similar to three-body abrasion wear, the pure FeCrSiB self-fluxing alloy based hardfacings are recommended only. Compared with steel Hardox 400, relative wear resistance of the abovementioned hardfacing is about 3 times higher compared to Hardox 400 and comparable with commercial wear plate CDP 112 (Table 20).

Table 20. Relative wear resistance to Hardox 400 at AIW

Designation	Wear rate, mm³/kg	Relative wear resistance to H400
P1	9.3	2.8
C5	108.6	0.2
CDP	8.2	3.2
H400	26.1	1.0

Table 21 shows conclusive information where tested composite hardfacings performed better compared to Hardox 400 (1), unreinforced hardfacing P1 (2), wear plate CDP 112 (3). If material was not compared in given conditions (-) is marked, when hardfacing performed worse compared to given material (0) is marked.

Table 21. Performance of composite hardfacings compared to reference materials

Designation	Technology	ARWW	Two-body abrasion		AEW		AIW
			AWW	AEMW	30°	90°	
C3	PM	1 2 3	1 2 0	- - -	- - -	1 2 -	0 0 -
C4	PM	1 0 3	1 2 0	- - -	- - -	- - -	- - -
C5	PM	1 2 3	1 2 3	- - -	1 2 -	1 2 -	0 0 0
S3	PM	- - -	- - -	- - -	- - -	1 2-	0 0 -
S5	PM	1 2 3	1 2 0	- - -	- - -	- - -	- - -
M5	PM	1 0 3	1 2 0	- - -	1 0 -	0 0 -	0 0 0
F5	PM	1 0 3	1 2 0	- - -	1 0 -	0 0 -	0 0 0

Table 22 shows conclusive information of the materials tested and the wear test conditions. Green marks that testing was done in the given conditions, red marks that testing was not done in these conditions. In the case of C5 and M5 it is also shown which technology produced the hardfacing used in the given test conditions.

Table 22. Hardfacings testing conditions

Designation	Technology	ARWW	Two-body abrasion		AEW		AIW
			AWW	AEMW	30°	90°	
P1	PM	green	green	red	green	green	green
C3	PM	green	green	red	red	green	green
C4	PM	green	green	red	red	red	red
C5	PM, PTAW	PM	PM, PTAW	PTAW	PM	PM	PM
S3	PM	red	red	red	red	green	green
S5	PM	green	green	red	red	red	red
M5	PM, PTAW	PM	PM, PTAW	red	PM	PM	PM
F5	PM	green	green	red	green	green	green
B1	SAW	red	green	green	red	red	red
B2	SAW	red	green	green	red	red	red
D	SAW	red	green	green	red	red	red
CDP112	Reference	green	green	red	green	green	green
Hardox 400	Reference	green	green	red	green	green	green

5. GENERAL CONCLUSIONS

Resulting from the studies of surfacing technologies (PM, PTAW and SAW), thick (> 2 mm) composite hardfacings based on recycled coarse (1.6 – 2.0 mm) hardmetal and FeCrSiB self-fluxing alloy powders were produced:

- PM technology enables production of hardfacings with high content of hardmetal reinforcement (in this thesis research up to 50 vol%, but higher amounts can be used) and variable hardness of the matrix (hardness increases with hardmetal reinforcement content).
- PTAW technology enables production of composite hardfacings with double-cemented structure – coarse composite ceramic-metallic (hardmetal) reinforcement (1.6 – 2 mm) in the iron-based matrix.
- Similarly to PTAW, SAW technology allows for the production of composite hardfacings with double-cemented structure with coarse hardmetal reinforcement. Wear performance of SAW hardfacings is comparable to PTAW hardfacing; the greatest difference is in the amount of dissolution of hardmetal particles, which is higher in the case of SAW hardfacings.

Based on the study of optimization of reinforcement parameters of MMC hardfacings for different abrasive wear applications, the following conclusions could be made:

- Angular reinforcement shows better wear resistance than spherical reinforcement, except in three-body abrasion (ARWW) conditions.
- In the three-body and two-body abrasion conditions, increasing hardmetal content in the hardfacing increases its wear resistance. In AEW and especially in AIW conditions, increasing the hardmetal content decreases the wear resistance of hardfacings.
- Coarse reinforcement (1.6 – 2.0 mm) usually performs better than fine (0.16 – 0.32 mm) and multisized reinforcement in all wear conditions compared.

Resulting from the studies of wear resistance and wear mechanisms of reinforced hardfacings at different abrasive wear conditions, the following main conclusions can be drawn:

- The best wear resistance is demonstrated by the hardfacing with coarse hardmetal reinforcement content of 50 vol% at the two-body abrasion (AWW) conditions – increase in the wear resistance is about 13 times compared to an unreinforced hardfacing.
- Wear resistance of composite hardmetal consisting hardfacings at free abrasive wear (where abrasive can move freely) conditions (ARWW, AEW, AIW) is low. Reinforcing increases the wear resistance by 10 – 20% only at ARWW, up to 2 times at AEW, while at AIW it decreases the wear resistance notably.
- The main wear mechanism at abrasion (ARWW, AWW) and low impact angle AEW is microcutting of the matrix and low-cycle fatigue of the matrix as well as reinforcement. At high impact angle AEW ($\alpha = 90°$) and impact wear (AIW), the wear mechanism dominating is the low-cycle fatigue of hardmetal reinforcement and direct fracture of the matrix material.

In the specific wear conditions, the following recommendations can be given for selection of hardfacings:

- At the three-body abrasion (ARWW), pure self-fluxing alloy based hardfacings are preferred as the reinforcement gives only marginal increase in the wear resistance and

does not justify the higher cost of these hardfacings.

- At the two-body abrasion (AWW, AEMW), composite hardfacings with coarse hardmetal reinforcement should be used. Optimal reinforcement content in the two-body abrasion seems to be around 50 vol% (within the range of tested materials).
- At the abrasive erosive wear (AEW) conditions, materials with the combination of high ductility and high hardness should be used. In AEW test conditions, the wear of C5 hardfacing was in the same range as the wear of unreinforced hardfacing; since the difference is small, it does not justify higher price of reinforced hardfacings.
- At the abrasive impact wear (AIW) conditions, materials with the combination of high ductility and high hardness should be used. In these conditions, best wear resistance was shown by unreinforced hardfacing and adding reinforcement decreases the wear resistance.

In the future, focus could be on the following studies:
- Commercialization of the PTAW surfacing technology: a) mechanization of the coarse reinforcement feeding process, and b) using slower cooling rate and additional tempering to reduce stresses in the structure and its effects on the structure
- Industrial testing of the proposed hardfacings.

REFERENCES

[1] Modern Surface Technology; F. -W. Bach; A. Laarmann; T. Wenz, (eds.), Wiley-VCH Verlag GmbH & Co. KGaA, Winheim, 2006

[2] H.-J. Kim, C.-H- Lee, S.-Y. Hwang. Superhard nano WC-12%Co coating by cold spray deposition. *Materials Science and Engineering A*, 2005, **391**(1-2), 243 – 248

[3] B. K. Reck, T. E. Graedel. Challenges in Metal Recycling, *Science*, 2012, **337**, 6095, 690 – 695

[4] M. Seddon, An Overview of Downstream Tungsten Markets. Argus Metal Pages Forum, 4th of August 2016, Tokyo: accessed 2017-10-05 at http://www.argusmedia.com/~/media/files/pdfs/regional-specific/jp/downloads/argus-metal-pages-forum-082016-tungsten.pdf?la=en

[5] T. Ishida, T. Itakura, H. Moriguchi, A. Ikegaya. Development of technologies for recycling cemented carbide scrap and reducing tungsten use in cemented carbide tools. *SEI Technical Review*, 2012, **75**, 38 – 46

[6] Tungsten: Global Industry, Markets & Outlook (Rockskill`s), accessed 2017-10-05 at: https://roskill.com/market-report/tungsten

[7] P. Kulu, S. Zimakov. Wear resistance of thermal sprayed hardfacings on the base of recycled hardmetal. *Surface and Hardfacings Technology*, 2000, **130**, 46 – 51

[8] P. Kulu, A. Surzhenkov, R. Tarbe, M. Viljus, M. Saarna, M. Tarraste. Hardfacings for extreme wear applications. *Proceedings of the 28th International Conference on Surface Modification Technologies*, Tampere, Finland, 16th – 18th of June 2014, 149 – 157

[9] Guide to Wear Problems and Testing for Industry, M. J. Neale, M. Gee, William Andrew Publishing LLC, 2001

[10] P. F. Mendez, N. Barnes, K. Bell, S. D. Borle, S. S. Gajapathi, S. D. Guest, H. Izadi, A. K. Gol, G. Wood. Welding processes for wear resistant overlays. *Journal of Manufacturing Processes*, 2014, **16**(1), 4 – 25

[11] R. Skirkus. *Reduction of wear and resistance to movement on soil tillage elements by modelling the geometrical parameters and strengthening surfaces with composite hardfacings*, PhD thesis, Aleksandras Stulginskis University, Akademija, 2017

[12] A. Misra, I. Finnie. A review of the abrasive wear of metals, *Journal of Engineering Materials and Technology*, 1982, **104**, 94 – 101

[13] *Surface Engineering for Corrosion and Wear Resistance*. J. R. Davis (ed.), ASM International, 2001

[14] ASM Handbook, Volume 8, *Mechanical Testing*, ASM International, Ohio, 2000

[15] I. Hussainova. On micromechanical problems of erosive wear of particle reinforced composites, *Proceedings of the Estonian Academy of Sciences*, 2005, **11**(1), 46 – 58

[16] A. Leyland, A. Matthews. On the significance of the H/E ratio in wear control: a nanocomposite coating approach to optimized tribological behaviour. *Wear*, 2000, **246**, 1 – 11

[17] D. L. Joslin, W. C. Oliver. A new method for analysing data from continuous depth-sensing microindendation tests. *Journal of Materials Research*, 1990, **5**(1), 123-126

[18] L. St-Georges. Development and characterization of composite Ni-Cr + WC laser cladding, *Wear*, 2007, **263**(1-6), 562 – 566

[19] J. Liu, S. Yang, W. Xia, X. Jiang, C. Gui. Microstructure and wear resistance performance of Cu-Ni-Mn alloy based hardfacing coatings reinforced by WC particles, *Journal of Alloys and Compounds*, 2016, **654**, 63 – 70

[20] Y. Xie, J. jiang, K. Y. Tufa, S. Yick. Wear resistance of materials used for slurry transport, *Wear*, 2015, **332-333**, 1104 – 1110

[21] B. S. Mann. High-energy impact wear resistance of hard hardfacings and their application in hydroturbines, *Wear*, 2000, **237**(1), 140 – 146

[22] J. Kübarsepp, H. Klaasen, J. Pirso. Behaviour of TiC-base cermets in different wear conditions, *Wear*, 2001, **249**(3-4), 229 – 234

[23] M. Lindroos, V. Ratia, M. Apostol, K. Valtonen, A. Laukkanen, W. Molnar, K. Holmberg, V-T. Kuokkola. The effect of impact conditions on the wear and deformation behaviour of wear resistant steels, *Wear*, 2015, **328-329**, 197 – 205

[24] P. Kulu, I. Hussainova, R. Veinthal. Solid particle erosion of thermal sprayed hardfacings, *Wear*, 2005, **258**(1-4), 488 – 496

[25] P. Kulu, T. Pihl. Selection criteria for wear resistant powder hardfacings under extreme erosive wear conditions, *Journal of Thermal Spray Technology*, 2002, **11**(4), 517 – 522

[26] A. Zikin, S. Ilo, P. Kulu, I. Hussainova, C. Katsich, E. Badisch. Plasma transferred ARC (PTA) hardfacing of recycled hardmetal reinforced nickel-matrix surface composites. *Materials Science (Medžiagotyra),* 2012, **18**(1), 12 – 17

[27] V. E. Buchanan. Solidification and microstructural characterization of iron-chromium based hardfaced coatings deposited by SMAW and electric arc spraying. *Surface and Coatings Technology*, 2009, **203**(23), 3638 – 3646

[28] *Handbook of Thermal Spray Technology*. J. R. Davis (ed.), ASM International, 2004

[29] F. Zhigang, J. A. Sue. Double cemented carbide composites, U.S. Patent no 5.880.382, 9. Mar 1999

[30] G. R. C. Pradeep, A. Ramesh, B. Durga. A review paper on hardfacing processes and materials. *International Journal of Engineering Science and Technology*, 2010, **2**(11), 6507 – 6510

[31] F. Otsubo, H. Era, K. Kishitake. Structure and phases in nickel-base self-fluxing alloy coating containing high chromium and boron. *Journal of Thermal Spray Technology*, 2000, **9**(1), 107 – 113

[32] O. M. Dubovyi, A. M. Stepanchuk. Coating technology by spraying. NUK, Mykolaiv, 2007 (in Ukrainian)

[33] W. Zhang, Z. Zhong, S. Kang. Microstructures and mechanical properties of a martensitic steel welded with flux-cored wires, *International Journal of Coal Science & Technology*, 2015, **2**(3), 254 – 260

[34] J. B. Wang, Y. F. Zhou, X. L. Xing, S. Liu, C. C. Zhao, Y. L. Yang, Q. X. Yang. The effect of nitrogen alloying to the microstructure and mechanical properties of martensitic stainless steel hardfacings, *Surface and Hardfacings Technology*, 2016, **294**, 115 – 121

[35] K. Simunovic, T. Saric, G. Simunovic, Different approaches to the investigation and testing of the Ni-based self-fluxing alloy hardfacings – A review. Part 1: general facts, wear and corrosion investigations, *Tribology Transactions*, 2014, **57**(6), 955 – 979

[36] I. N. Kravchenko, A. A. Kolomeychenko, D. M. Butenko, A. V. Kolomeichenko. Plasma spraying of self-fluxing alloys with a remote arc with melting of the hardfacing, *Welding International*, 2017, **31**(9), 722 – 724

[37] Q. Y. Hou. Influence of molybdenum on the microstructure and properties of a FeCrBSi alloy hardfacing deposited by plasma transferred arc hardfacing, *Surface and Hardfacings Technology*, 2013, **225**, 11 – 20

[38] G. Bolleli, B. Bonferroni, J. laurila, L. Lusvarghi, A. Milanti, K. Niemi, P. Vuoristo. Micromechanical properties and sliding wear behaviour of HVOF-sprayed Fe-based alloy coatings, *Wear*, 2012, **276-277**, 29 – 47

[39] A. Surzhenkov, D. Goljandin, R. Traksmaa, M. Viljus, K. Talviste, A. Aruniit, J. Latokartano, P. Kulu. High temperature erosion wear of cermet particles reinforced self-fluxing alloy HVOF sprayed coatings, *Materials Science (Medžiagotyra),* 2015, **21**(3), 386 – 390

[40] P. Kulu, J. Halling. Recycled and hard metal-base wear resistant composite coatings, *Journal of Thermal Spray Technology*, 1998, **7**(2), 173 – 178

[41] M. Riddihough. Stellite as wear-resistant material. *Tribology International*, 1970, **3**(4), 211 – 215

[42] J. Yao, Z. Li, B. Li, L. Yang. Characteristics and bonding behaviour of Stellite 6 alloy hardfacing processed with supersonic laser reposition, *Journal of Alloys and Compounds*, 2016, **661**, 526 – 534

[43] S. Apay, B. Gulenc. Wear properties of AISI 1015 steel coated with Stellite 6 by microlaser welding, *Materials & Design*, 2014, **55**, 1 – 8

[44] K. C. Antony. Wear-resistant cobalt-base alloys. *Journal of Metals*, 1983, **35**(2), 52 – 60

[45] J. Wang, T. Liu, Y. Zhou, X. Xing, S. Liu, Y. Yang, Q. Yang. Effect of nitrogen alloying on the microstructure and abrasive impact wear resistance of Fe-Cr-C-Ti-Nb hardfacing alloy, *Surface and Hardfacings Technology*, 2017, **309**, 1072 – 1080

[46] N. Yüksel, S.Sahin. Wear behaviour-hardness-microstructure relation of Fe-Cr-C and Fe-Cr-C-B based hardfacing alloys, *Materials & Design*, 2014, **58**, 491 – 498

[47] A. Zikin, M. Antonov, I. Hussainova, L. Katona, A. Gavrilović. High temperature wear of cermet particle reinforced NiCrBSi hardfacings, *Tribology International*, 2013, **68**, 45 – 55

[48] B. Venkatesh, K. Striker, VSV Prabhakar, Wear characteristics of hardfacing alloys: state-of-the-art, *Procedia Materials Science 10*, 2015, 527 – 532

[49] G. D. Nelson, G. L. F. Powell, V. M. Linton. Investigation of the wear resistance of high chromium white irons, *Proceedings of the 19th International Conference on surface Modification Technologies,* August 1-3, 2005, Minnesota, USA

[50] ASM Handbook, Volume 2, *Properties and Selection: Nonferrous Alloys and Special-Purpose Materials*, ASM International, Ohio, 1993

[51] C.C. Onuoha, C. Jin, Z. N. Farhat, J. Kipouros, K. P. Plucknett. The effects of TiC grain size and steel binder content on the reciprocating wear behaviour of TiC-316L stainless steel cermets, *Wear*, **350-351**, 116 – 129

[52] A. Rajabi, M. J. Ghazali, A. R. Daud. Chemical composition, microstructure and sintering temperature modifications on mechanical properties of TiC-based cermet – A review, *Materials & Design*, 2015, **67**, 95 – 100

[53] A. Rajabi, M.J. Ghazali, J. Syarif, A. R. Daud. Development and application of tool wear: A review of the characterization of TiC-based cermets with different binders, *Chemical Engineering Journal*, 2014, **255**, 445 – 452

[54] L. Janka, J. Norpoth, R. Trache, S. Thiele, L. M. Berger. HVOF- and HVAF-sprayed Cr_3C_2-NiCr hardfacings deposited from feedstock powders of spherical morphology: microstructure formation and high-stress abrasive wear resistance up to 800 °C, *Journal of Thermal Spray Technology*, 2017, **26**(7), 1720 – 1731

[55] C-C. Zang, Y-Z. Wang, Y-D. Zhang, J-H. Li, H. Zeng, D-Q. Zhang, Microstructure and wear-resistant properties of NiCr-Cr3C2 hardfacing with Ni45 transition layer produced by laser cladding, *Rare Metals*, 2015, **34**(7), 491 – 497

[56] S. Tang, D. Liu, P. Li, Y. Chen, X. Xiao. Formation of wear-resistant graded surfaces on titanium carbonitride-based cermets by microwave assisted nitriding sintering, *International Journal of Refractory Metals and Hard Materials*, 2015, **48**, 217 – 221

[57] E. Chicardi, Y. Torres, J. M. Córdoba, P. Hvizdoš, F. J. Cotor. Effect of tantalum content on the microstructure and mechanical behaviour of cermets based on $(Ti_xTa_{1-x})(C_{0.5}N_{0.5})$ solid solutions, *Materials & Design*, 2014, **53**, 435 – 444

[58] H. Wang, H. Li, H. Zhu, F. Cheng, D. Wang, Z. Li. A comparative study of plasma sprayed TiB_2-NiCr and Cr_3C_2-NiCr composite, *Materials Letters*, 2015, **153**, 110 – 113

[59] F. Yang, Y. Wu, J. Han, J. Meng, Microstructure, mechanical and tribological properties of Mo2FeB2 based cermets with Mn addition, *Journal of Alloys and Compounds*, 2016, **665**, 373 – 380

[60] B. Song, S. Dong, H. Liao, C. Coddet. Microstructure and wear resistance of $FeAl/Al_2O_3$ intermetallic composite hardfacing prepared by atmospheric plasma spraying, *Surface and Hardfacings Technology,* 2015, **268**, 24 – 29

[61] L. Singh, N. K. Grover, V. Chawla, J. S. Greval. Microstructure and characterization of detonation gun sprayed Al203 hardfacing, *Asian Journal of Engineering and Applied Technology*, 2016, **5**(1), 15 – 17

[62] L-M. Berger, Application of hardmetals as thermal spray coatings, *International Journal of Refractory Metals and Hard Materials*, 2015, **49**, 350 – 364

[63] K. Szymański, A. hernas, G. Moskal, H. Myalska. Thermally sprayed coatings resistant to erosion and corrosion for power plant boilers – A review, *Surface & Coatings Technologies*, 2015, **268**, 153 – 164

[64] Md. A. Islam, J. Jiang, Y. Xie, P. Fiala. Investigation of erosion-corrosion behaviour of (WTi)C based weld overlays, *Wear*, 2017, **390 – 391**, 155 – 165

[65] M. Qunshuang, L. Yaijang, W. Juan, L. Kun. Microstructure evaluation and growth control of ceramic particles in wide-band laser clad Ni60/WC composite hardfacings, *Materials & Design*, 2016, **92**, 897 – 905

[66] F. Weng, H. Yu, C. Chen, J. Liu, L. Zhao, J. Dai. Microstructure and property of composite hardfacings on titanium alloy deposited by laser cladding with Co42 + TiN mixed powders, *Journal of Alloys and Compounds*, 2016, **686**, 74 – 81

[67] A. K. Lakshminarayanan, C. S. Ramachandran, V. Balasubramanian. Feasibility of surface-coated friction stir welding tools to join AISI 304 grade austenitic stainless steel, *Defence Technology*, 2014, **10**(4), 360 – 370

[68] P. Kulu, H. Käerdi, A. Surzenkov, R. Tarbe, R. Veinthal, D. Goljandin, A. Zikin. Recycled hardmetal-based powder composite coatings: optimization of composition, structure and properties, *International Journal of Materials and Product Technology*, 2014, **49**(2-3), 180 – 202

[69] H. Sarjas, D. Goljandin, P. Kulu, V. Mikli, A. Surženkov, P. Vuoristo. Wear resistant thermal sprayed composite coatings based on iron self-fluxing alloy and recycled cermet powders, *Materials Science (Medžiagotyra),* 2012, **18**(1), 34 – 39

[70] ASM Handbook, Volume 5, *Surface Engineering*, ASM International, Ohio, 1994

[71] G. Hou, Y. An, X. Zhao, H. Zhou, J. Chen. Effect of alumina dispersion on oxidation behaviour as well as friction and wear behaviour of HVOF-sprayed CoCrAlYTaCSi hardfacing at elevated temperature up to 1000 °C, *Acta Materiala*, 2015, **95**, 164 – 175

[72] C. Karaoglani, H. Dikici, Y. Kucuk. Effects of heat treatment on adhesion strength of thermal barrier hardfacing systems, Eng*ineering Failure Analysis*, 2013, **32**, 16 – 22

[73] A. Surzhenkov, M. Antonov, D. Goljandin, P. Kulu, M. Viljus, R. Traksmaa, A. Mere. High-temperature erosion of Fe-based coatings reinforced with cermet particles, *Surface Engineering*, 2016, **32**(8), 624 – 630

[74] G. Bolelli, T. Börner, A. Milanti, L. Lusvarghi, J. Laurila, H. Koivuluoto, K. Niemi, P. Vuoristo. Tribological behaviour of HVOF- and HVAF-sprayed composite coatings based on Fe-ally+WC-12%Co, *Surface and Coatings Technology*, 2014, **248**, 104 – 112

[75] A. Surzhenkov, M. Antonov, D. Goljandin, T. Vilgo, V. Mikli, M. Viljus, P. Kulu. Sliding wear of TiC-NiMo and Cr3C2-Ni cermet particles reinforced FeCrSiB matrix HVOF sprayed coatings. *Estonian Journal of Engineering*, 2013, **19**(3), 203 – 210

[76] T. Terajima, F. Takeuchi, K. Nakata, S. Adachi, K. Nakashima, T. Igarashi. Composite coating containing WC/12Co cermet and Fe-based metallic glass deposited by high-velocity-oxy-fuel spraying. *Journal of Alloys and Compounds,* 2010, **504**, 288 – 291

[77] A. Surzhenkov, M. Antonov, V. Mikli, J. Latokartano, T. Vilgo, P. Kulu. Sliding wear resistance of HVOF sprayed self-fluxing alloy matrix cermet particles reinforced composite coatings

[78] A. Surzhenkov, J. Baroninš, M. Viljus, R. Traksmaa, P. Kulu. Sliding Wear of Composite Stainless Steel Hardfacing under Room and Elevated Temperature, Solid State Phenomena, 2017, **267**, 195 – 200

[79] X. H. Wang, Z. D. Zou, S. Y. Qu, S. L. Song. Microstructure and wear properties of Fe-based hardfacing coating reinforced by TiC particles. *Journal of Materials Processing Technology*, 2005, **168(1)**, 89 – 94

[80] ASM Handbook, Volume 6, *Welding, Brazing and Soldering*, ASM International, Ohio, 1993

[81] R. G. P. Kamaraj, M. Srinivasa, R. Bakshi. Hardfacing of AISI H13 tool steel with Stellite 21 alloy using cold metal transfer welding process, Surface and Hardfacings Technology, 2017, **326**(A), 63 – 71

[82] A. Zikin, I. Hussainova, C. Katsich, E. Badisch, C. Tomastik. Advanced chromium carbide-based hardfacings. *Surface & Coatings Technology*, 2012, **206**, 4270 – 4278
[83] R. Zahiri, R. Sundaramoorthy, P. Lysz, C. Subramanian. Hardfacing using ferro-alloy powder mixtures by submerged arc welding, *Surface and Hardfacings Technology*, 2014, **260**, 220 – 229

[84] M. Aghakhani, P. Naderian, Modeling and optimization of dilution in SAW in the presence of Cr_2O_3 nano-particles, *The International Journal of Advanced Manufacturing Technology*, 2015, **78**(9-12), 1665 – 1676

[85] R. Bendikiene, A. Ciuplys, L. Kavaliauskiene. Preparation and wear behaviour of steel turning tools surfaced using the submerged arc welding technique, *Proceedings of the Estonian Academy of Sciences*, 2016, **65**(2), 117 – 122

[86] P. Ambroza, R. Bendikiene, L. Kavaliauskiene. Submerged arc surfacing of structural steel using metals powder added to flux, *Proceedings of the 5th IASME/WSEAS Internatonal Conference on Heat Transfer, Thermal Engineering and Environment*, Greece, 2007, 184 – 187

[87] K. Yang, Z. X. Zhang, W. Q. Hu, Y. F. Bao, Y. F. Jiang. A new type of submerged-arc flux-cored wire used for hardfacing continuous casting rolls, *Journal of Iron and Steel Research, International*, 2011, **18**(11), 74 – 79

[88] S. H. Choo, C. K. Kim, K. Euh, S. Lee, J. Y. Jung, S. Ahn. Correlation of microstructure with the wear resistance and fracture toughness of hardfacing alloys reinforced with complex carbides, *Metallurgical and Materials Transactions, A*, 2000, **31**(12), 3041 – 3052

[89] R. Bendikiene, E. Pupelis. Application of surfaced cutters for machining of wood based materials. *Wood Research*, 2016, **61**(1), 155 – 162

[90] S-P. Lu, D-Y. Kwon, Y. Guo. Wear behaviour of WC/NiCrBSi(Co) composite coatings, *Wear*, 2003, **254**(5-6), 421 – 428

[91] A. Röttger, S. Weber, W. Theisen. Supersolidus liquid-phase sintering of ultrahigh-boron high-carbon steels for wear-protection applications, *Materials Science and Engineering: A*, 2012, **532**, 511 – 521

[92] J. M. Córdoba, E. Chicardi, F. J. Gotor. Liquid-phase sintering of Ti(C,N)-based cermets. The effects of binder nature and content on the solubility and wettability of hard ceramic phases, *Journal of Alloys and Compounds*, 2013, **559**, 34 – 38

[93] C. D. Opris, R. Liu, M. X. Yao, X. J. Wu. Development of Stellite alloy composites with sintering/HIPing technique for wear-resistant applications, *Materials & Design*, 2007, **28**(2), 581 – 591

[94] H. Berns, A. Saltykova, A. Röttger, D. Heger. Wear protection by Fe-B-C hard phases, *Steel Research International*, 2011, **82**(7), 786 – 794

[95] H. Berns, A. Saltykova. Wear resistance of in situ MMC produced by supersolidus liquid phase sintering (SLPS), *Wear*, 2009, **267**(11), 1791 – 1797

[96] H. Yu, W. Liu, Y. Zheng. Microstructure and mechanical properties of liquid phase sintered Mo2FeB2 based cermets. *Materials & Design*, 2011, **32**(6), 3521 – 3525

[97] H. Rojacz, M. Varga, H. Kerber, H. Winkelmann. Processing and wear of cast MMCs with cemented carbide scrap. *Journal of Materials Processing Technology*, 2014, **214**, 1285 – 1292

[98] T. Simson, P. Kulu, A. Surzenkov, R. Tarbe, M. Viljus, D. Goljandin. Optimization of reinforcement content of powder metallurgy hardfacings in abrasive wear conditions, *Proceedings of the Estonian Academy of Sciences*. 2016, **65**(2), 90 – 96

[99] D. Goljandin, Disintegrator milling systems development and Milling Technologies of Different Materials, PhD thesis, 2013

[100] Castolin Eutectic homepage, CDP112 wear plate data, https://www.castolin.com/product/cdp-112, 04.01.2018

[101] Nippon Steel & Sumikin Welding Co, Ltd homepage, accessed 14.12.2017 http://www.welding.nssmc.com/product/techniqueE.html

[102] K. G. Budinski "*Friction, Wear and Erosion Atlas*", CRC Press, Boca Raton, 2013

[103] D. K. Shetty, I. G. Wright. Indendation fracture of WCCo cermets. *Journal of Materials Sciences*. 1985, 20, 1873 – 1883

[104] A. Surzhenkov, R. Tarbe, M. Tarraste, T. Simson, M. Viljus, P. Kulu. Optimization of hardmetal reinforcement content in Fe-based hardfacings for abrasive-impact wear conditions. *Proceedings of European Conference of Heat Treatme*nt, 11.05 – 13.05.2016, Prague

[105] R. Tarbe, *Abrasive Impact Wear: Tester, Wear and Grindability Studies*. PhD Thesis. Tallinn University of Technology, 2009

[106] http://www.taylorspecialsteels.co.uk/pages/main/conchart.htm Vickers to Rockwell hardness conversion table, accessed 16.03.2018

[107] H. T. Liu, L. Z. Sun. Effects of thermal residual stresses on effective elastoplastic behaviour of metal matrix composites. *International Journal of Solids and Structures*, 2004, **41**(8), 2189 – 2203

[108] J. Pirso, M. Viljus, S. Letunovitš, K. Juhani, R. Joost. Three-body abrasive wear of cermets. *Wear*, 2011, **271**(11-12), 2868 – 2878

[109] J. Pirso, M. Viljus, K. Juhani, S. Letunovitš. Two-body dry abrasive wear of cermets. *Wear*, 2009, **266**(1-2), 21 – 29

ABSTARCT

Development of coarse recycled hardmetal reinforced hardfacings

Wear is a problem present in all sections of the industry and it is the main reason for material and economic losses. Severest problems occur in places where abrasive wear is encountered, such as mining, drilling and road maintenance. These problems are dealt with use of wear resistant coatings – hardfacings that improve the life time of a component or a machine part. However, many materials used for the production of hardfacings are either expensive or scarce (and their recycling rate is low). Therefore, it is necessary to find ways to use recycled hard materials for the production of new hardfacings. For that reason, a disintegrator milled hardmetal was chosen as reinforcement material for the hardfacings studied in this thesis.

Another important aspect is the production technologies of hardfacings. Suitable technologies should be cheap to use, have high productivity and able to use a wide variety of hardfacing materials. Different technologies can be compared by thermal spray technologies, such as HVOF, fusion technologies, such as PTAW and SAW, and bulk melting technologies, such as PM technology. However, for use of reinforcement with large particle sizes (> 1 mm), only fusion and bulk melting technologies are applicable, and for use of hardface complex components with large sizes, only fusion technologies suit. Therefore, from the production aspect, only PTAW and SAW technologies were compared.

To analyse the influence of recycled hardmetal reinforcement particle size, shape and content, different hardfacings were produced using the PM technology. These hardfacings contained different hardmetal reinforcement content, particle sizes and different particle shapes. Microstructure of these hardfacings was analysed by using SEM images of cross-sections of these hardfacings, also EDS and XRD analysis was performed where necessary. In addition, macrohardness and microhardness of both matrix and reinforcement were measured. PM hardfacings were used in all types of wear tests.

Wear testing of hardfacings was done by four different methods: three-body abrsasion (ARWW), two-body abrasion (AWW and AEMW), low-energy abrasion erosion wear (AEW), and high-energy abrasion impact wear (AIW). These methods should cover all possible scenarios that may occur during abrasive wear. PTAW and SAW hardfacings were tested only in the two-body abrasion as early tests showed that reinforcement gives no or little gain in three-body abrasion and in almost all cases in AEW and AIW is actually detrimental to wear resistance. First, wear testing results were compared with an unreinforced hardfacing and Hardox 400 steel, as well as with commercial wear plate CDP 112 (Castolon Eutectic®). Wear testing results showed that in the three-body abrasion, pure self-fluxing alloy hardfacings should be preferred as hardmetal reinforcement gives only a small gain and does not justify their higher price. In the two-body abrasion, hardfacings with coarse hardmetal reinforcement should be preferred. Optimal reinforcement content seems to be around 50 vol%. In AEW and AIW conditions, materials with the combination of high hardness and high ductility, such as pure self-fluxing alloy (FeCrSiB) or Hardox 400 steel, should be preferred.

From the production technology point of view, SAW hardfacings should have better wear resistance than PTAW hardfacings. In addition, SAW hardfacings had better surface quality than PTAW hardfacings. On the other hand, working-in period of PTAW hardfacings was faster than that of SAW hardfacings. If the wear plates are produced, then the PM technology can be used; in addition, the PM technology enables the best control over the process parameters during production.

KOKKUVÕTE

Taaskasutatava jämekõvasulamarmatuuriga kõvapinnete arendus

Kulumine on probleem, mis eksisteerib kõikjal tööstuses ning on peamiseks põhjuseks materjali- ja majanduslikele kadudele. Eriti suur on probleem kohtades, kus leiab aset abrasiivkulumine, näiteks kaevandamisel, pinnase teisaldamisel ja teehooldusel. Nende probleemidega saab võidelda, kasutades kulumiskindlaid kõvapindeid, mis aitavad tõsta detaili või konstruktsiooni eluiga. Mitmed materjalid aga, mida kasutatakse kõvapinnete tootmisel, on kas kallid või piiratud varudega. Seetõttu tuleb leida viise taaskasutatavate materjalide kasutamiseks uute kulumiskindlate kõvapinnete tootmisel. Sel põhjusel on uuritud antud töös kasutatud kõvasulami taaskasutust armatuurina komposiit-kõvapinnetes.

Teine oluline aspekt on kõvapinnete tootmistehnoloogiad. Sobilikud tehnoloogiad peaksid olema odavad kasutada, suure tootlikkusega ja võimega kasutada laia valikut pindematerjale. Kui vaadelda erinevaid pindamistehnoloogiaid, siis pihustustehnoloogiad (kiirleekpihustus), keevitus-tehnoloogiaid (plasmakaarkeevitus ja räbustikaarkeevitus) ning pealesulatustehnoloogiaid (vedelfaaspaagutus, jt) on sobilikud pinnete saamiseks. Kuid kui me soovime kasutada suure osakesete suurusega armatuuri (> 1 mm), siis jäävad valikusse vaid keevitus- ja pealesulatustehnoloogiad. Soovides aga saada pakse pindeid suuremõõtmelistel detailidel, on eelkõige sobilikud keevitustehnoloogiad. Sel põhjusel, tootmistehnoloogiate vaatenurgast, on antud töös vaatluse all vaid plasmakaarkeevituse ja räbustikaarkeevituse tehnoloogiaid.

Analüüsimaks taaskasutatava kõvasulami sisalduse, osakeste suuruse ja nende kuju mõju kõvapindele, toodeti erinevaid kõvapindeid vedelfaaspaagutuse abil. Saadud kõvapinded olid erineva kõvasulami sisaldusega, osakeste suuruse ja kujuga. Nende kõvapinnete mikrostruktuuri analüüsiti pinnete ristlihvidel skaneeriva elektronmikroskoopia (SEM) abil. Lisaks analüüsiti osasid pindeid elektronspektroskoopia (EDS) ja difraktsioonianalüüsi (XRD) abil. Samuti analüüsiti pinnete makrokõvadust ja maatriksi ning armatuuri mikrokõvadust.

Kõvapinnete kulutamiskatsed viidi läbi neljal erineval meetodil: vaba abrasiiviga abrasioon (kummiratta katse), fikseeritud abrasiiviga abrasioon (abrasiivketta ja liivapaberikatse), abrasiiv-erosioonkulumine ja abrasiiv-löökkulumine. Antud kulutamismeetodid peaks katma kõik võimalikud stsenaariumid, mis võivad esineda abrasiivkulumise tingimustes. Vedelfaaspaagutatud pindeid sai uuritud ka kõigis kulutamise tingimustes. Plasmakaarkeevitatud ja räbustikaarkeevitatud pindeid katsetati ainult fikseeritud abrasiiviga abrasiooni tingimustes, kuna varasemad testid näitasid, et armatuur ei anna olulist efekti vaba abrasiiviga abrasioonkulumise tingimustes ning pea kõigil juhtudel abrasiiv-erosioonkulumise ja abrasiiv-löökkulumise tingimustes pigem saavutatakse vastupidine mõju kulumiskindlusele. Kulutamiskatsete tulemusi võrreldi armeerimata kõvapindega, et vaadata, kas armeerimine annab soovitud efekti. Võimalikku tugevdamisefekti saavutamiseks võrreldi pindeid aga Hardox 400 terasega, sest kulumiskindlad terased on materjalid, mida soovitakse kaitsta või asendada kohtades, kus on nõutud suur kulumiskindlus. Lisaks võrreldi tulemusi kaubandusliku kulutamiskindlaplaadi CDP 112-ga, et vaadata, kas laboris toodetud taaskasutatavat kõvasulamit sisaldavad kõvapinded on konkurentsivõimelised tööstuslike toodetega või mitte.

Kulutamiskatsete tulemused näitasid, et vaba abrasiiviga abrasiooni korral tuleks eelistada puhast iseräbustuval sulamil (FeCrSiB) põhinevat pinnet, sest kõvasulam armatuur annab vaid marginaalse võidu kulumiskinduses ja ei õigusta seega selle kõrgemat hinda. Fikseeritud abrasiiviga abrasioonil tuleks eelistada jämeda kõvasulamarmatuuriga kõvapindeid. Optimaalne kõvasulami sisaldus on ligikaudu 50 mahuprotsenti. Abrasiiv-erosioonkulumise ja abrasiiv-löökkulumise tingimustes tuleks eelistada pindeid, millel on nii suur sitkus kui ka suur kõvadus,

seega mittearmeeritud pinded, nt. iseräbustuvast sulamist pindeid.

Tootmistehnoloogiate seisukohast vaadatuna näitasid räbustikaarkeevitatud pinded paremat kulumiskindlust võrrelduna plasmakaarkeevitatud pinnetega. Lisaks oli räbustikaarkeevitatud pinnetel parem pinnakvaliteet võrrelduna plasmakaarkeevitatud pinnetega. Teisest küljest vaadatuna oli plasmakaarkeevitatud pinnete sissetöötamisperiood lühem räbustikaarkeevitatud pinnetega võrreldes. Kulumiskindlate plaatide tootmisel on sobilikuim vedelfaaspaagutus, sest see võimaldab parimat kontrolli protsessi parameetrite üle tootmise käigus ja puuduvad piirangud kõvasulamarmatuuri osakeste koostise suhtes.

Acknowledgements

I would like to express my sincere gratitude to my supervisors professor emeritus Priit Kulu and teaching assistant Andrei Surženkov from the Department of Mechanical and Industrial Engineering of Tallinn University of Technology for their support and guidance. I appreciate their time spent and their patience all through my doctoral studies.

APPENDIX

PUBLICATION 1
T. Simson, P. Kulu, A. Surženkov, D. Goljandin, R. Tarbe, M. Tarraste, M. Viljus, Optimization of structure of hardmetal reinforced iron-based PM hardfacings for abrasive wear conditions, *Key Engineering Materials*, 2017, **721**, 351 – 355.

Optimization of structure of hardmetal reinforced iron-based PM hardfacings for abrasive wear conditions

Taavi Simson[1a*], Priit Kulu[1b], Andrei Surženkov[1c], Dmitri Goljandin[1d], Riho Tarbe[1e], Marek Tarraste[1f], Mart Viljus[2g]

[1]Department of Materials Engineering, Tallinn University of Technology, Ehitajate tee 5, 19086, Tallinn, Estonia
[2]Centre for Materials Research, Tallinn University of Technology, Ehitajate tee 5, 19086 Tallinn, Estonia
[a]taavi.simson@ttu.ee, [b]priit.kulu@ttu.ee, [c]andrei.surzenkov@ttu.ee, [d]dmitri.goljandin@ttu.ee, [e]riho.tarbe@ttu.ee, [f]marek.tarraste@ttu.ee, [g]mart.viljus@ttu.ee

ABSTRACT: This paper focuses on the influence of hardmetal reinforcement amount, shape and size on the abrasive wear resistance of composite iron self-fluxing alloy (FeCrSiB) based hardfacings produced by the powder metallurgy (PM) technology. First, the size of the reinforcement (1 – 2.5 mm) was fixed, but its shape (angular or spherical) and amount (0 – 50 vol%) were varied. Then the reinforcement shape (angular) and amount (50 vol%) were kept constant, while its size (0.16 – 0.315 mm fine reinforcement and 1 – 2.5 mm coarse reinforcement) and proportion of fine and coarse reinforcement (all fine, all coarse, half fine-half coarse) were varied. ASTM G65 abrasive rubber wheel wear test was applied to find out the wear resistance of the hardfacings; an unreinforced self-luxing alloy (FeCrSiB) hardfacing was the reference material. Volumetric wear rate was calculated according to the weight loss. Worn surfaces were studied under scanning electron microscope. As a result, an optimal composition of the hardmetal containing Fe-based hardfacings based on the reinforcement amount (vol%), shape (irregular or spherical) and size (fine or coarse) is given.

Keywords: hardfacing, hardmetal reinforcement, powder metallurgy, twomodal reinforcement, abrasive wear

1. INTRODUCTION

WC-Co hardmetal has higher ductility than other cermets, which makes it particularly useful in hardfacings [1]. Hardfacings containing hardmetal hardphase have proven to exhibit excellent wear resistance in abrasive wear conditions [2]. Hardfacings containing coarse hardmetal reinforcement have been found to show higher wear resistance [3].

Composite hardfacings can be produced by different means: thermal spray [4], cladding [5], casting [6], and powder metallurgy (PM) technology [7]. Latter can be used if coarse reinforcement is needed.

Previous research has focused on the influence of size [3] and content [7] of hardmetal reinforcement in the composite hardfacings on the wear resistance. To our best knowledge, neither the influence of coarse particle shape on wear resistance, nor the influence of twomodal reinforcement size composition have been studied in detail. Therefore, this paper focuses on the morphology of the hardmetal reinforcement [8] and the influence of the shape of reinforcement on abrasive wear resistance. In our study, hardfacings with different reinforcement shapes (angular and spherical) and particle sizes (fine, coarse and twomodal) produced by powder metallurgy (PM) technology were analyzed in abrasive wear conditions.

2. EXPERIMENTAL

2.1. Materials and production of hardfacings

To produce the hardfacings, experimental disintegrator milled recycled angular WC-Co hardmetal powder with 12 – 20 vol% cobalt binder content as reinforcement and commercial Fe-based self-fluxing alloy powder (Höganas AB, 6 AB) as matrix were used. Composition of the hardfacings is given in Table 1.

Spherical hardmetal WC-Co reinforcement from Wansheng Cemented Carbide Ltd was used for comparison with angular reinforcement in abrasive wear tests.

A layer of hardmetal and self-fluxing alloy powder mixture on a steel S235 substrate (wt%: 0.17 C, 1.40 Mn, 0.55 C, 0.025 P, 0.025 S, 0.012 N, bal Fe) was subjected to vacuum pressureless sintering at 1100 ℃ for 30 min. Based on previous experiments, these process parameters have been found optimal.

As a result, the self-fluxing alloy melts down, but surrounded hardmetal particles remain unmolten. During cooling down and solidification, a hardfacing with hardmetal reinforcement and self-fluxing alloy matrix is formed. Thickness of the hardfacings obtained was about 3.5 mm.

Table. 1: Composition of hardfacings					
Designation	Composition, [vol%]	Reinforcement shape	Reinforcement size, [mm]	Density ρ, [mg/mm^3]	Porosity[c]
P1	100 FeCrSiB[a]	-	-	7.4	Low
R3	30 WC-Co + FeCrSiB[a]	Angular	1 – 2.5	9.6	Medium
R4	40 WC-Co + FeCrSiB[a]	Angular	1 – 2.5	10.3	Medium
R5	50 WC-Co + FeCrSiB[a]	Angular	1 – 2.5	11.04	Medium
F5	50 WC-Co + FeCrSiB[a]	Angular	0.16 – 0.315	11.04	High
C5	50 (25+25) WC-Co + FeCrSiB[a]	Angular	0.16 – 0.315 1 – 2.5	11.04	High
S5	50 WC-Co[b] + FeCrSiB[a]	Spherical	Ø 2.8	11.04	Medium

[a] 6 AB from Höganäs AB, with 15 – 53 μm particle size ; 13.7 Cr, 2.7 Si, 3.4 B, 6.0 Ni, 2.1 C, bal Fe
[b] Commercial spherical WC-Co, Wansheng Cemented Carbide Ltd.
[c] Low – under 5%, medium – 5 – 10%, high – over 10%

2.2. Characterization of hardfacings

Vickers macrohardness HV30 (load 298 N) was measured to find the surface hardness and microhardness HV0.3 (load 2.98 N) was measured at the polished cross-section of the hardfacings. Hardness results were based on ten tests on each specimen.

The microstructure of the produced hardfacings was analyzed using scanning electron microscope (SEM) EVO MA-15 (Carl-Zeiss). In addition, the distribution of chemical elements in the hardfacings was found out using energy dispersive X-ray spectroscopy (EDS).

2.3. Abrasive wear testing

Abrasive rubber wheel wear (ARWW) test according to the standard ASTM G65 was used to determine the wear resistance of produced hardfacings. Quartz sand (1000 – 1100 HV) with a particle size of 0.2 – 0.3 mm was used as an abrasive.

Test parameters are presented in Table. 2. In each test, three specimens were used.

Weight loss was measured after each test and volumetric wear rate (mm^3/kg) was calculated. Test results were compared to pure self-fluxing iron-based alloy (6 AB, Höganäs AB) and relative wear resistance ε was calculated as the ratio of volumetric wear rate of the reference material (P1) and a studied hardfacing.

Table. 2: Abrasive wear test parameters			
Type of wear test	Velocity, [m/s]	Quantity of abrading material, [kg]	Impact angle,[°]
Abrasive rubber wheel wear (ARWW)	2.4	3.75	0

3. RESULTS AND DISCUSSION

3.1 Microstructure and hardness of hardfacings

Our study of the microstructure showed that all the hardfacings containing WC-Co reinforcement exhibited pores and cracks in the structure, independent of the size or shape of the reinforcement (Fig. 1). The amount of cracks and pores decreased with the decreasing hardmetal content (R3, R4). These cracks are caused by different thermal expansion coefficients of WC-Co reinforcement and iron-based self-fluxing alloy matrix. Coefficients of thermal expansion are $5 \cdot 10^{-6}$ 1/K in the case of hardmetal and $16.1 \cdot 10^{-6}$ 1/K in the case of iron-based alloy; the difference is more than three times [9].
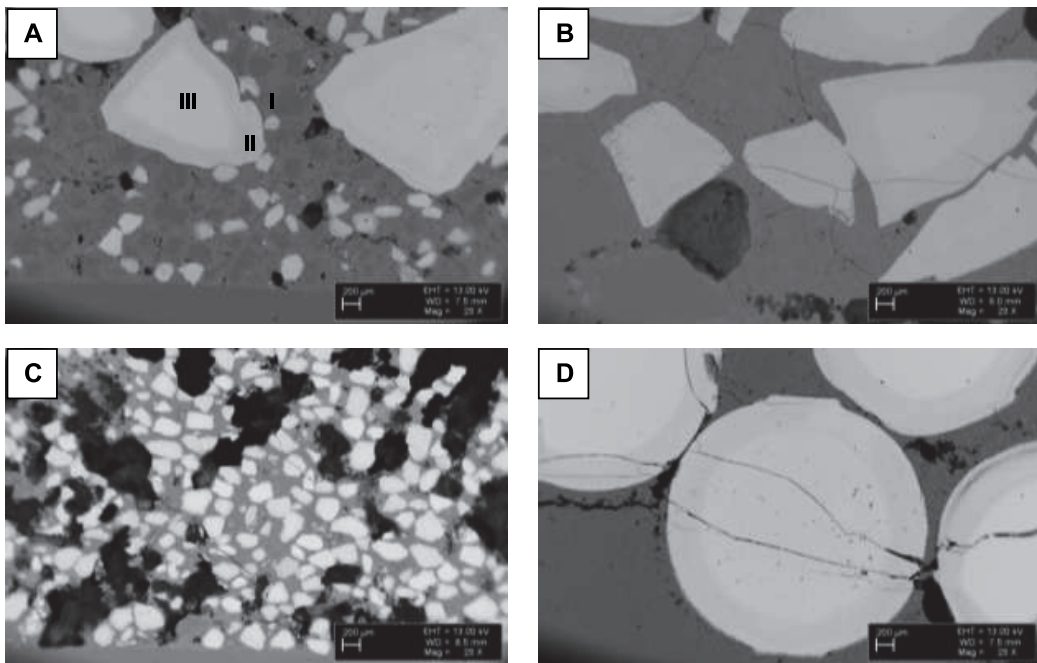
Fig. 1: Microstructure on 50 vol% WC-Co reinforced hardfacings. 20x magnification. A) C5, B) R5, C) F5, D) S5, dark grey represents the matrix, light grey - reinforcement particles and black - porosity.
Zones in the microstructure: I – dissolution- reprecipitation zone, II – dissolution zone, III – core zone.

Porosity of a hardfacing containing fine reinforcement can be caused by a higher amount of moisture and impurities due to a larger specific surface area of reinforcement powder compared to hardfacings containing coarse hardmetal; hardfacings containing fine reinforcement had much higher porosity (Fig. 1, C).
All hardfacings exhibited three zones in the structure (Fig. 1, A): dissolution-reprecipitation zone in the matrix (I), dissolution zone in reinforcement (II) and hardmetal core zone (III). Similar zones were reported in previous research also [21].
Zone I contains micrometrical grains of primary WC, which became loose during the sintering process due to the dissolution of the cobalt binder. These grains are embedded in the reprecipitated

iron, chromium and tungsten carbides. In zone II, cobalt binder is partially replaced by iron, and on a smaller scale, by nickel and chromium due to interdiffusion between the matrix and reinforcement. In zone III, the inital hardmetal structure is preseved.

Surface macrohardness measurements are presented in Table. 3. A hardfacing based on pure iron-based self-fluxing alloy (P1) showed minimal fluctuation in hardness results. Average macrohardness of a hardfacing using 50 vol% fine hardmetal reinforcement (F5) was lower than that of the pure iron-based self-fluxing alloy hardfacing. This can be explained by the high porosity of the hardfacing. (Fig. 1, C).

Hardfacing with twomodal reinforcement (C5) using 25 vol% of fine and 25 vol% of coarse angular WC-Co reinforcements showed very high average macrohardness results. The reason can be that the indentor touched the WC-Co hardphase most of the time and when using both coarse and fine reinforcement, the surface area of the hardphase on the hardfacing surface is high.

Hardfacings consisting of 50 vol% coarse angular reinforcement (R5) or 50 vol% coarse spherical reinforcement (S5) showed similar macrohardness results, both average and fluctuation were close. Even though average hardness values of R5 were higher than those of S5, hardfacings containing spherical reinforcement (S5) performed better in the ARWW test.

Table. 3: Hardness of hardfacings			
Designation	Macrohardness, HV30	Microhardness, HV0.3	
		Matrix	Reinforcement
P1	868 ± 28	1035 ± 70	-
F5	830 ± 161	900 ± 90	1444 ± 136
C5	1714 ± 296	817 ± 63	1482 ± 126
S5	1161 ± 420	950 ± 107	1637 ± 117
R5	1260 ± 436	1005 ± 41	1856 ± 67
R4	1154 ± 351	1047 ± 68	1911 ± 135
R3	1098 ± 308	978 ± 54	1912 ± 97

3.2 Abrasive wear resistance

The results of the ARWW test are given in Table 4 and Fig. 2. Higher wear rate of hardfacings with fine reinforcement (F5 and C5) can be attributed to higher porosity (Fig. 1, A and C) of these hardfacings.

As it follows from Fig. 2, coarse hardmetal reinforcement containing hardfacings (R5 and S5) performed better than the pure self-fluxing alloy based hardfacing P1. The wear resistance of hardfacing with spherical reinforcement (S5), in turn, was almost twice higher than that of a hardfacing with angular reinforcement (R5). The reason might be in the shape factor, in hardfacings with spherical reinforcement, the residual stresses are spread more equally in different directions [10]. The quality of the hardmetal used can also play a role.

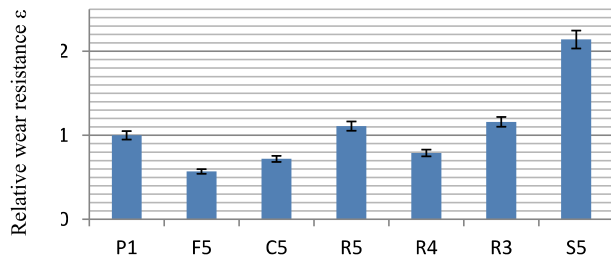| Table. 4: ARWW test results	
Designation	Wear rate, [mm^3/kg]
P1	1.67
F5	2.91
C5	2.31
S5	0.78
R5	1.51
R4	2.10
R3	1.43

Fig. 2: Relative wear resistance ε of hardfacings at the ARWW test.

4. CONCLUSIONS

It was demonstrated that the iron self-fluxing alloy based hardfacings produced by the PM technology with hardmetal reinforcement have considerable porosity and cracks due to the different coefficients of thermal expansion of the components.

Based on the results of abrasive wear tests, the following conclusions can be made:

- In ARWW test, hardfacings containing coarse reinforcement showed better wear resitance than hardfacings containing fine or twomodal reinforcement; their relative wear reistance compared to the pure self-fluxing alloy based hardfacings was lower in both cases. Hardfacings with spherical coarse reinforcement performed better than those with angular coarse reinforcement.
- Low wear resistance of hardfacings with fine and twomodal reinforcements can be mostly attributed to high porosity (higher compared to hardfacings with coarse reinforcement) and their defective structure (cracks, residual stresses).
- Regarding the composition, the best results were achieved with coarse reinforcement and spherical in shape. An optimal amount of reinforcement can be estimated to be in the range of 30 to 50 vol% in the wear conditions studied.

REFERENCES
[1] P. Kulu, J. Halling, Recycled hard metal-base wear resistant composite coatings, J. Therm. Spray. Techn., 7 (1998) 173-178.
[2] P. Kulu, R. Tarbe, A. Žikin, H. Sarjas, A. Surženkov, Abrasive wear resistance of recycled hardmetal reinforced thick coating. Key. Eng. Mat., 527 (2013) 185-190.
[3] P. Kulu, A. Surzhenkov, R. Tarbe, M. Viljus, M. Saarna, M. Tarraste, Hardfacings for abrasive wear applications. Proc. 28th Int. Conf. Surface Modification Technologies, Tampere, Finland, 16-18th of June 2014, 149-157.
[4] H. Sarjas, D. Goljandin, P. Kulu, V. Mikli, A. Surženkov, P. Vuoristo, Wear resistant thermal sprayed composite coatings based on iron self-fluxing alloy and recycled cermet powders. Mater. Sci-Medzg 18 (2012) 34-39.
[5] A. Zikin, I. Sotiraq, P. Kulu, I. Hussainova, C. Katsich, E. Badisch, Plasma Transferred Arc (PTA) hardfacing of recycled hardmetal reinforced nickel-matrix surface composites. Mater Sci-Medzg 18 (2012) 12-17.
[6] H. Rojacz, M. Varga, H. Kerber, H. Winkelmann, Processing and wear of cast MMCs with cemented carbide scrap. J. Mater. Process. Tech. 214 (2014) 1285-1292.
[7] T. Simson, P. Kulu, A. Surženkov, R. Tarbe, M. Viljus, M. Tarraste, D. Goljandin, Optimization of reinforcement content of powder metallurgy hardfacings in abrasive wear conditions. Proc. Estonian Acad. Sci. 65 (2016) 90-96.
[8] V. Mikli, H. Käerdi, P. Kulu, M. Besterci, Characterization of powder particle morphology. Proc. Estonian Acad. Sci. Eng. 7 (2001) 22-34.
[9] Mechanical and Metal Trades Handbook (Estonian translation), TUT Press, 2012, 116-117
[10] I. Hussainova, On micromechanical problems of erosive wear of particle reinforced composites, Proc. Estonian Acad. Sci. Eng. 11 (2005) 47-58.

PUBLICATION 2
T. Simson, P. Kulu, A. Surženkov, R. Tarbe, D. Goljandin, M. Tarraste, M. Viljus, R. Traksmaa, Wear resistance of sintered composite hardfacings under different abrasive wear conditions. *Materials Science (Medžiagotyra)*, 2017, **23**(3), 249 – 253.

Wear Resistance of Sintered Composite Hardfacings under Different Abrasive Wear Conditions

Taavi SIMSON *, **Priit KULU, Andrei SURŽENKOV, Riho TARBE, Dmitri GOLJANDIN, Marek TARRASTE, Mart VILJUS, Rainer TRAKSMAA**

Department of Mechanical and Industrial Engineering, Tallinn University of Technology, Ehitajate tee 5, 19086 Tallinn

The article focuses on vacuum liquid phase sintered (PM) composite hardfacings and their behaviour under different abrasive wear conditions. Hardfacings studied contained 30 – 50 vol % fine, coarse or multimodal (fine and coarse) hardmetal reinforcement. For wear resistance studies, we used the Abrasive Rubber Wheel Wear (ARWW) test as a three-body abrasive wear test, the Abrasive Wheel Wear (AWW) test as a two-body abrasive wear test and the Abrasive-Impact Erosion wear (AIEW) test as an abrasive-erosive wear test. Tested materials were compared to Hardox 400 steel and CDP112 wear plate (Castolin Eutectic® Ltd.). It was found that under three-body abrasion conditions (ARWW test) hardfacings with high content of spherical coarse reinforcement are suitable; their wear resistance is about two times higher than that of unreinforced hardfacings. Under two-body abrasive wear (AWW test), hardfacings with a high content of coarse reinforcement are recommended; their wear resistance is up to eight times higher than that of unreinforced hardfacings from the figures and graphs mentioned in the text. Under abrasive-erosive wear (AIEW test), unreinforced ductile materials are recommended; they have two to three times higher wear resistance than composite hardfacings reinforced with fine or multimodal reinforcement.

Keywords: hardfacing, powder metallurgy, abrasive wear, impact erosion.

1. INTRODUCTION

Hardmetal reinforced composite hardfacings provide efficient protection under different abrasive wear conditions [1, 2]. Hardfacings containing coarse hardmetal reinforcment have been found particularly effective [3]. However, because of tungsten content and mining of it, hardmetals have impact on the environment; in addition, their price is increasing. Therefore, the aim is to find ways of recycling or reuse of hardmetal scrap [4]. Use of recycled industrial hardmetal waste has been studied in [5] as well.

Many scientists have studied composite hardfacings with Ni, Co and Fe based matrixes [6 – 8]. Fe-based composite hardfacings are favoured due to their low price [9, 10].

Vacuum liquid phase sintering (PM technology) [3], plasma transferred arc welding (PTA) [11] and submerged arc welding (SAW) [12] have been proven to suit for production of those hardfacings. PM technology is safer for the operator, because of no ozone formation and UV radiation. Furthermore, no local deformation is caused by local heating; in PM technology all parts are heated equally.

Our previous research has focused on the effect of recycled hardmetal content in hardfacings [13] and on the effect of particle size and shape [14] on the wear resistance. Our findings indicate that the best results can be obtained with 30-50 vol% coarse reinforcement content [13].

In this paper, focus is on the behaviour of composite hardfacings in wear conditions, with loose abrasive (analysed by the ARWW and AIEW test) and fixed abrasive (analysed by the AWW test). Results are compared to commercial materials (CDP 112 wear plate, Hardox 400 steel). Hardox 400 is chosen as reference material because it is common material in wear resistant steel structures such as jaw crusher or ball mills. CDP 112 is chosen as reference material so experimental hardfacings could be compared to existing commercial product.

Based on the results, conditions for use of composite hardfacings are specified and recommended. This research was conducted because to the authors` best knowledge, no studies have reported comparisons of hardfacings with coarse recycled hardmetal reinforcement in different abrasion conditions.

2. EXPERIMENTAL

2.1. Feedstock materials and manufacturing of hardfacings

Recycled (disintegrator milled) WC-Co hardmetal powder with fine and coarse fractions and commercial WC-Co sintered spherical hardmetal as reinforcement and commercial iron-based self-fluxing alloy powder as matrix were chosen as feedstock materials to produce the hardfacings (see Table 1). Disintegrator milled hardmetal particles were angular in shape and had size of 0.16 to 0.31 mm (fine fraction) and 1.6 to 2.0 mm (coarse fraction). Commercial spherical hardmetal had a diameter of 2.8 mm.

The layer of powder mixtures was layed on steel S235 (wt.%: 0.17 C, 1.40 Mn, 0.55 Cu, 0.025 P, 0.012 N, bal Fe) substrate and subjected to sintering in vacuum at 1100 °C

---

* Corresponding author. Tel.: + 372 58 208 242.
E-mail address: *taavi.simson@ttu.ee* (T. Simson)

for 30 min. Based on previous experiments [3], these parameters have been found to be optimal.

During the sintering process, self-fluxing alloy powder particles melt, while hardmetal particles remain unmelted. Melted self-fluxing alloy surrounds hardmetal particles and during cooling composite hardfacing is formed.

2.2. Abrasive wear testing

Three different wear testing methods were used to compare the wear resistance of produced hardfacings in wear conditions with a loose and fixed abrasive.

First, abrasive rubber wheel wear (ARWW) was used according to ASTM G65 [16] standard, other methods were experimental abrasive wheel wear (AWW) test [17], developed in Tallinn University of Technology, and abrasive-impact erosion wear (AIEW) test according to GOST 23-201-78 standard [18].

Table 1. Composition of hardfacings

Designation	Composition, vol %	Reinforcement size, mm
P1	100 FeCrSiB[b]	-
C3	30 WC-Co [a], 70 FeCrSiB [b]	$1.6-2.0$
C4	40 WC-Co [a], 60 FeCrSiB [b]	$1.6-2.0$
C5	50 WC-Co [a], 50 FeCrSiB [b]	$1.6-2.0$
S5	50 WC-Co [d], 50 FeCrSiB [b]	$d-2.8$
M5	50 WC-Co [a], 50 FeCrSiB [b]	$0.16-0.31/1.6-2.0$
F5	50 WC-Co [a], 50 FeCrSiB [b]	$0.16-0.31$
CDP [e]	35 WC, 65 NiCrSiB (wt.%)	$-$
H400	Steel [c]	$-$

[a] Experimental, from waste hardmetal
[b] 6 AB from Höganäs AB, with $+15-53$ μm particle size; 13.7 Cr, 2.7 Si, 3.4 B, 6.0 Ni, 2.1 C, bal Fe.
[c] Hardox 400 steel, 0.32 C, 0.70 Si, 1.60 Mn, 0.025 P, 0.010 S, 1.40 Cr, 0.60 Mo, 0.004 B, bal Fe
[d] Commercial WC-Co, Wansheng Cemented Carbide Ltd.
[e] Wear plate CDP 112, Castolin Eutectic® Ltd. [15]

Test results of abrasive rubber wheel wear (ARWW) show how composite hardfacings perform under abrasion with loose abrasive. It can be viewed as three-body abrasion.

Abrasive wheel wear (AWW) method is basically a testbody against a grinding wheel. This test shows how hardfacings perform under abrasion with fixed abrasive. AWW test can also be viewed as two-body abrasion.

Table 2. Parameters of wear tests

Test	Parameter
ARWW	Velocity -2.4 m/s, duration -10 min, abrasive $-$ silica sand, particle size 0.2 $-$ 0.3 mm, hardness $1000-1100$ HV, distance 1440 m, quantity of abrasive -3.75 kg
AWW	Velocity -2.4 m/s, duration -10 min, no free abrasive, distance 1440 m, abrasive $-$ SiC, particle size $600-800$ μm, wheel hardness 35 HRC
AIEW	Velocity -80 m/s, impact angle 30°, abrasive $-$ silica sand, partcile size 0.2 $-$ 0.3 mm, quantity of abrasive -6 kg

Abrasive-impact erosion wear (AIEW) test, similar to the ARWW test, uses loose abrasive but it can-not be viewed as three-body abrasion because except for the kinetic energy of impacting particles, no added force is acting upon testbodies.

Parameters of the ARWW and AWW (Table 2) were chosen as similar as possible such that the results could be compared. AIEW test parameters are presented in Table 2.

2.3. Characterization of hardfacings

Vickers macro- and microhardness of hardfacings were measured. Macrohardness HV30 (298 N) was measured to find the surface hardness and microhardness HV0.3 (2.98 N) was measured to find the matrix and hardphase microhardnesses separately. Results of hardness measurements are presented in Table 3.

Microstructures of received hardfacings were studied under scanning electron microscope (SEM) EVO MA-15 from Carl-Zeiss and using XRD analysis of C5 material.

3. RESULTS AND DISCUSSION

3.1. Analysis of hardfacings microstructure

SEM image of C5 in Fig. 1, S5 in Fig. 2, F5 in Fig. 3 and M5 in Fig. 4. Structures of C3 and C4 are simillar to C5 and therefore their SEM images are not given.

Hardfacings are characterized by cracks shown in Fig. 1 $-$ Fig. 4.
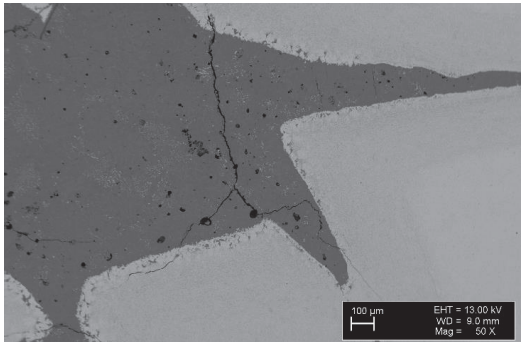

Fig. 1. SEM image of microstructure of C5: I $-$ dissolution-percipitation zone; II $-$ diffusion zone; III $-$ core zone of hardmetal particle
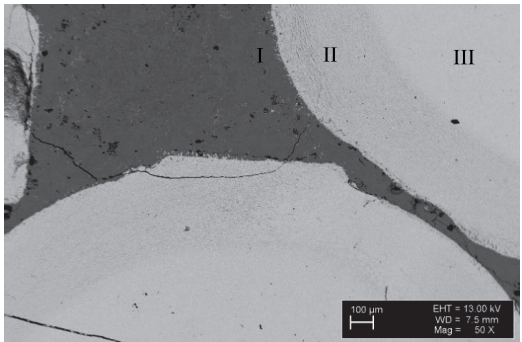

Fig. 2. SEM image of microstructure of S5

They are caused by different thermal expansion coefficients of FeCrSiB matrix and hardmetal reinforcement [3]. Hardfacings containing finer reinforce-ment (Fig. 3, Fig. 4) have higher porosity. Porosity is most likely to be caused by entrapped moisture as well as by different

shrinkage of the components [19]. Most of the pores, those that are large and uneven in shape, are shrinkage pores. Small and round pores are caused by moisture evaporation [3]. In Fig. 1, Fig. 2 and Fig. 4, dark and lighter gray areas can be seen on hardmetal particles (pointed out in Fig. 1). These areas represent different zones in the contact area of the matrix and hardmetal particles. In zone (I), dissolution of cobalt and WC into a matrix and formation of new carbides takes place. This is caused by reactions between self-fluxing alloy and carbides and cobalt, due to corrosive nature of molten matrix material. In diffuson zone (II), Co is substituted by iron from the matrix. Size of diffusion zone is dependant on sintering temperature and time, the bigger the heat input, the larger the diffusion zone. Temperature in the diffusion zone is not high enough to cause the dissolution of WC, but is high enough to cause cobalt difusion. This is why sintering temperature is chosen high enough to cause matrix melting but low enough to avoid to big diffusion zone. No changes take place in the core zone (III). This is due to fact that temperature in core zone is not high enough to cause any changes to hardmetal.

XRD analysis showed that new carbides form during sintering process. Most noticeable were Fe_5C_2 and $Fe_{23}C_6$. Phases formed due to dissolution of hardmetal were $Cr_{0.04}Fe_{0.955}$, WcoB and $Cr_{2.4}W_{0.6}B4$ and CrB.
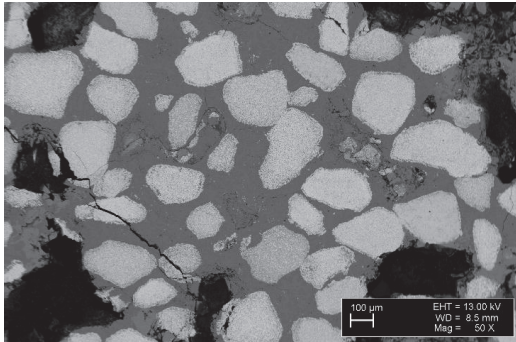

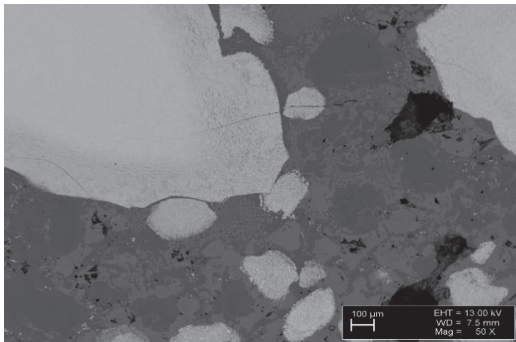**Fig. 3.** SEM image of microstructure of F5

Fig. 4. SEM image of microstructure of M5

3.2. Analysis of hardness measurements

Results of materials hardness are presented in Table 3. Hardfacings with smaller reinforcement content have lower macrohardness. Hardfacings reinforced with fine or

multimodal reinforcement also have lower macrohardness. Differences in reinforcement microhardness are caused by different cobalt binder content in hardmetal scrap used. Porosity influences microhardness of the matrix (F5 and M5) and to some extent macrohardness. There in no large difference in the microhardness values of reinforcement in the case of commercial and recycled hardmetal.

Table 3. Hardness of studied materials

Designation	Macrohardness, HV30	Microhardness, HV0.3	
		Matrix	Reinforcement
P1	868 ± 28	1035 ± 70	–
C3	1098 ± 308	978 ± 54	1444 ± 136
C4	1154 ± 351	1047 ± 68	1911 ± 135
C5	1260 ± 436	1005 ± 41	1856 ± 67
S5	1161 ± 420	950 ± 107	1637 ± 117
M5	1714 ± 296	817 ± 63	1482 ± 126
F5	830 ± 161	900 ± 90	1444 ± 136
CDP	548 ± 50	524 ± 111	1730 ± 318
H400	425 ± 25 [a]	–	–
[a] Manufacturer data			

3.3. Analysis of wear results

Results of the ARWW and AWW test are presented in Table 4 and results of the AIEW test in Table 5. As can be seen from the results, in the ARWW test, the wear rates are much higher than the results of the AWW test.

One of the reasons is that during the ARWW, the abrasive particles move freely and are pushed into the softer matrix by the rubber wheel. This results in cutting away the matrix and some hardmetal particles becoming loose, contributing to higher wear rate.

In the AWW test, on the other hand, abrasive particles are embedded in the abrasive wheel. This means that abrasive particles cannot reach to cut away the matrix and therefore hardmetal particles in the matrix are more effective protecting the surface from the wear.

Interesting phenomena can be seen when comparing Hardox 400 and P1 hardfacing. In the ARWW test conditions where there is loose abrasive and macrohardness and resistance to cutting plays more importnat role, P1 is more wear resistant. In AWW where abrasive particles are fixed, Hardox 400 is more wear resistant on the basis of received results. However, the reason for that is yet unknown.

Similar trends can be seen when comparing self-fluxing alloy hardfacing P1 and commercial composite wear plate CDP112. In the ARWW test, material P1 is more wear resistant, in the AWW test, it is material CDP 112. Material CDP112 is more wear resistant thanks to WC particles in the matrix, which make the surface of CDP 112 more wear resistant. Reasons for better performance of Hardox 400 compared to P1 in AWW need a further study.

In the AIEW tests steel Hardox 400 seems to be the best material, because it is more available than CDP 112 and the difference in their wear resistance is small. Self-fluxing alloy hardfacing P1, even though it is harder than Hardox, gives only a small advantage in abrasive-erosive wear conditions. The reason is that high hardness from carbides that form during the sintering process lower the fatigue resistance of the material. Fatigue plays a role in erosion wear when impacting particles have lower hardness or their

hardness is only slightly higher than the material they wear [20, 21].

Reinforcement particle size, at AIEW using fine or a mixture of fine and coarse reinforcement, is even detrimental to the results and gives no benefit. Using coarse reinforcement gives only a small benefit as compared to Hardox 400 and no benefit compared to a pure self-fluxing alloy. Therefore, it can be seen that in the abrasive-erosive wear conditions, unreinforced hardfacings with high ductility are beneficial while composite hardfacings should not be used in these conditions.

Table 4. ARWW and AWW test results

Designation	Wear, mm³	
	ARWW	AWW
P1	4.99	6.15
C3	4.44	1.43
C4	5.93	0.68
C5	3.90	0.46
S5	2.92	1.02
M5	8.66	3.18
F5	10.91	2.98
CDP112	11.8	0.67
Hardox 400	57.5	3.66

Table 5. AIEW test results

Designation	Wear rate, mm³/kg
P1	26.9
C5	30.2
M5	76.3
F5	90.3
H400	32.8

Relative volumetric wear resistance ε at the ARWW, AWW and AIEW test was compared to that of Hardox 400. Results are given in Fig. 6 – Fig. 8.

As can be seen, at the ARWW test, the differences are much higher. With the exception of C4, the rule of thumb is that the coarse hardmetal reinforcement the hardfacing contains, the higher the wear resistance of the hardfacing is. This is true to a certain extent, as too much reinforcment weakens the hardfacing. An optimal reinforcement content with coarse reinforcement seems to be around 50 vol %, which is in good agreement with the previous results [8].

At the AWW test, the differences between the wear of materials are smaller than at the ARWW test. Again, it can be seen that the higher the coarse hardmetal content the higher the wear resistance.

When comparing a composite hardfacing with a pure self-fluxing alloy (P1), in the ARWW test, reinforcement in the matrix gives only minor improvement in the wear resistance. At the AWW test or two-body abrasion on the other hand, additional reinforcement in the matrix gives a multi-fold increase in the wear resistance. Therefore, in the three-body abrasion, unreinforced hardfacings seem to be more reasonable and in the two-body abrasion composite hardfacing have the advantage.

At the AIEW test, P1 gives only a small increase in the wear resistance as compared to Hardox 400. Using coarse reinforcement (C5) does not improve wear resistance and using fine or multimodal reinforcement in fact decreases the wear resistance of the hardfacing. Thus, in abrasion impact

conditions steel or pure self-fluxing alloy gives the best results in terms of wear resistance.
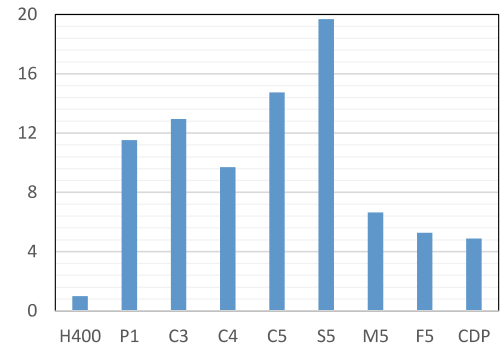

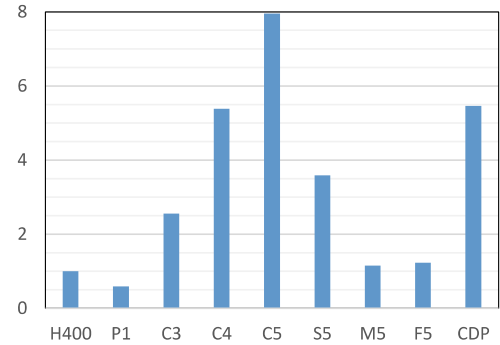**Fig. 6.** Relative wear resistane ε at ARWW test compared to Hardox 400

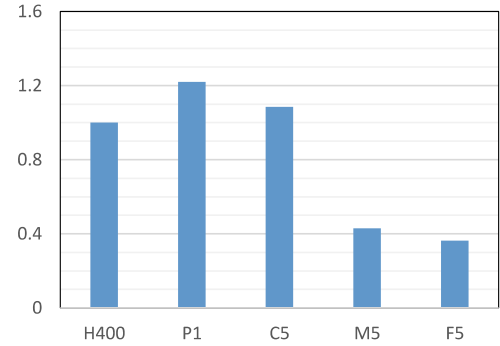**Fig. 7.** Relative wear resistance ε at AWW test compared to Hardox 400

Fig. 8. Relative wear resistance ε at AIEW test compared to Hardox 400

4. CONCLUSIONS

Based on our test results, composite hardfacings containing coarse hardmetal reinforcement suit well for use in the wear conditions where abrasion with fixed particles or two-body abrasion occur.

1. At two-body abrasion or abrasion with fixed particles, hardfacings with 50 vol% coarse angular hardmetal reinforcement content are most suitable.
2. At three-body abrasion hardfacings with 50 vol% spherical hardmetal content are recommended.
3. At the abrasive impact erosion wear conditions, hardmetal reinforcement gives a detrimental effect to the wear resistance.

Acknowledgments

REFERENCES

1. **Kulu, P., Zimakov, S.** Wear Resistance of Thermal Sprayed Coatings on the Base of Recycled Hardmetal *Surface Coatings Technology* 130 (1) 2000: pp. 46−51
https://doi.org/10.1016/S0257-8972(00)00687-3
2. **Kulu, P., Halling, J.** Recycled Hard-metal-based Wearresistant Composite Coatings *Journal of Thermal Spray Technology* 7 (2) 1998: pp. 173−178.
https://doi.org/10.1361/105996398770350882
3. **Kulu, P., Surzhenkov, A., Tarbe, R., Viljus, M., Saarna, M., Tarraste, M.** Hardfacings for Abrasive Wear Applications *Proceedings of the 28th International Conference on Surface Modification Technologies* 2014: pp. 149−157.
4. **Ishida, T., Itakura, T., Moriguchi, H., Ikegava, A.** Development of Technologies for Recycling Cemented Carbide Scrap and Reducing Use in Cemented Carbide Tools *SEI Technical Review* 75 2012: pp. 38−46.
5. **Bendikiene, R. Ciuplys, A., Pupelis, E.** Research on Possibilities to Replace Industrial Wear Plates by Surfaced Coatings Using Waste Materials *International Journal of Surface Science and Engineering* 10 (4) 2016: pp. 330−338.
https://doi.org/10.1504/IJSURFSE.2016.077535
6. **Badisch, E., Kirchgaßner, M.** Influence of Welding Parameters on Microstructure and Wear Behaviour of a Typical Nicrbsi Hardfacing Alloy Reinforced with Tungsten Carbide *Surface and Coatings Technology* 202 (24) 2008: pp. 6016−6022.
https://doi.org/10.1016/j.surfcoat.2008.06.185
7. **Zikin, A., Antonov, M., Hussainova, I., Katona, L., Gavrilović, A.** High Temperature Wear of Cermet Particle Reinforced NiCrBSi Hardfacings *Tribology International* 68 2013: pp. 45−55.
https://doi.org/10.1016/j.triboint.2012.08.013
8. **Ming-xi, L., He, Y., Sun, G.** Laser Cladding Co-based Alloy/SiCp Composite Coatings on IF Steel *Materials & Design* 25 (4) 2004: pp. 355−358.

https://doi.org/10.1016/j.matdes.2003.08.006
9. **Bolelli, G., Bonferroni, B., Laurila, J. Lusvarghi, L., Milanti, A., Niemi, K., Vuoristo, P.** Micromechanical Properties and Sliding Wear Behavior of HVOF-sprayed Fe-bsed Alloy Coatings *Wear* 276−277 2012: pp. 29−47.
https://doi.org/10.1016/j.wear.2011.12.001
10. **Li, R., He, Y.D., Zhou, Z., Wang, Z.J., Song, X.Y.** Wear and High Temperature Oxidation Behaviorof Wire Arc Sprayed Iron Based Coatings *Surface Engineering* 30 (11) 2014: pp. 784−790.
http://dx.doi.org/10.1179/1743294414Y.0000000331
11. **Zikin, A., Ilo, S., Kulu, P., Hussainova, I., Katsich, C., Badisch, C.** Plasma Transferred ARC (PTA) Hardfacing of Recycled Hardmetal Reinforced Nickel-matrix Surface Composite *Materials Science (Medziagotyra)* 18 (1) 2012: pp. 12−17.
http://dx.doi.org/10.5755/j01.ms.18.1.1334
12. **Bendikiene, R., Ciuplys, A., Kavaliauskiene, L.** Preparation and Wear Behaviour of Steel Turning Tools Surfaced Using the Submerged Arc Welding Technique *Proceedings of the Estonian Academy of Sciences* 65 (2) 2016: pp. 117−122.
http://dx.doi.org/10.3176/proc.2016.2.01
13. **Simson, T., Kulu, P., Surženkov, A., Tarbe, R., Viljus, M., Tarraste, M., Goljandin, D.** Optimization of Reinforcement Content of Powder Metallurgy Hardfacings in Abrasive Wear Conditions *Proceedings of the Estonian Academy of Sciences* 65 (2) 2016: pp. 90−96.
http://dx.doi.org/10.3176/proc.2016.2.03
14. **Simson, T., Kulu, P. Surženkov, A., Goljandin, D., Tarraste, M., Viljus, M.** Optimization of Composition of Hardmetal Reinforced Fe-Based PM Hardfacings in Abrasive Wear Conditions *Key Engineering Materials* 721 2017: pp. 351−355.
15. Castolin Eutectic homepage, CDP112 wear plate data, https://www.castolin.com/product/cdp-112, 02.02.2017.
16. ASTM G65−16, *Standard Test Method for Measuring Abrasion Using the Dry Sand/Rubber Wheel Apparatus.*
17. **Talviste, K.** Strengthening Technologies for Road Maintenance Machinery Wear Parts *MSc thesis* Tallinn University of Technology, 2013 (in Estonian).
18. GOST 23.201-78, *Gas Abrasive Wear Testing of Materials and Coatings with a Centrifugal Accelerator.*
19. *Mechanical and Metal Trades Handbook*, Verlag Europa-Lehrmittel
20. **Sapate, S.G., RamaRao, A.V.** Erosive Wear Behaviour of Weld Hardfacing High Chromium Cast Irons: Effect of Erodent Particles *Tribology International* 39 (3) 2006: pp. 206−212.
https://doi.org/10.1016/j.triboint.2004.10.013
21. **ElTobgy, M.S., Ng, E., Elbestawi, M.A.** Finite Element Modeling of Erosive Wear *International Journal of Machine Tools and Manufacture* 45 (11) 2005: pp. 1337−1346.
https://doi.org/10.1016/j.ijmachtools.2005.01.007

PUBLICATION 3
T. Simson, P. Kulu, A. Surženkov, A. Ciuplys, M. Viljus ,G. Zaldarys, Comparison of plasma transferred arc and submerged arc welded abrasive wear resistant composite hardfacings, *Materials Science (Medžiagotyra)*, 2018, **24**(2), 172 – 176.

Comparison of Plasma Transferred Arc and Submerged Arc Welded Abrasive Wear Resistant Composite Hardfacings

Taavi SIMSON [1] *, **Priit KULU** [1], **Andrei SURŽENKOV** [1], **Antanas CIUPLYS** [2], **Mart VILJUS** [1], **Gintautas ZALDARYS** [2]

[1] *Department of Mechanical and Industrial Engineering, Tallinn University of Technology, Ehitajate tee 5, 19086 Tallinn, Estonia*
[2] *Department of Production Engineering, Kaunas University of Technology, Studentu str. 56, 51424 Kaunas, Lithuania*

Composite hardfacings produced by Plasma Transferred Arc Welding (PTAW) and Submerged Arc Welding (SAW) possess a good combination of hardness, wear resistance and fracture toughness, thus providing high wear resistance. Although they cannot substitute and be compared with conventional WC-Co based hardmetals, still they can be used in many applications where high wear resistance, hardness and toughness are in great demand. In this study two different hardfacing production technologies PTAW and SAW, were used to produce the hardfacings for abrasive wear conditions. In both cases hardfacings were welded on the top of low alloy steel using different proportions of disintegrator milled hardmetal WC-Co powder of different fractions as a reinforcement and self-fluxing alloy as a matrix. They were analysed in regard to Rockwell and Vickers hardness, wear behaviour, and microstructural analysis. SAW hardfacings were subjected to Rockwell hardness test after process and after two cycles of tempering; secondary hardness effect was detected as increment of hardness values from 39 HRC to 58 HRC after first cycle of tempering. High Vickers hardness values did not correlate with wear results, as it commonly shows hardness of hardmetal particles. Dissolution of hardmetal particles in the matrix was observed in both PTAW and SAW hardfacings with higher amount in the later. This amount correlated with heat input during welding process. Wear test results in abrasive emery wear (AEMW) and abrasive wheel wear test (AWW) showed almost analogous tendency, with slightly lower wear in later. Both types of hardfacings have shown promising results in intensive wear conditions.

Keywords: hardfacing, plasma transfer arc welding, submerged arc welding, wear resistance, recycled powder.

1. INTRODUCTION

In the majority of wear parts applications there is a great demand for hard materials with superior wear resistance in the form of coatings or hardfacings [1]. Hardfacing procedure can be used for the production of new overlays as well as for restoration of worn surfaces [2]. Different types of welding, brazing, powder metallurgy (liquid phase sintering), laser-cladding, thermal spraying, etc., are widely used for the production of hardfacings [3].

Among other hardfacing methods, welding is considered as an economical choice [4]. A solid wire is used as an electrode to form a hard high wear resistant layer on the surface of a substrate using different welding processes such as Gas Tungsten Arc Welding (GTAW), Flux Cored Arc Welding (FCAW), Gas Metal Arc Welding (GMAW) or Submerged Arc Welding (SAW). SAW is a fascinating method for the production of hardfacings because of its high deposition rates. The SAW hardfacing process may indeed mean melting a pre-placed highly alloyed powder, which contains elements such a chromium, carbon, molybdenum, tungsten, and manganese, by the electric arc under the layer of flux [5, 6].

Generally, SAW hardfacings are used in abrasion, erosion, corrosion or impact wear conditions: mineral processing, mining, cement production, and paper manufacturing. Some of specific applications are similar to those of Plasma Transferred Arc Welded (PTAW) hardfacings such as crusher teeth, hydro transport screens, and pumps [7, 8].

In its turn, PTAW is among the favoured production technologies to produce hardfacings with lower manufacturing cost and higher productivity compared with thermal spraying, laser cladding or a similar technology [9]. The main advantages of these coatings are their density and high thickness that are necessary for mining, oil-sand industries, mixer blades, furnace chutes, etc. [10, 11]. PTAW iron-based hardfacings, reinforced with WC-Co particles, may provide over 9 times higher resistance to abrasive wear, than commonly used wear resistant steels [12]. This process normally uses powder mixture carried into the arc area using powder feeding system [5]. There are only a few different powder materials systems that are typical to PTAW and SAW: chromium carbide, WC-Ni and WC-Co, etc. Because of comparatively high price of PTAW equipment it is impractical to produce relatively low value added hardfacings such as chromium carbide overlays, therefore more expensive materials systems such a WC, WC-Co, self-fluxing alloys, Fe-Cr-C alloys, stellites, etc., are used; on the other hand, SAW technique is seldom used for production of tungsten carbide based coatings because of extremely high weld arc temperatures, which can initiate

---

* Corresponding author. Tel.: +372-58-208242.
E-mail address: *taavi.simson@ttu.ee* (T. Simson)

the dissolution of tungsten carbide. Considering process parameters: hardfacing rate, voltage, and feed rate a direct dependence was observed between the dissolution rate and the content of WC [13]. The maximum WC content of 19 % at dissolution rate of 5 % was only realised with low feed speed and voltage. In the case of the PTAW process, the WC content may approach 30 % [14].

Taking into account these considerations the main objective of presented study is applying two common welding technologies − PTAW and SAW − to produce hardfacings, compare and analyse mechanical their properties, formed microstructures and wear resistance in intensive abrasive emery wear and abrasive wheel wear conditions.

2. EXPERIMENTAL

Recycled (disintegrator milled) hardmetal WC-Co powder, with size of $1.6 - 2.0$ mm (coarse fraction) and $0.16 - 0.315$ mm (fine fraction) as reinforcement and commercial iron-based self-fluxing alloy powder with fraction size of $15 - 53$ µm as matrix were used as the feedstock materials for PTAW. In case of SAW, in addition to hardmetal and the above-mentioned self-fluxing alloy powders, a low carbon wire was applied as the consumable. Composition of hardfacings is presented in Table 1.

Table 1. Composition of hardfacings

No.	Powder composition, vol.%	Method
C5	50 WC-Co [2] + 50 FeCrSiB [1]	PTAW
B1	50 WC-Co [2], 50 LCW [4]	SAW
B2	25 WC-Co [2] + 25 FeCrSiB [1] + + 50 LCW [4]	SAW
D	25 WC-Co [2] + 25 WC-Co [3] + + 50 LCW [4]	SAW
[1] Iron-based self fluxing alloy 6AB (Höganäs AB): Cr 13.7 wt.%, Si 2.7 wt.%, B 3.4 wt.%, Ni wt.6.0 %, C 2.1 wt.%, bal. Fe; [2] Disintegrator milled WC-Co powder (Tallinn University of Technology); particle size $1.6 - 2.0$ mm; [3] Disintegrator milled WC-Co powder (Tallinn University of Technology); particle size $0.6 - 0.315$ mm; [4] LCW − low carbon wire (C < 0.1 wt.%, Si < 0.03 wt.%, Mn $0.35 - 0.6$ wt.%, Cr < 0.15 wt.%, Ni < 0.3 wt.%).		

The PTAW hardfacing process was carried out in three steps. Firstly, the matrix self-fluxing alloy bond layer was deposited, with the deposition rate of 50 mm³/s and current of 65 A. Secondly, the hardmetal layer with thickness of ~2 mm was manually placed on that layer. Final step was the deposition of the third layer of the matrix self-fluxing alloy with the deposition rate of 40 mm³/s and current of 55 A.

The SAW hardfacing process was performed in a single pass using standard flux AMS1 (LST EN 10204:2004; SiO_2 $38 - 44$ wt.%, MnO $38 - 44$ wt.%, CaF_2 $6 - 9$ wt.%, CaO < 6.5 wt.%, MgO < 2.5 wt.%, Al_2O_3 < 5 wt.%, Fe_2O_3 < 2 wt.%, S < 0.15 wt.%, P < 0.15 wt.%) to shield and prevent contamination of the welding area. Low carbon single electrode wire with diameter of 1.2 mm was fed at the 25.2 m/h rate into the welding zone under preliminarily chosen process parameters: welding current $180 - 200$ A, voltage $22 - 24$ V, travel speed − 14.4 m/h [15]. SAW was carried out with an automatic welding device − torch

MIG/MAG EN 500 78). As substrate material for production of composite hardfacings structural steel S235 (C 0.17 wt.%, Mn $0.55 - 0.65$ wt.%, S ≤ 0.05 wt.%, P ≤ 0.04wt.%) provided as bars with 10×10 mm cross-section was used. The hardfacing was deposited on 10×100 mm samples with hardmetal powder mixture (~ 2 mm) spread on the surface of substrate under the flux.

Harfacings obtained using SAW were tempered after welding, at first for 1 h at 550 °C, with following tempering for 1 h at 600 °C.

Scanning electron microscope (SEM) images of harfacings were obtained using SEM EVO MA-15 from Carl-Zeiss.

Rockwell hardness of hardfacings was measured on the wrought (as welded) and heat treated (tempered) samples using Universal hardness tester Verzus 750CCD at the load of 1470 N with diamond indenter. Vickers hardness (9.8 N) was measured using Buehler Micromet 2001 hardness tester. An average of 10 for Rockwell and 20 for Vickers hardness readings are reported in the results.

Two different wear testing methods were used to evaluate and compare wear resistance of produced hardfacings: Abrasive Emery Wear Test (AEMW) (Fig. 1) and Abrasive Wheel Wear (AWW) (Fig. 2). Technological parameters of wear test methods are given in Table 2.
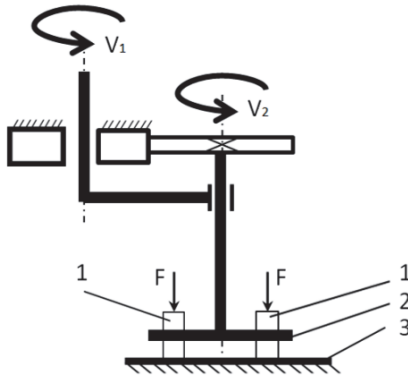

Fig. 1. Scheme of abrasive emery wear test: 1 − worn samples; 2 − holder; 3 − emery substrate

Table 2. Parameters of wear testing methods

Wear testing methods	
AEMW	Speed − 0.4 m/s, duration − 60 min, distance − 1440 m, abrasive − electrocorundum/white aluminium oxide 15A8HM with 8H mesh size
AWW	Speed − 2.4 m/s, duration − 10 min, distance − 1440 m, abrasive − SiC, particle size − $600 - 800$ µm; wheel hardness − 35 HRC

Samples for AEMW test (Fig. 1) with dimensions 6×20 mm were pressed to the emery substrate with 5 N load. Wear samples have been rotating round the holder axis with velocity of 63 r/min. Mass loss has been checked after each 10 min of test (~ 240 m of wear path) on the scales with 0.0001 g accuracy. Electrocorundum/white aluminium oxide was used as abrasive emery substrate; it was changed every 5 min (~ 120 m of wear path).

AWW test was carried out by testing machinery assembled in Tallinn University of Technology. AWW test (Fig. 2) imitates two-body abrasive wear conditions, in which test body is pressed against revolving abrasive wheel with fixed abrasive at speeds that are similar to Abrasive Rubber Wheel Wear (ARWW) test, carried out according to ASTM G65 standard.

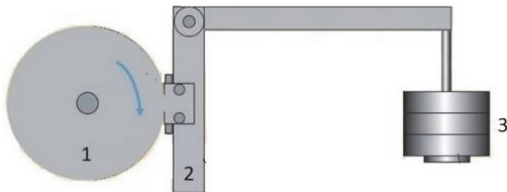Each presented hardfacing C5, B1, B2, D was tested four times, and just the average results of hardness and wear were analysed and discussed.

Fig. 2. Scheme of abrasive wheel wear: 1 − abrasive wheel; 2 − testbody holder; 3 − weight

3. RESULTS AND DISCUSSION

The purpose of multiple step tempering was to reduce the stresses and initiate transformation of possibly retained austenite [6]. After the first tempering at a temperature of 550 ºC, hardness of hardfacings B1 and B2 reached 55 HRC (Table 3). Further tempering at 600 °C did not affect hardness values of this testing lot. Different results were observed for the sample D, produced from the hardmetal powder of fine and coarse fracture. Fine particles dissolved completely forming highly alloyed matrix, while coarse particles remained almost unaffected. Obviously hardness of sample D as welded was just 39 HRC, though it increased to 58 HRC and 54 HRC respectively after tempering at 550 °C and 600 °C. This is typical to the so called secondary hardening of e.g. high speed steels and high alloyed tool steels. Secondary hardness was caused by the transformation of retained austenite or by the precipitation of carbides.

Table 3. Hardness of hardfacings

Rockwell hardness of SAW hardfacings after tempering		
No.	As welded, HRC	After tempering, HRC
		550 °C (I cycle)	600 °C (II cycle)
B1	55	55	54
B2	54	53	50
D	39	58	54
Vickers hardness, HV1			
Matrix	C5	B1	B2	D
846	1425	1441	1557	1436

The microstructures hardfacings' cross-section views produced using SAW clearly revealed hardmetal particles with narrow diffusion zones, where iron from matrix substitues cobalt, (I) tightly distributed into the metal matrix (II) Between hardmetal particles and matrix there is also precipitation zone (III), where loose WC are precipitated in the matrix (Fig. 3, Fig. 4, Fig. 5) [18].
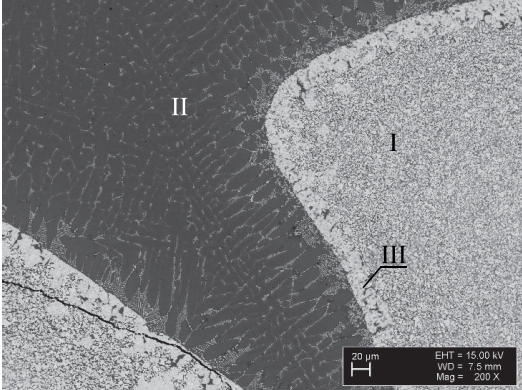

Fig. 3. Microstructures of SAW hardfacing B1: I − diffusion zone II − metal matrix; III − precipitation zone
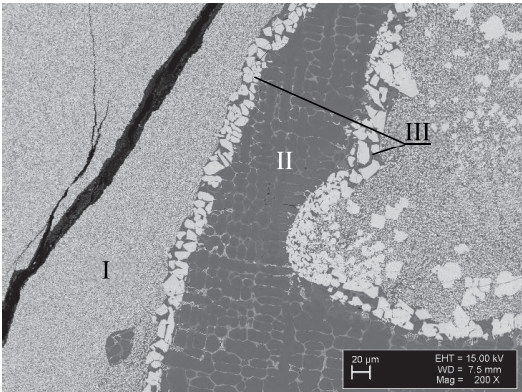

Fig. 4. Microstructures of SAW hardfacing B2: I − diffusion zone; II − metal matrix; III − precipitation zone
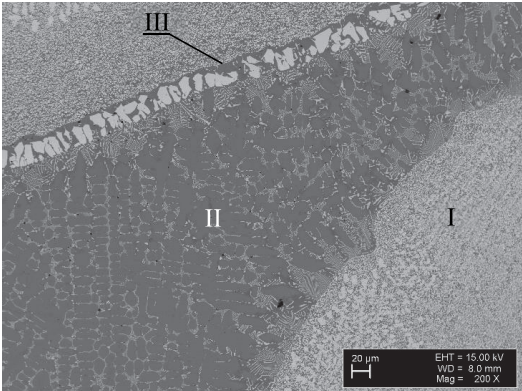

Fig. 5. Microstructures of SAW hardfacing D: I − diffusion zone; II − metal matrix; III − precipitation zone

It is clearly seen in microstructure images of hardfacings B1, B2 and D (Fig. 3 – Fig. 5) that tungsten carbide-cobalt powder particles dissolute (II) under the influence of high SAW weld pool temperature. Such a dissolution of WC-Co increases hardness of the matrix, but

probably would decrease overall wear resistance of the hardfacings [5, 15].

The solidification of hardfacings started when primary carbides were formed, followed by eutectic change of liquid solution to austenite. The ledeburitic eutectic surrounds the primary carbides and forms matrix of SAW hardfacings (dark grey sectors around the WC-Co particles). Low carbon wire and self-fluxing alloy form a matrix in the coating with a structure similar to a cast structure (II).

Some relief cracks have appeared almost in all microsections in the area of hardmetal particles during mechanical operations of sections preparations: cutting, grinding and polishing. These cracks have caused just initial increase of mass loss during wear test.

As can be seen from Fig. 6, during PTAW welding similar dissolution of hardmetal particles in the matrix takes place as in SAW (II). Amount of dissolution is in correlation with heat input during welding process. Former investigations [16] confirmed this statement: the decreased content of WC was related to thermally induced degradation from increased dissolution and increased iron content in the melt.
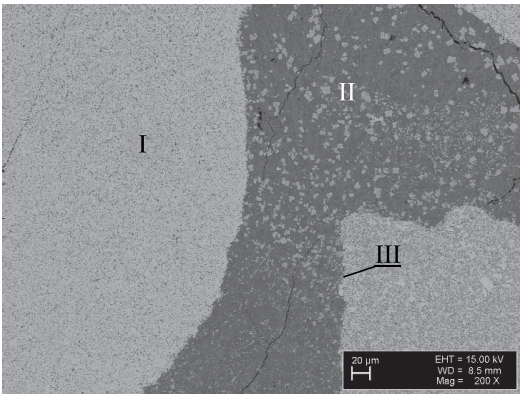

Fig. 6. Microstructure of PTAW hardfacing C5: I − diffusion zone; II − metal matrix; III − precipitation zone

SAW and PTAW produced hardfacings were tested in two abrasive wear conditions: emery wear (Fig. 7) and abrasive wheel wear (Fig. 8). Mass loss results were registered for two wear scars in abrasive emery wear test and four wear scars in abrasive wheel wear test. Generally, first wear scar associates with intensive wear, because heavier WC-Co particles precipitate at the bottom of coating.

Matrix material is cut out by abrasive particles at the beginning. At later test abrasive cannot reach matrix no more, so then it is protected by hardmetal particles.

As can be seen, values of first wear scar tests are quite high for the both experimental tests: maximum mass loss in AEMW was 136.4 mg, in AWW test − 126.8 mg (Fig. 7 and Fig. 8 respectively). After reaching such a high mass loss for all tested samples, it was decided by grinding operation to remove approximately the 1.5 mm from the surface of hardfacings tested on AEMW (2 wear scars), and to carry out additional wear tests on the hardfacings in the case of AWW test (4 wear scars).
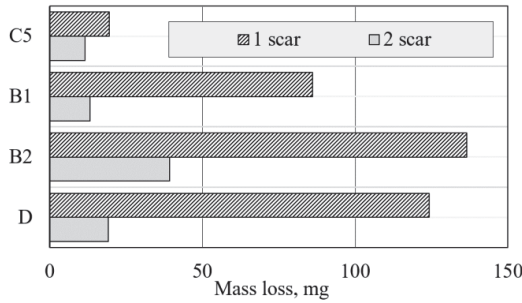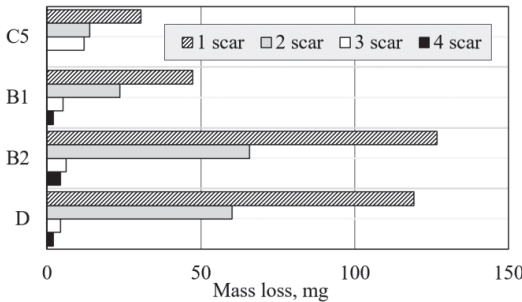

Fig. 7. Abrasive emery wear test results of hardfacings

	B1	B2	D
☐ 3 scar, mg	5.20	6.2	4.30
■ 4 scar, mg	2.05	4.45	2.1

Fig. 8. Abrasive wheel wear test results of hardfacings

Obtained results have proved the presumption that heavy hardmetal particles lay at the bottom − wear resistance of ground hardfacing B1 has been increased by 6 times: initial mass loss − 86.05 mg, after removal of superficial layer − 13.2 mg. The same tendency is seen for hardfacing D − mass loss has been decreased by 6 times too while for B2 this difference was two times lower (Fig. 7). PTAW produced hardfacing C5 was less sensitive to the second wear test after grinding − mass loss values were just 1.6 times lower.

Wear resistance of hardfacings tested on AWW machinery have been increasing after each 1440 m of wear path. It was depicted in the previous research [17] that composite hardfacings containing coarse WC-Co reinforcement (1.6 − 2.0 mm) suit well for two-body abrasion condition (AWW). Total length of wear path was 5760 m; as can be seen in Fig. 8, character of wear behaviour of SAW and PTAW samples in wheel test was analogous to the emery wear test. Mass loss after second test for all hardfacings was approximately 2 times lower than after the first one. The maximum reduction in worn mass loss was reached after third wear test − for all hardfacings in average by 9 times. Results of further wear test for B1, B2, and D hardfacings showed subsequent increase in wear resistance (on average twice) demonstrating suitability of produced hardfacings for long-term intensive wear, because deeper portions of coatings showed gradually increasing wear resistance.

4. CONCLUSIONS

Wear test results in abrasive emery wear and abrasive wheel wear test showed almost analogous tendency (when comparing first and second scars), with slightly lower wear values in AWW compared to AEMW.

PTAW produced hardfacing C5 showed better wear resistance than SAW hardfacings B1, B2, and D in both wear test conditions: mass loss of the former was by 5.9 and 2 times lower after first and second wear test respectively in abrasive emery test, and on average by 3.2 lower in abrasive wheel test.

Behaviour of SAW hardfacings B1, B2, and D is promising – third and fourth test series showed very high wear resistance, indicating that hardfacings need "working in" before achieving maximum wear resistance.

Secondary hardening effect was observed after two cycles of tempering of hardfacings produced by submerged arc welding. It led to the formation of high wear resistant substrate.

REFERENCES

1. **Hinners, H., Konyashin, I., Ries, B., Petrzhik, M., Levashov, E.A., Park, D., Weirich, T., Mayer, J., Mazilkin, A.A.** Novel Hardmetals with Nano-Grain Reinforced Binder for Hard-Facings *International Journal of Refractory Metals and Hard Materials* 67 2017: pp. 98 – 104.
https://doi.org/10.1016/j.ijrmhm.2017.05.011

2. **Bendikienė, R., Pupelis, E., Kavaliauskienė, L.** Effects of Surface Alloying and Laser Beam Treatment on the Microstructure and Wear Behaviour of Surfaces Modified Using Submerged Metal Arc Welding *Materials Science (Medžiagotyra)* 22 (1) 2016: pp. 44 – 48.
http://dx.doi.org/10.5755/j01.ms.22.1.7621

3. **Flores, J.F, Neville, A., Kapur, N., Gnanavelu, A.** An Experimental Study of the Erosion-Corrosion Behaviour of Plasma Transferred Arc MMCs *Wear* 267 2009: pp. 213 – 222.
https://doi.org/10.1016/j.wear.2008.11.015

4. 50 Hardfacing Tips. Form no. 9220. Victor Technologies, 2012; available at http://studylib.net/doc/18905505/50-hardfacing-tips---victor-technologies]

5. **Mendez, P.F., Barnes, N., Bell, K., Borle, S.D., Gajapathi, S.S., Guest, S.D., Izadi, H., Gol, A.K., Wood, G.** Welding Processes for Wear Resistant Overlays *Journal of Manufacturing Processes* 16 2014: pp. 4 – 25.
https://doi.org/10.1016/j.jmapro.2013.06.011

6. **Bendikiene, R., Ciuplys, A., Pupelis, E.** Research on Possibilities to Replace Industrial Wear Plates by Surfaced Coatings using Waste Materials *International Journal of Surface Science and Engineering* 10 (4) 2016: pp. 330 – 338.

7. **Chang, C.M., Chen, L.H., Lin, J.H., Fan, C.M., Wu, W.** Microstructure and Wear Characteristics of Hypereutectic Fe-Cr-C Cladding with Various Carbon Contents *Surface & Coatings Technology* 205 2010: pp. 245 – 250.
https://doi.org/10.1016/j.surfcoat.2010.06.021

8. **Kirchgaßner, M., Badisch, E., Franek, F.** Behaviour of Iron-based Hardfacing alloys under abrasion and Impact *Wear* 265 2008: pp. 772 – 779.
https://doi.org/10.1016/j.wear.2008.01.004

9. **Rojacz, H., Zikin, A., Mozelt, C., Winkelmann, H., Badisch, E.** High Temperature Corrosion Studies of Cermet Particle Reinforced NiCrBSi Hardfacings *Surface & Coatings Technology* 222 2013: pp. 90 – 96.
https://doi.org/10.1016/j.surfcoat.2013.02.009

10. **Zahiri, R., Sundaramoorthy, R., Lysz, P., Subramanian, C.** Hardfacing Using Ferro-Alloy Powder Mixtures by Submerged Arc Welding *Surface & Coatings Technology* 260 2014: pp. 220 – 229.
https://doi.org/10.1016/j.surfcoat.2014.08.076

11. **Saha, A., Mondal, S.C.** Multi-objective Optimization of Manual Metal Arc Welding Process Parameters for Nano-structured Hardfacing Material Using Hybrid Approach *Measurement* 102 2017: pp. 80 – 89.
https://doi.org/10.1016/j.measurement.2017.01.048

12. **Kulu, P., Tarbe, R., Žikin, A., Sarjas, H., Surženkov, A.** Abrasive Wear Resistance of Recycled Hardmetal Reinforced Thick Coating *Key Engineering Materials* 527 2013: pp. 185 – 190.
https://doi.org/10.4028/www.scientific.net/KEM.527.185

13. **Günther, K., Liefeith, J., Henckell, P., Ali, Y., Bergmann, J.P.** Influence of Processing Conditions on the Degradation Kinetics of Fused Tungsten Carbides in Hardfacings *International Journal of Refractory Metals and Hard Materials* 70 2018: pp. 224 – 331.
https://doi.org/10.1016/j.ijrmhm.2017.10.015

14. **Surzhenkov, A., Baroninš, J., Viljus, M., Traksmaa, R., Kulu, P.** Sliding Wear of Composite Stainless Steel Hardfacing under Room and Elevated Temperature *Solid State Phenomena* 267 2017: pp. 195 – 200.
https://doi.org/10.4028/www.scientific.net/SSP.267.195

15. **Liyanage, T., Fisher, G., Gerlich, A.P.** Microstructures and Abrasive Wear Performance of PTAW Deposited Ni-WC Overlays Using Different Ni-alloy Chemistries *Wear* 274 – 275 2012: pp. 345 – 354.
https://doi.org/10.1016/j.wear.2011.10.001

16. **Choi, L., Wolfe, M., Yarmurch, M., Gerlich, A.** Effect of Welding Parameters on Tungsten Carbide-metal Matrix Composites Produced by GMAW *Proceedings of Canadian Welding Association Conference* 2011.

17. **Simson, T., Kulu, P., Surženkov, A., Tarbe, R., Goljandin, D., Tarraste, M., Viljus, M., Traksmaa, R.** Wear Resistance of Sintered Composite Hardfacings under Different Abrasive Wear Conditions *Materials Science (Medžiagotyra)* 23 (3) 2017: pp. 249 – 253.
http://dx.doi.org/10.5755/j01.ms.23.3.16323

18. **Simson, T., Kulu, P., Surženkov, A., Goljandin, D., Tarbe, R., Tarraste, M., Viljus, M.** Optimization of Structure of Hardmetal Reinforced Iron-Based PM Hardfacings For Abrasive Wear Conditions *Key Engineering Materials* 721 2017: pp. 351 – 355.
https://doi.org/10.4028/www.scientific.net/KEM.721.351

https://doi.org/10.1504/IJSURFSE.2016.077535

PUBLICATION 4

A. Surzhenkov, M. Viljus, **T. Simson**, R. Tarbe, M. Saarna, F. Casesnoves, Wear resistance and mechanisms of composite hardfacings at abrasive impact erosion wear, *Journal of Physics: Conference Series*, 2017, **843**, 012060.

PAPER • OPEN ACCESS

Wear resistance and mechanisms of composite hardfacings at abrasive impact erosion wear

View the article online for updates and enhancements.

Wear resistance and mechanisms of composite hardfacings at abrasive impact erosion wear

A Surzhenkov, M Viljus, T Simson, R Tarbe, M Saarna and F Casesnoves

Department of Mechanical and Industrial Engineering, Tallinn University of Technology, Ehitajate tee 5, 19086 Tallinn, Estonia

andrei.surzenkov@ttu.ee

Abstract. Tungsten carbide based hardmetal containing sprayed and melted composite hardfacings are prospective for protection against abrasive wear. For selection of abrasive wear resistant hardfacings under intensive impact wear conditions, both mechanical properties (hardness, fracture toughness, etc.) and abrasive wear conditions (type of abrasive, impact velocity, etc.) should be considered.
This study focuses on the wear (wear rate and mechanisms) of thick metal-matrix composite hardfacings with hardmetal (WC-Co) reinforcement produced by powder metallurgy technology. The influence of the hardmetal reinforcement type on the wear resistance at different abrasive impact erosion wear (AIEW) conditions was studied. An optimal reinforcement for various wear conditions is described. Based on wear mechanism studies, a mathematical model for wear prediction was drafted.

1. Introduction

Abrasive impact erosion wear (AIEW) of materials depends on their mechanical properties and on wear parameters. The dominating mechanisms at AIEW may generally be predicted on the grounds of the material / abrasive hardness ratio (H_m/H_a) and the impact angle (0...90º). Depending on the first ratio, these mechanisms are [1,2]:

  − $H_m < H_a$: microcutting or plastic deformation with surface fatigue;
  − $H_m \approx H_a$: deformation with microcutting and/or surface fatigue;
  − $H_m > H_a$: deformation with surface fatigue and direct fracture.

Toughness of a material is another important mechanical characteristic that determines the behavior of a material at impact erosion. Depending on fracture toughness, the following mechanisms of wear may occur [3,4]:

  − in brittle materials (low K_{1c}): plastic deformation with surface fatigue and great probability of direct fracture;
  − in ductile materials (high K_{1c}): deformation with microcutting and/or surface fatigue [3,4].

Thick metal matrix composite (MMC) hardfacings are recommended for extreme abrasive wear conditions (i.e., high abrasivity, hardness and impact velocity of abrasive particles) due to their optimal hardness-toughness ratio. In this case, different wear mechanisms may simultaneously exist.

Such hardfacings may be produced, for example, by casting, plasma transferred arc (PTA) welding and submerged arc welding (SAW), vacuum sintering (VS), spray-fusion (SF), and high velocity spraying (HVS) [5–10].

The concept of plastic deformation and brittle fracture and a combined model of erosion were proposed to calculate the wear of composite structure materials [11]. A relatively soft metal matrix allows for use of the energetic theory of wear with the mean hardness and dimensionless specific energy parameter τ_o/e_s. In the wear calculations of hardphase, the models of plastic deformation and brittle fracture using hardness distribution and fracture probability must be taken into consideration [2,11].

The calculated and the experimental results showed that the wear rates of the Ni-based matrix composite coating with a relatively low hardness ($H_m < H_a$) have very good coincidence [12].

In the analysis of the abrasive wear resistance of HVOF-spayed, PTA-welded and PM hardfacings in different wear conditions (abrasion at rubber wheel, impact erosion) in [13], potential application areas of selected composite hardfacings were proposed.

Wear of matrix material at impact erosion is contributed from erosion by microcutting [1,2]. As not all impacts lead to the formation of a clean machined chip that is removed, at multiple impacts within the plastic strain field of the previous impacts, it may be possible for material to be removed. In [14] that kind of wear is classified as fatigue wear for only two overhapping impacts.

The aim of the present research was (a) to study wear resistance and wear mechanisms of surface damage of thick MMC hardfacings at different AIEW modes (oblique and normal impact), and (b) to propose criteria for selection of hardfacings for the above-mentioned conditions based on the mechanical properties (hardness-toughness ratio) and microstructure (reinforcement content, size and shape).

2. Experimental

2.1 Materials

Metal matrix composite hardfacings were produced by powder metallurgy (PM) technology using vacuum liquid-phase sintering. For matrix iron based self-fluxing alloy powder Höganās 6AB with composition, wt.%: 13.72 Cr, 2.67 Si, 0.32 Mn, 2.07 C, 0.02 S, 3.40 B, 6.04 Ni, bal. Fe was used. As a reinforcement, WC-15Co hardmetal powder produced by mechanical milling using a disintegrator milling system [15], with a particle size of 1.0–2.5 mm (coarse), 0.16–0.315 mm (fine) and their mixture (50% coarse + 50% fine) was used. The amount of 50% (optimal) was determined in our previous studies [8].

Table 1 shows the composition and hardness and Figure 1 − the microstructures of the studied hardfacings. As a reference material, Hardox 400 steel was used.

Table 1. Designation, composition and hardness of studied hardfacings.

Designation	Reinforcement		Hardness [16]	
	Particle size, mm	Content, vol.%	HV30	HV1[a]
P1	–	0	870 ±30	1035 ±70
	Coarse angular (C)			
C5	1.0–2.5	50	1260±435	1005±40/1855±65
	Fine angular (F)			
F5	0.160–0.315	50	830±160	900±90/1445±135
M5	Mixture 50C + 50F	50	1715±295	815±65/1480±125
	Reference steel			
H400	Hardox 400	–	425±25	–

[a] metal matrix/hard phase
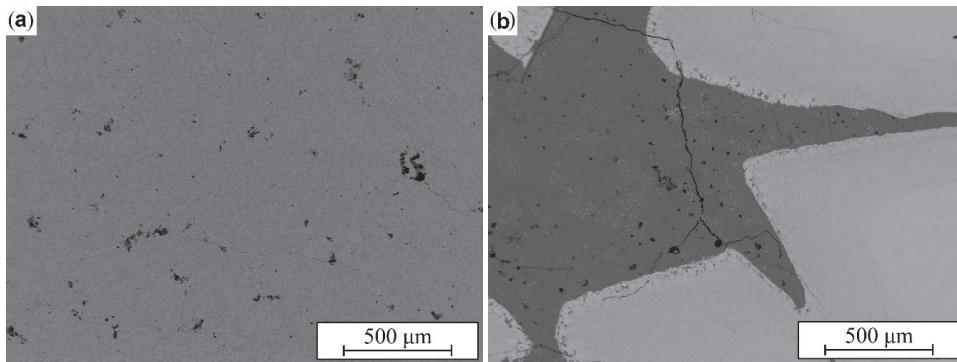
Figure 1. Microstructures of the studied hardfacings: a – P1 (unreinforced), b – C5 (50 vol.% WC-Co angular reinforcement) [16].

2.2 Abrasive wear studies

Abrasive impact erosion wear (AIEW) tests were used to determine the wear resistance of the hardfacings. At the low-energy wear test, granite and quartz sand of fraction 0.2–0.3 mm and centrifugal type tester CAK were used; at the high-energy wear test, granite gravel of fraction 3.0–5.6 mm and a disintegrator type tester DESI (Figure 3) were used.

The schemes and parameters of AIEW are given in Tables 2 and 3.

Based on the weight loss of abraded hardfacings, the volumetric wear rate (loss of volume per 1 kg of abrading material) in mm^3/kg was determined.

The relative wear resistance ε was calculated as the ratio of volumetric wear rates of the reference material (Hardox 400) to the wear rate of the studied hardfacing.

Mechanisms of the impact erosion wear were studied using a scanning electron microscope (SEM) EVO MA-15 (Carl Zeiss, Germany).

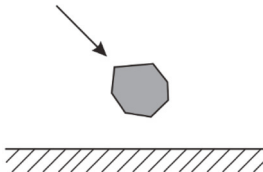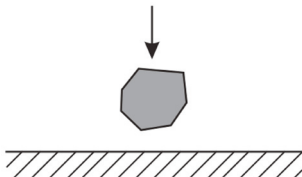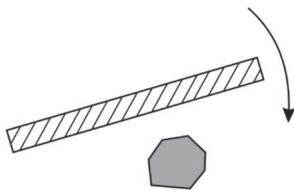**Table 2.** Abrasive impact erosion wear (AIEW) modes.

Oblique impact erosion wear $0º > α < 90º$	Normal impact erosion wear $α = 90º$

Abrasive 0.2–0.3 mm

Kinetic energy E_k at v = 40 m/s $3.0×10^{-5}$ J
at v = 80 m/s $1.2×10^{-4}$ J

Abrasive 3.0–5.6 mm

Kinetic energy E_k at v = 40 m/s $1.4×10^{-2}$ J
at v = 80 m/s $5.6×10^{-1}$ J

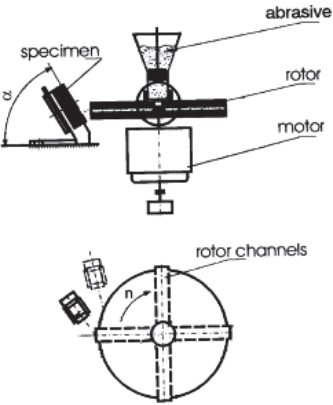**Table 3.** Abrasive impact erosion wear (AIEW) parameters (a).

Scheme of wear tester	Wear test parameters
	Quartz sand 0.2–0.3 mm, 1000–1100 HV Granite sand 0.2–0.3 mm, 900–950 HV Impact angle $α = 30º$ and $90º$ Impact velocity v = 40 m/s and 80 m/s Quantity of abrasive Q = 6 kg

Figure 2. AIEW tester CAK.

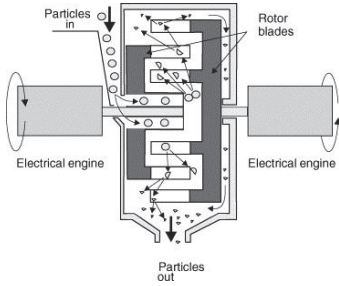**Table 3 (continues).** Abrasive impact erosion (AIEW) parameters (b).

Scheme of wear tester	Wear test parameters
	Granite gravel 3.0–5.6 mm; 900–950 HV Impact angle $\alpha \approx 90^{\circ}$ Impact velocity v = 40 m/s and 80 m/s Quantity of abrasive Q = 15 kg
Figure 3. AIEW tester DESI.	

3. Results and discussion

3.1 Wear resistance of hardfacings at AIEW

3.1.1 Influence of abrasive hardness. Results of low-energy AIEW are given in Table 4 and Figure 4. As it follows from Figure 4, the wear resistance of hardfacings is better with a softer abrasive – granite (abrasive hardness is comparable with matrix hardness); relative wear resistance exceeds that of steel Hardox 400 by about 3 times. With a harder abrasive – quartz sand ($H_a \approx 1.2 \, H_m$), the wear resistance of the studied hardfacings is low; relative wear resistance is at the same level or below that in comparison with Hardox 400.

Table 4. Wear rate (mm^3/kg) of hardfacings at low-energy AIEW.

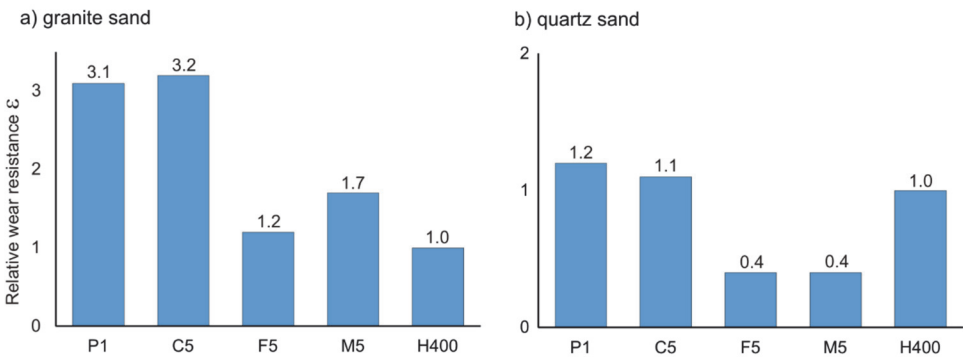| Designation	Granite sand HV 900–950	Quartz sand HV 1000–1100
P1	12.0	26.9
C5	11.7	30.2
F5	30.2	90.3
M5	21.9	76.3
H400	37.0	32.8

Figure 4. Relative wear resistance of hardfacings at low-energy AIEW with different abrasives (reference material – steel Hardox 400).

3.1.2 Influence of impact angle at AIEW. The results of wear resistance comparison of studied hardfacings at oblique impact ($\alpha = 30^\circ$) and at normal impact ($\alpha = 90^\circ$) show that the wear rate at straight impact is approximately 1.5 times higher (see Table 2). The relative wear resistance of the best hardfacing (C5) at $\alpha = 30^\circ$ was 3.2 times higher, at normal impact ($\alpha \approx 90^\circ$) it is only 1.9 times higher (Figure 5).

Table 5. Wear rates (mm^3/kg) of hardfacings at different impact angles at low-energy AIEW (abrasive – granite sand, impact velocity v = 80 m/s).

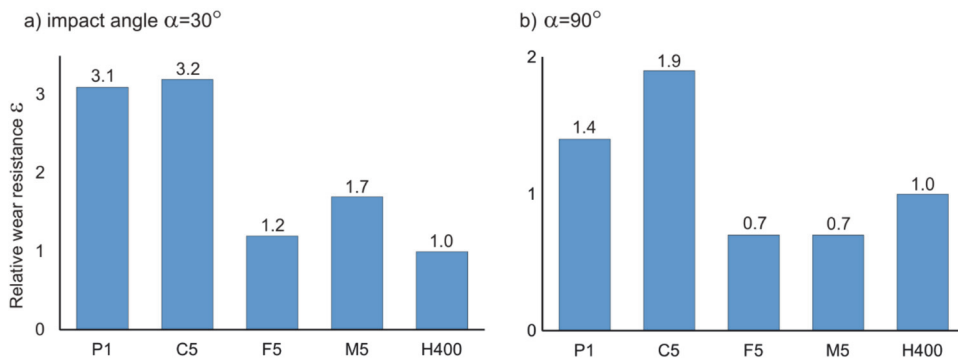| Designation	Impact angle, α	
	$\alpha = 30°$	$\alpha = 90°$
P1	12.0	21.5
C5	11.7	15.5
F5	30.2	41.0
M5	21.9	40.4
Hardox 400	37.0	30.0

Figure 5. Relative wear resistance of hardfacings at low-energy AIEW under different impact angles (abrasive – granite sand, reference material – Hardox 400).

3.1.3 Influence of abrasive particle velocity. The results of wear rate comparison of studied hardfacings at 40 m/s and 80 m/s (Table 6 and Figure 6) show that the wear rate of reinforced hardfacings at higher velocities is 3–4 times higher when the wear of the reference steel Hardox 400 is 7–8 times higher.

Thus, at low velocity (in the range $\varepsilon = 0.3$–0.8), the relative wear resistance is lower to compare with Hardox 400; at high velocity, wear resistance of composite hardfacings is very low (in the range $\varepsilon = 0.1$–0.2). It can be explained by the differences in the wear mechanisms of hardened steel as compared with metal matrix composite hardfacings.

Table 6. Wear rates (mm^3/kg) at different velocities at low-energy AIEW (abrasive – granite sand, impact angle α = 90º).

Designation	Velocity of abrasive particles, v	
	v = 40 m/s	v = 80 m/s
P1	10.0	21.5
C5	4.8	15.5
F5	13.8	41.0
M5	5.6	40.4
H400	3.8	30.0
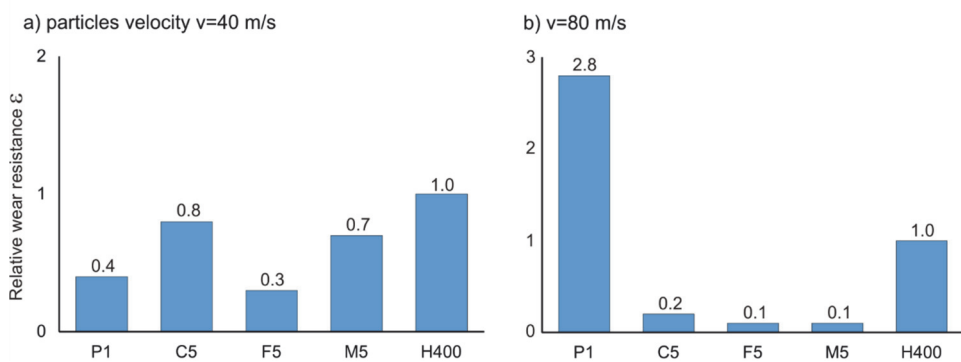
Figure 6. Relative wear resistance of hardfacings under different impact velocities (abrasive – granite sand, reference material – steel Hardox 400).

3.1.4 Influence of impact energy of abrasive particles. As the difference in studied impact energies is high (ratio of kinetic energies of high and low energy impact at v = 40 m/s is about 500 times), it influences the wear resistance significantly (see Table 7 and Figure 7). Wear rates of best hardfacing C5 differ about 23 times while the difference of the reference steel is only about 7 times.

Table 7. Wear rates (mm^3/kg) at different impact energies (abrasive – granite, v = 40 m/s, α = 90º).

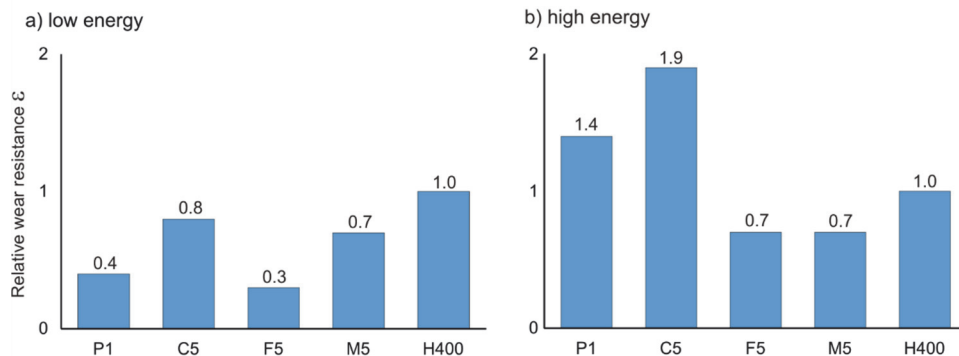| Designation	Low energy (sand) $E_k = 3.0 \times 10^{-4}$ J	High energy (gravel) $E_k = 1.4 \times 10^{-2}$ J
P1	10.0	9.3
C5	4.8	108.6
F5	13.8	215.2
M5	5.6	348.6
Hardox 400	3.8	26.1

Figure 7. Relative wear resistance of hardfacings at low-energy and high-energy AIEW (abrasive – granite, reference material – steel Hardox 400).

3.2 Mechanisms of AIEW

As the unreinforced hardfacing (P1) and the hardfacing reinforced with the coarse hardmetal (C5) exhibited the lowest wear among the studied hardfacings, they were taken as the object for our analysis of wear mechanisms. Both under low-energy and under high-energy AIEW conditions, the general wear process took place in two stages: firstly, destruction of the matrix and secondly, loss of loose WC-Co particles (Figures 8 and 9). Because the wear of the matrix was much more intensive than the wear of the reinforcement, higher magnification pictures of the first are demonstrated separately.

Under the low-energy AIEW conditions, the wear of both the FeCrSiB matrix (both in unreinforced and composite hardfacing) and the WC-Co reinforcement occurred by the low-cycle fatigue mechanism (Figure 8) [2]. In the first case, it included the stages of work hardening by the impact particles, resulting in the formation and development of lateral cracks [17] and, finally, spalling of flat fragments. It is interesting to note that the wear of the FeCrSiB matrix was more extensive in the composite hardfacing, and in the proximity of the reinforcing particles (Figure 8 b,c), it became most remarkable. The most probable cause for that is the thermally induced tensile stresses at the matrix-reinforcement interface [8], which favor the removal of the material [18]. At reinforcement, the wear started with the extrusion of the binder and continued by the subsequent chipping of the exposed carbide particles, as described in [4] (not shown in Figures 8, 9).

Under high-energy AIEW conditions, the wear mechanism of the reinforcement was identical to that under the low-energy AIEW conditions. However, the wear mechanism of FeCrSiB alloy underwent some changes (Figure 9). In addition to lateral cracks, median ones [17] may be seen (Figure 9). Thus, the wear mechanism of the FeCrSiB matrix may be described as a combination of low-cycle surface fatigue and direct fracture. As at the low-energy AEIW, the wear of the FeCrSiB matrix was higher at the composite hardfacing (Figures 8 b,c) for the same reason.
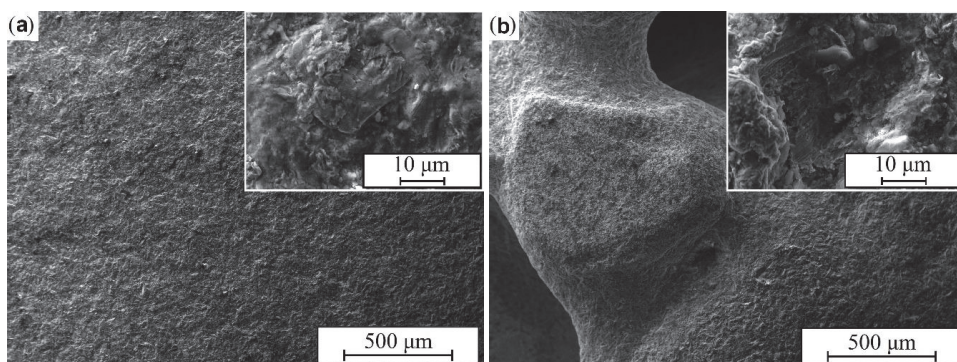
Figure 8. Worn surfaces of the hardfacings under low-energy AIEW conditions (v = 80 m/s): a – P1 (unreinforced), b – C5 (50 vol.% angular WC-Co reinforcement).
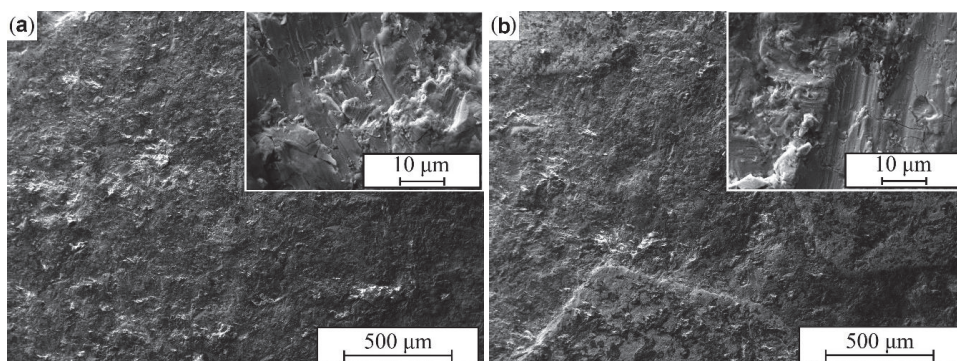

Figure 9. Worn surfaces of the hardfacings under high-energy AIEW conditions (v = 40 m/s): a – P1 (unreinforced), b – C5 (50 vol.% angular WC-Co reinforcement).

4. Conclusions

1. Wear rate of AIEW of studied composite WC-Co containing hardfacings depends first on the wear parameters (type and hardness of abrasive, velocity and kinetic energy of particles). Relative volumetric wear resistance of better hardfacings (coarse angular reinforcement, C5) exceeds that of the reference steel Hardox 400 about 3 times at low-energy AIEW with the abrasive – granite sand. At high velocity, AIEW relative wear resistance is low.

2. The dominating wear mechanism of both matrix and reinforcement at the low-energy AIEW was surface fatigue, at the high-energy AIEW – a combination of surface fatigue and direct fracture at the matrix and surface fatigue at the reinforcement.

3. The criteria for coating selection by composition and hardness-toughness ratio for hardmetals containing hardfacings are the following:

   a) at oblique impact AIEW – maximal hardphase content and higher hardness of the composite;

   b) at normal impact AIEW – lower hardphase content and hardness of metal matrix and higher toughness of hardphase.

5. References

[1]   Hutchings I M, Winter R E and Field J E 1976 *Proc. Roy. Soc. London* A **348** 379–92
[2]   Kleis I and Kulu P 2008 *Solid Particle Erosion. Occurrence, Prediction and Control* (London:

            Springer Verlag) p 206

[3]   Kulu P 2002 *Adv. Eng. Mater.* **4** 392–7

[4]   Hussainova I, Kübarsepp J and Pirso J 2001 *Wear* **250** 818–25

[5]   Rojacz H, Varga M, Kerber H and Winkelmann H 2014 *J. Mater. Process. Tech.* **214** 1285–92

[6]   Kulu P, Tarbe R, Saarna M, Surženkov A, Peetsalu P and Talviste K 2015 *Int. J. Microstructure and Materials Properties* **10** 101–13

[7]   Bendikiene R, Ciuplys A and Kavaliauskiene L 2016 *Proc. Est. Acad. Sci.* **65** 117–22

[8]   Simson T, Kulu P, Surženkov A, Tarbe R, Viljus M, Tarraste M and Goljandin D 2016 *Proc. Est. Acad. Sci.* **65** 90–6

[9]   *Reparation and wear protection technologies*. Product Catalogue, Castolin Eutectic, 2010

[10] Surzhenkov A, Vallikivi A, Mikli V, Viljus M, Vilgo T and Kulu P 2012 *Proc. 2nd Int. Conf. Manufacturing Engineering & Management 2012 (Prešov, Slovak Republic)* ed S Hloch et al. (Prešov: Udulibri) 34–7

[11] Kulu P, Veinthal R and Kaerdi H 2007 *Int. J. Mater. Prod. Tech.* **28** 425–47

[12] Veinthal R 2005 *Characterization and Modelling of Erosion Wear of Powder Composite Materials and Coatings* PhD Thesis (Tallinn: TUT Press) p 61

[13] Kulu P, Surženkov A, Simson T and Sarjas H 2016 *Proc. European Conf. Heat Treatment 2016 & 3rd Int. Conf. Heat Treatment and Surface Engineering in Automotive Applications*, 11–13 May 2016, Prague, Czech Republic (Prague: Asociace pro tepelné zpracování kovů)

[14] Andrews D R 1980 *The Erosion of Metals* PhD Thesis (London: Cambridge Press) p 156

[15] Goljandin D and Kulu P 2015 *Disintegrators and Disintegrator Treatment of Materials* (Lambert Academic Publishing) p 162

[16] Simson T, Kulu P, Surženkov A, Goljandin D, Tarbe R, Tarraste M and Viljus M 2017 *Key Eng. Mat.* **721** 351–5

[17] Sheldon G L and Finnie I 1966 *Am. Soc. Mech. Eng. Trans. J. Eng. Ind.* **88** 393–9

[18] Stewart D A, Shipway P H and McCartney D G 1998 *Surf. Coat. Tech.* **105** 13–24

PUBLICATION 5

T. Simson, R. Tarbe, M. Tarraste, M. Viljus, Abrasive impact erosion of composite Fe-based hardfacings with coarse WC-Co reinforcement, *Proceedings of the 24th IFHTSE Congress*, 26th – 29th of June 2017, Nizza, France.

Abrasive Impact Erosion of Composite Fe-based Hardfacings with Coarse WC-Co Reinforcement

Taavi Simson[a], Riho Tarbe[b], Marek Tarraste[c], Mart Viljus[d]

Department of Materials Engineering, Tallinn University of Technology, Ehitajate tee 5, 19086 Tallinn, Estonia

[a]taavi.simson@ttu.ee, [b]riho.tarbe@ttu.ee, [c]marek.tarraste@ttu.ee, [d]mart.viljus@ttu.ee

Abstract. The aim is to find an optimal coarse (1–2.5 mm) WC-Co reinforcement content (0/30/50 vol.%) and shape (angular/spherical) in the composite FeCrBSi-alloy based hardfacings subjected to low-energy (with fine (0.1–0.3 mm) erodent particles) and high-energy (with coarse (4.0–5.6 mm) erodent particles) abrasive impact erosion wear (AIEW) under the normal impact angle. The hardfacings were produced by the vacuum pressureless sintering at 1100 ºC from the pre-mixed blends of matrix and reinforcement powders. The impact velocity of the erodent particles was 40 and 80 m/s under both tests. The roles of hardness, modulus of elasticity, fracture toughness and porosity in the wear resistance of the hardfacings were analysed, and wear mechanisms were determined using SEM. The volume fraction of 30 vol.% WC-Co reinforcement was found optimal for low-energy AIEW conditions at 40 m/s and 50 vol.% WC-Co – at 80 m/s. Under high-energy AIEW conditions, the addition of WC-Co reinforcement decreases the wear resistance of the matrix alloy. The wear mechanism of both the matrix and the reinforcement was low-cycle surface fatigue under low-energy AIEW conditions, a combination of low-cycle surface fatigue and direct fracture in the case of matrix and low-cycle surface fatigue in the case of reinforcement under high-energy AIEW.

Introduction

Wear resistance of metal matrix composites (MMCs) depends on many factors, such as hardness [1,2], volume fraction [1–3], size [1–3], shape [1,4], and distribution [1,3] of the reinforcement and on the other hand, on porosity and residual stresses in the matrix [3]. In the case of abrasive erosive wear, resistance of a MMC to wear depends basically on its hardness and fracture toughness [3], whereas the importance of the latter grows with the increase of the impact angle [5]. Due to this reason, under normal impact angle abrasive erosive wear or abrasive impact erosion wear (AIEW), metal matrix structure with the reinforcement volume fraction less than 50% is recommended [6]. In its turn, coarse reinforcement with a composite structure (e.g. WC-Co) is more advantageous than a monolythic one of the same size because of higher fracture toughness [5].
MMCs with coarse composite reinforcement were reported to be produced by various welding [7,8], casting [9,10] and sintering [11] routes. Resistance of the sintered composite hardfacings reinforced with coarse WC-Co to a flow of erodent particles at the normal impact angle was found to increase with the increase of the reinforcement size [11]. At the same time, for example, optimal volume fraction was reported to be dependent on the parameters of the wear test [12,13]; therefore, the results obtained are not always comparable, which was the reason for our research.. In this study, composite hardfacings reinforced with different volume fractions of angular or spherical WC-Co reinforcement are tested under various abrasive impact erosion wear conditions. The influence of mechanical and structural properties of the matrix and reinforcement on the wear resistance of the hardfacings and wear

mechanisms is analysed.

Experimental

Preparation of hardfacings. Table 1 shows parameters of the hardfacing components. Hardfacings were produced by the liquid phase sintering of the mechanically pre-mixed components in vacuum (1100 °C, 30 min). The designation and composition of the hardfacings is listed in Table 2. In all the cases, the resultant thickness of the hardfacings was in the range 4.5–5 mm.

Table 1. Parameters of the hardfacing components

Type of component	Type of material	Manufacturer	Production method	Chemical composition [wt.%]	Particle size [mm]
Matrix	Fe-based self-fluxing alloy (FeCrBSi)	Höganäs AB (Sweden)	Gas atomization	13.72 Cr, 2.67 Si, 0.32 Mn, 2.07 C, 0.02 S, 3.40 B, 6.04 Ni, bal. Fe	0.010–0.053
Reinforcement	Angular WC-Co hardmetal	Tallinn University of Technology (Estonia)	Disintegrator milling from hardmetal scrap	85–97 WC, 15–3 Co	1–2.5
	Spherical WC-Co hardmetal	Wangsheng Cemented Carbide Ltd. (People's Republic of China)	Vacuum sintering	85 WC, 15 Co	⌀2.8

Table 2. Designation and composition of the hardfacings

Designation	Composition [wt.%]	Reinforcement shape
Un	100 FeCrBSi	–
A30	70 FeCrBSi, 30 WC-Co	Angular
A50	50 FeCrBSi, 50 WC-Co	Angular
S30	70 FeCrBSi, 30 WC-Co	Spherical
S50	50 FeCrBSi, 50 WC-Co	Spherical

Microstructure analysis and indentation properties. Polished cross-sections of the hardfacings were studied under the scanning electron microscope (SEM) EVO MA-15 (Carl Zeiss, Germany). Porosity of the hardfacings was estimated according to the standard ISO/TR 26946:2011, using the optical microscope Axiovert 25 (Carl Zeiss, Germany) and Buehler® Omnimet® software.

Universal hardness (HU) and modulus of elasticity (E) were simultaneously determined according to the standard EN/ISO 14577-02 using the universal hardness tester 2.5/TS (Zwick, Germany). The applied load and the indentation depth were respectively 50 N and 100 μm. The average values of HU and E were calculated on the basis of five measurements.

Fracture toughness was determined as

$$K_{IC} = \frac{(HV \cdot P)^{0.5}}{3 \cdot (1 - v^2) \cdot (2^{0.5} \cdot \pi \cdot tan\varphi)^{1/3} \cdot (4 \cdot a)^{0.5}}$$ [14], where (1)

K_{IC} is the fracture toughness, MPam$^{-0.5}$;
H is the Vickers hardness, kgf/mm^2;
P is the load, N, P = 50 N;
v is the Poisson's ratio, v = 0.23;
φ is a half aperture angle, $2\varphi = 136°$;
a is the median radial crack length, μm.

Abrasive impact erosion wear (AIEW) testing. Hardfacings were subjected to low-energy (erodent particle size range 0.1–0.3 mm) and high-energy (erodent particle size range 4.0–5.6 mm) abrasive impact erosion wear (AIEW) tests. The equipment and parameters of the wear tests are listed in Table 3.

Table 3. Equipment and parameters of the AIEW tests

Type of the test	Equipment	Abrasive type	Abrasive size [mm]	Abrasive quantity [kg]	Impact velocity [m/s]	Impact angle [º]
Low-energy	Four-channel centrifugal type abrasive-erosive wear tester CAK-2 [15]	Granite sand	0.1–0.3	6	40; 80	90
High-energy	Impact tester DESI [16]	Granite gravel	4.0–5.6	15	40; 80	90

The wear rate of a single specimen was calculated as

$$I_v = \frac{\Delta m \cdot 360}{M \cdot \delta \cdot \rho}, \text{where}$$ (2)

I_v is the wear rate, mm^3/kg;
Δm is the weight loss of the specimen, mg;
M is the total weight of the abrasive used in the test, kg;
δ is the angle, during which the jet of abrasive particles impacts the specimen, $\delta = 8.5°$ in the low-energy AIEW test and $\delta=9.4°$ in the high-energy AIEW test;
ρ is the density of the material subjected to wear, mg/mm^3.
The average wear rate was calculated on the basis of three specimens. Worn surfaces of the hardfacings were studied under SEM EVO MA-15 (Carl Zeiss, Germany) and wear mechanisms were determined.

Results and discussion

Microstructure studies. The microstructure of the hardfacings reinforced with WC-Co had the same features; therefore, only the microstructure of the hardfacings with 50 vol.% WC-Co is demonstrated here. Unreinforced hardfacing had a fine-grained structure with some residual porosity and negligible cracking (Fig. 1a). On the basis of the EDS analysis and our previous research [17], it may be

suggested that the dark rectangular-shape crystals are a complex mixture of Fe and Cr carbides and borocarbides embedded in the light Si-rich Fe-Cr-Ni-Co based matrix.

Both pores and cracks in the unreinforced hardfacing are suggested to appear due to a mismatch between the coefficients of thermal expansion (CTEs) of the FeCrBSi alloy and the steel substrate [11]. A higher mismatch between the CTEs of the FeCrBSi alloy and the WC-Co hardmetal [13] is assumed to cause higher porosity and more intensive cracking in the case of the reinforced hardfacings (Fig. 1b,c, Table 3).

A good wetting of the disintegrator milled angular WC-Co reinforcement by the molten matrix is shown in Fig. 1b; however, in the case of the sintered spherical WC-Co reinforcement, some unwetted areas can be seen (Fig. 1c). The most apparent reason for a poorer wettability of the spherical WC-Co is the formation of sinter skin on the surface of the hardmetal balls [18].

At good wetting, four zones may be distinguished at the matrix-reinforcement interface of the hardfacings reinforced by both angular and spherical hardmetal (Fig. 1d): matrix zone I where the original eutectic structure of the FeCrBSi alloy enriched with W and Co is present; dissolution and reprecipitation zone II laid up by primary WC carbide particles embedded in the reprecipitated Fe-Cr-W carbides; diffusion zone III where the structure of initial WC-Co grains preserves but where cobalt is replaced by iron; zone IV where the initial structure and chemical composition of WC-Co has preserved.
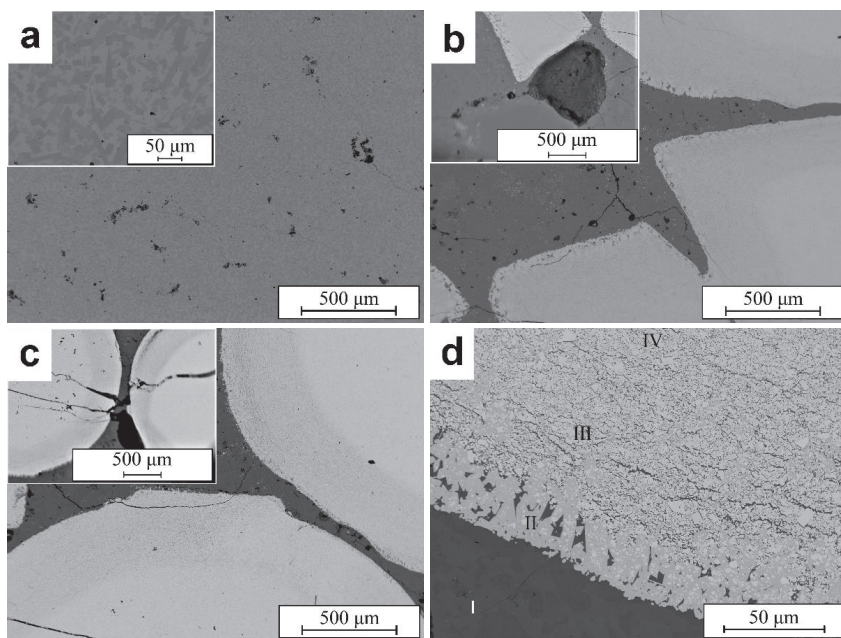

Fig. 1. Microstructure of the studied hardfacings: a - unreinforced hardfacing, b - composite hardfacing with 50 vol.% angular WC-Co reinforcement, c - composite hardfacing with 50 vol.% spherical WC-Co reinforcement, d - zones in the composite hardfacing: I − matrix structure, II − dissolution and reprecipitation zone, III − diffusion zone, IV − reinforcement structure (hardfacing with 50 vol. % WC-Co).

Indentation properties. The universal hardness of the FeCrBSi alloy with the addition of WC-Co reinforcement first increases slightly and then decreases again when the modulus of elasticity and

fracture toughness decrease linearly (Table 4; fracture toughness of the reinforcement could not be reliably determined under the current measuring conditions; therefore, it is not given here). At the same time, the resistance to plastic indentation (the H/E^2 ratio [19]) grows with the increase of the reinforcement volume fraction.

The increase of universal hardness values with the addition of 30 vol.% WC-Co may be explained by the dissolution of W and Co in the Fe-based matrix and subsequent formation of intermetallides and/or carbides [17,20]. With the increase of the reinforcement volume fraction, the residual tensile stresses induced by the different CTEs of the matrix and the reinforcement would increase [21], causing changes in the mechanical properties [22]. Most probably, the drop of universal hardness values and the discussed decrease of the modulus of elasticity and fracture toughness are caused by these growing tensile stresses.

Table 4. Porosity values and indentation properties of the studied hardfacings

Hardfacing designation	Porosity [%]	HU [MPa]	E [GPa]	HU/E^2, ×10^{-8}	Fracture toughness [MPa·m$^{-0.5}$]
Un	1.9	6695±695	290.9±26.7	8.0±1.3	14.5±3.3
S3 matrix reinforcement	3.0	6338±746 12697±906	256.4±15.5 547.4±64.3	9.7±1.0 4.3±0.9	12.0±1.2
A3 matrix reinforcement	4.6	6959±364 12025±564	243.5±18.0 449.7±30.3	11.8±1.3 6.0±0.8	12.6±1.4
S5 matrix reinforcement	1.8	5968±462 11826±637	221.4±20.5 433.5±46.0	12.3±3.2 6.4±1.4	11.7±3.3
A5 matrix reinforcement	4.8	6050±735 12802±2684	215.3±42.9 483.4±156.4	13.7±5.5 5.8±2.0	11.2±0.3

Wear of the studied hardfacings. Under fine abrasive AIEW conditions, the addition of hardmetal reinforcement gives a wear rate decrease of 2.2–2.9 times at the low impact velocity and a wear rate decrease of 1.2–2.2 times at the high impact velocity (Fig. 2a). Under low impact velocity (40 m/s), hardfacings reinforced with 30 and 50 vol.% angular WC-Co, as well as hardfacings reinforced with 30 vol.% spherical WC-Co exhibited nearly identical wear rates. Under high impact velocity (80 m/s), hardfacings with 50 vol.% WC-Co showed better wear resistance than the rest of the hardfacings. Under coarse abrasive AIEW conditions, the addition of hardmetal reinforcement deteriorates the wear resistance of the hardfacings by 3.3–30.7 times under low impact velocity and 1.5–10.6 times – under high impact velocity (Fig. 3b). The wear rates grow with the increase of the hardmetal reinforcement content, whereas the addition of the spherical reinforcement leads to higher wear.
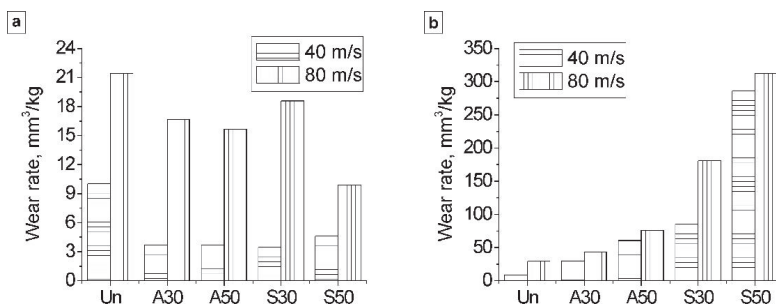
Fig. 2. Wear of the studied hardfacings: a - under low-energy AIEW conditions, b - under high-energy AIEW conditions.

Low-energy AIEW mechanisms. Under low-energy AIEW conditions, the wear mechanism of both the FeCrBSi alloy in the unreinforced and in the reinforced hardfacings, as well as the WC-Co reinforcement showed the low-cycle surface fatigue (Fig. 3) [15]. In the FeCrBSi alloy, work hardening by the repeating impacts of the erodent particles led to the appearance and growth of lateral cracks underneath the worn surface, resulting in chipping of flat fragments (Fig. 1a). In the WC-Co reinforcement, the repeating impingements of the erodent particles resulted in the loss of the binder and subsequent delamination of loose carbide grains (Fig. 1d), as described in [23].
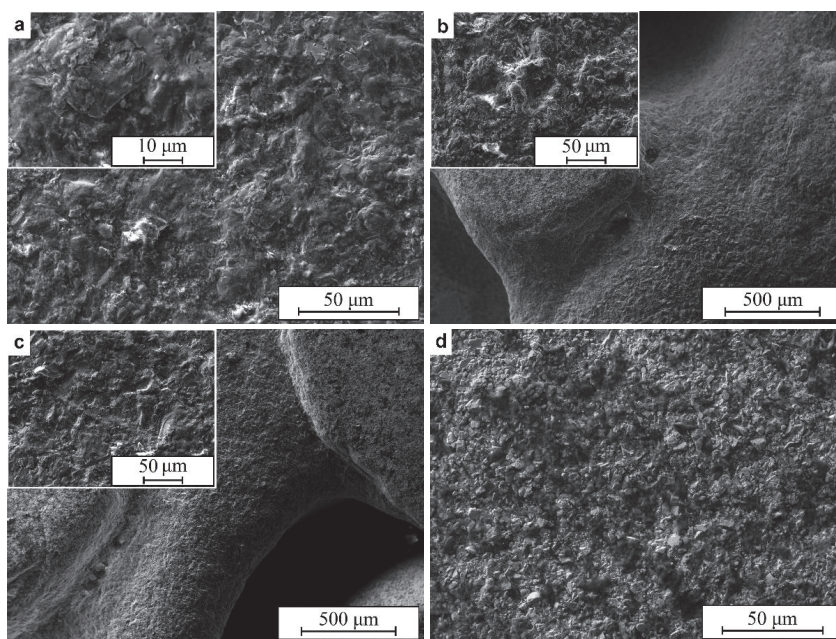

Fig. 3. Worn surfaces of the hardfacings (low-energy AEIW): a – unreinforced hardfacing, b – hardfacing with 50 vol.% angular WC-Co (wear of the matrix is shown on the left upper corner figure), c – hardfacing with 50 vo.% spherical WC-Co reinforcement (wear of the matrix is shown on the left upper corner figure), d – worn surface of a WC-Co particle (R5 hardfacing).

High-energy AIEW mechanisms. Under high-energy AIEW conditions, the wear mechanism of the reinforcement remained unchanged (Fig. 4d). However, in the case of the FeCrBSi alloy (Fig. 4a–c), the formation of radian cracks could be observed, indicating brittle fracture. Also, more extensive loss of the matrix was observed in the proximity of the spherical WC-Co as a result of poor wetting of the reinforcement (Fig. 4c).
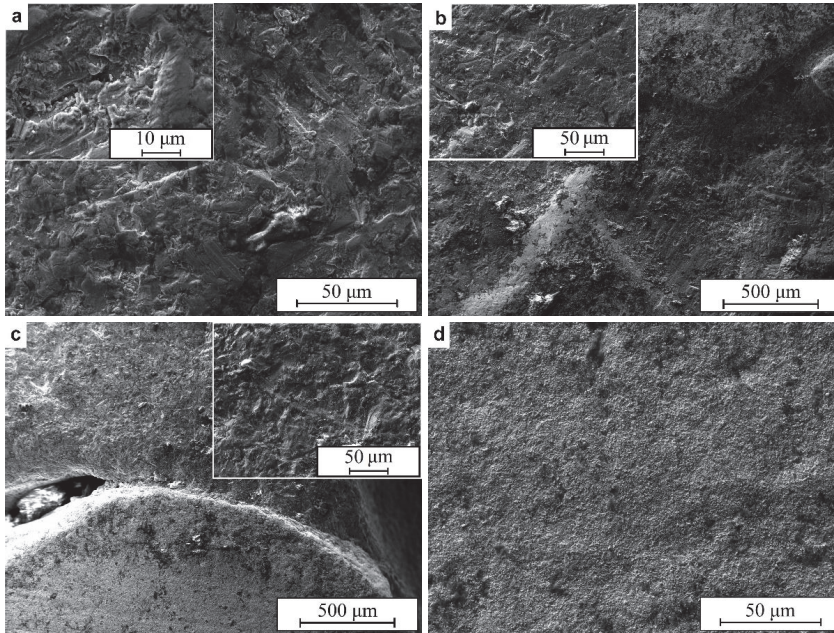

Fig. 4. Worn surfaces of the hardfacings (high-energy AIEW): a – unreinforced hardfacing, b – hardfacing with 50 vol.% WC-Co (wear of the matrix is shown on the left upper corner), c – hardfacing with 50 vol.% spherical WC-Co reinforcement (wear of the matrix is shown on the right upper corner), d – worn surface of a WC-Co grain (R5 hardfacing).

Discussion

Low-energy AIEW. No instant correlation between porosity and fracture toughness, and on the other hand, the wear rates of the hardfacings was discovered. Neither could any clear dependence of the wear rates on other parameters be found. Despite the statement in [23] that a higher elastic modulus should lead to lower wear by providing better resistance to penetration by the erodent particles, no such tendency was observed here. A higher resistance to plastic deformation (the H/E^2 ratio) of the matrix and reinforcement in some cases leads to lower wear, as prognosed in [19]. However, such a dependence is found only in the case of the unreinforced hardfacing, when it is compared to hardfacings that are reinforced with the angular WC-Co. In the case of the hardfacings reinforced with the spherical WC-Co, no correlations that may be explained by the effect of poorer wetting of reinforcement by the molten matrix were observed.

High-energy AIEW. In contrast to low-energy AIEW where impinging erodent particles cause basically only elastic deformation [23], here the impacting particles have a higher kinetic energy. The latter causes a higher deformation rate, probably exceeding the elastic strain limit, especially in the case of the matrix FeCrBSi alloy [24]. Therefore, the fracture toughness should become more important here

than the hardness and modulus of elasticity. This assumption correlates well with Table 3 and Fig. 2b. A higher wear of the hardfacings reinforced by the spherical WC-Co is most probably influenced by the poor wettability of it by the molten matrix. As a result, unsupported WC-Co particles break more easily; on the other hand, the discontinuities formed due to insufficient wetting may play a role of stress concentrators.

Conclusions

1. Generally, under low-energy abrasive impact erosion wear (AIEW) conditions, no clear effect of the reinforcement volume fraction on the wear resistance of the composite hardfacings was found. Under low impact velocity (40 m/s), addition of 30 vol. % WC-Co reinforcement provided lower wear rates of the FeCrBSi alloy. Under high impact velocity (80 m/s), hardfacings reinforced with 50 vol.% WC-Co exhibited lower wear.
2. Under high-energy AIEW conditions, the addition of WC-Co reinforcement had a detrimental effect upon the wear resistance of the FeCrBSi alloy, whereas the wear rates of the composite hardfacings increased with the increase of the volume fraction of the reinforcement.
3. Studied angular disintegrator milled WC-Co reinforcement generally results in a higher increase of the wear resistance than the studied sintered spherical WC-Co reinforcement due to better wetting by the molten matrix.
4. Under low-energy AEW conditions, the wear of the hardfacings is generally governed by the H/E^2 ratio (resistance to plastic indentation) and wetting of the reinforcement by the molten matrix. Under high-energy AIEW conditions, the wear of the hardfacings generally depends on the fracture toughness of the matrix and the wetting of the reinforcement by the molten matrix.
5. Under low-energy AIEW, the wear mechanism of both the matrix and the reinforcement is low-cycle surface fatigue. Under high-energy AIEW, the wear mechanism of the matrix is a combination of low-cycle surface fatigue and direct fracture, the wear mechanism of the reinforcement is low-cycle surface fatigue.

Acknowledgements

References

1. E. Pagounis, M. Talvitie, V.K. Lindroos, Influence of reinforcement volume fraction and size on the microstructure and abrasion wear resistance of hot isostatic pressed white iron matrix, Metall. Mater. Trans. A 27 (1996) 4171-4181.
2. Z.F. Zhang, L.C. Zhang, Y.-W. Mai, Particle effects on fraction and wear of aluminium matrix composites, J. Mater. Sci. 30 (1995) 5999-6004.

3. I. Hussainova, On micromechanical problems of erosive wear of particle reinforcement composites, Proc. Estonian Acad. Sci. Eng. 11 (2005) 46-58.
4. K. Van Acker, D. Vanhoyweghen, R. Persoons, J. Vangrunderbeek, Influence of tungsten carbide particle and distribution on the wear resistance of laser clad WC/Ni coatings, Wear 258 (2005) 194-202.
5. P. Kulu, I. Hussainova, R. Veinthal, Solid particle erosion of thermal sprayed coatings, Wear 258 (2005) 488-496.
6. P. Kulu, T.Pihl, Selection criteria for wear resistant powder coatings under extreme erosive wear conditions, J. Therm. Spray Tech. 11 (2002) 517-522.
7. P. Kulu, R. Tarbe, A. Zikin, H. Sarjas, A. Surženkov, Abrasive wear resistance of recycled hardmetal reinforced thick coating, Key Eng. Mat. 527 (2013) 185-190.
8. R. Bendikiene, A. Ciuplys, L. Kavaliauskiene, Preparation and wear behaviour of steel turning tools surfaced using the submerged arc welding technique, P. Est. Acad. Sci. 65 (2016) 117-122.
9. H. Rojacz, M. Varga, H. Kerber, H. Winkelmann, Processing and wear of cast MMCs with cemented carbide scrap, J. Mater. Process. Tech. 214 (2014) 1285-1292.
10. A.N. Stepanchuk, Manufacturing of composite materials and coatings from self-fluxing alloys and hardmetal scrap, 2011, http://cla.kpi.ua/handle/123456789/5381 (accessed 28/5/2015).
11. P. Kulu, A. Surzhenkov, R. Tarbe, M. Viljus, M. Saarna, M. Tarraste, Hardfacings for abrasive wear applications, Proc. 28th Int. Conf. Surface Modification Technologies, 16th–18th of June, 2014, Tampere, Finland, 149-157.
12. T. Simson, P. Kulu, A. Surženkov, R. Tarbe, M. Viljus, M. Tarraste, D. Goljandin, Optimization of reinforcement content of powder metallurgy hardfacings in abrasive wear conditions, P. Est. Acad. Sci. 65 (2016) 90-96.
13. A. Surzhenkov, R. Tarbe, M. Tarraste, T. Simson, M. Viljus, P. Kulu, Optimization of hardmetal reinforcement content in Fe-based hardfacings for abrasive-impact wear conditions, Proc. Eur. Conf. Heat Treat. 2016 and 3rd Int. Conf. Heat Treat. Surf. Eng. Automotive Applications, 11–13 May 2016, Prague, Czech Republic.
14. D.K. Shetty, I.G. Wright, Indentation fracture of WCCo cermets, J. Mater. Sci. 20 (1985) 1873-1883.
15. I. Kleis, P. Kulu, Solid Particle Erosion: Occurrence, Prediction and Control, Springer Verlag, London, 2007.
16. R. Tarbe, P. Kulu, Impact wear tester for the study of abrasive erosion and milling process, Proc. 6th Int. DAAAM Baltic Conf. INDUSTRIAL ENGINEERING, 24th–26th of April 2008, Tallinn, Estonia, 561-566.
17. A. Surzhenkov, M. Antonov, D. Goljandin, P. Kulu, M. Viljus, R. Traksmaa, A. Mere, High-temperature erosion of Fe-based coatings reinforced with cermet particles, Surf. Eng. 32 (2016) 624-630.
18. Z. Mirski, T. Piwowarczyk, Wettability of hardmetal surfaces prepared for brazing with various methods, Arch. Civ. Mech. Eng. 11 (2011) 411-419.
19. D.L. Joslin, W.C. Oliver, A new method for analysing data from continuous depth-sensing microindentation tests, J. Mat. Res. 5 (1990) 123-126.

20. A. Surzhenkov, D. Goljandin, R. Traksmaa, M. Viljus, K. Talviste, A. A. Aruniit, P. Kulu, High temperature erosion wear of cermet particles reinforced with self-fluxing alloy matrix HVOF sprayed coatings, Mat. Sci. (Medzd.) 21 (2015) 386-390.
21. H.T. Liu, L.Z. Sun, Effects of thermal residual stresses on effective elastoplastic behaviour of metal matrix composites, Int. J. Solids Struct. 41 (2004) 2189-2203.
22. T. Lu, J. Hutchinson, Effect of matrix cracking on the overall thermal conductivity of fiber reinforced composites, Philos. Trans. R. Soc. A 351 (1995) 595-610.
23. I. Hussainova, J. Kübarsepp, J. Pirso, Mechanical properties and features of erosion of cermets, Wear 250 (2001) 818-825.
24. R. Tarbe, Abrasive Impact Wear: Tester, Wear and Grindability Studies, PhD Thesis, TUT Press, Tallinn, 2009.

PUBLICATION 6

P. Kulu, F. Casesnoves, **T. Simson**, R. Tarbe. Prediction of abrasive erosion impact wear, *Solid State Phenomena*, 2017, **267**, 201 – 206.

Prediction of Abrasive Erosion Impact Wear of Composite Hardfacings

Priit Kulu[a*], Francisco Casesnoves[b], Taavi Simson[c] and Riho Tarbe[d]

Department of Mechanical and Industrial Engineering, Tallinn University of Technology,
Ehitajate tee 5, 19086 Tallinn, Estonia

[a]priit.kulu@ttu.ee, [b]frcase@ttu.ee, [c]taavi.simson@ttu.ee, [d]riho.tarbe@ttu.ee

Abstract. In this paper an attempt is made to consider for wear prediction apart from the plastic and brittle components also the fatigue component. As example, wear of the WC-Co hardmetal reinforced composite hardfacings under abrasive impact erosion wear conditions was calculated at low and high impact energy, accountig microcutting with surface fatigue for the wear of matrix and brittle fracture, surface fatigue and microcutting for the wear of reinforcement. Calculated wear rates are compared with data obtained from experimental tests. The results of the comparison show that the applied surface fatigue wear model is not applicable in the current case; the recommendations for the further improvement of the model are issued.

Introduction

Abrasive impact erosion wear (AIEW) under extreme conditions (high hardness and velocity of erodent particles, cyclic impact loads, etc.) is a serious problem in industrial equipment, e.g. milling and mixing devices. Based on structural features and material properties, wear mechanisms may have various nature: in brittle solids, the direct fracture mechanism is dominating; in ductile ones, the microcutting and/or low-cycle surface fatigue mechanism prevails [1]. In AIEW that involves solid particle impact at the metal surface, plastic deformation occurs. The correspondent theories of erosion, which enable to find the wear rate at erosion, has been created and developed [2].

The concept of plastic deformation is also applicable to harder and more brittle materials, such as ceramics, but here the mechanism of plastic deformation is accompanied by the mechanism of brittle fracture. The question usually is, what mechanism is predominant [3]. Examples of wear comparison between the theory and experimental data may be found both for plastic [2] and brittle [3,4] materials, not looking to non-predictable parameters, such as fracture toughness of the erodent and the material to be tested, etc. A comparison of the experimental and calculation results demonstrated a satisfactory coincidence in the case of metallic materials [1,5].

Tribological materials and coatings are usually composite materials with a heterogeneous structure: hard particles in a relatively soft matrix. Most of the information available on their tribological properties has been derived from laboratory tests rather than from engineering applications. Attempts have been made to correlate erosion rates – experimental and calculated – with materials parameters [6]. In these models, hardness and fracture toughness emerge as the main material parameters that control erosion; a high hardness increases resistance to plastic deformation, while high fracture toughness increases resistance to fracture.

In papers [6,7] an attempt was made to predict the erosion wear of composite materials and to correlate erosion wear rates with experimental results and material parameters. The metal-matrix composite material containing about 20 vol.% WC reinforcement and thermal spray-fused NiCrSiB-alloy based composite coating containing about 20 vol.% WC-Co hardmetal reinforcement served as examples.

It is well known that there is a big difference between ductile and brittle materials, if the erosion wear rate is measured as a function of the impact angle [1]. Cermets and hardfacings have been considered sufficient to reduce scratching and micromachining damage of a surface, exposed to erodent particles at low impact angle, due to their hardness and stiffness. At the high impact angle, the exposed surface should be able to withstand repeated deformation, and material removal takes

place, after some critical deformation value is exceeded. Therefore the wear mechanism at high angles may be handled as a low-cycle fatigue [8,9].

The main aim of this study was to find out the possibility of prediction of wear of homogeneous and composite materials under combined wear mechanisms (microcutting, brittle fracture and surface fatigue).

Used Mathematical Models

Wear Modes and Studied Materials. AIEW at low-energy (at oblique (30º) and normal (90º) impact angles) and high-energy (at normal impact angle) conditions was under the study (Fig. 1, Table 1). The choice of the impact angle and velocity values was dictated by the differences in the assumed wear mechanisms and intensities under small and high impact angles and velocities.
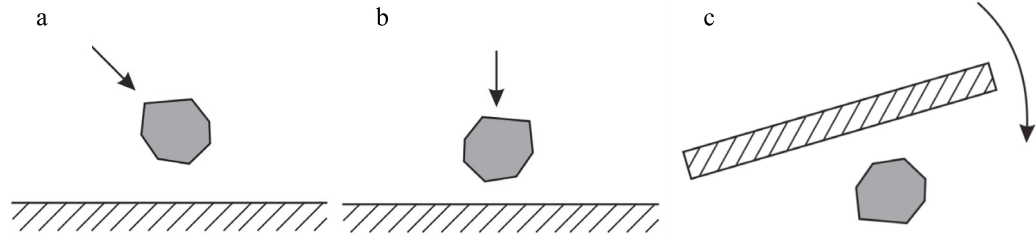

Fig. 1. AIEW conditions: a – oblique angle (30º) low-energy impact; b – normal angle (90º) low-energy impact; c – normal angle (90º) high-energy impact

Table 1. Abrasive impact erosion wear (AIEW) parameters

AIEW type	Abrasive type	Abrasive hardness HV1	Abrasive size [mm]	Impact angle [º]	Particle	
					Velocity [m/s]	Energy [J]
Low-energy	Granite sand	900–950	0.2 – 0.3	30; 90	40	3.0×10^{-5}
					80	1.2×10^{-4}
High-energy	Granite gravel		3.0 – 5.6	90	40	1.4×10^{-2}
					80	5.6×10^{-1}

As homogeneous materials, the wear resistant steel Hardox 400 and the unreinforced FeCrSiB hardfacing were used. As composite materials, iron-based self-fluxing alloy (FeCrSiB) matrix hardfacings with coarse (1.0 – 2.8 mm) WC-Co reinforcement were studied (Table 2).

Table 2. Studied materials

Designation	Composition	Hardness HV1
H400	Steel Hardox 400[1)	425 ± 25
P1	Unreinforced FeCrSiB[2)	870 ± 30
C3	70 vol.% FeCrSiB[2) + 30 vol.% WC-Co[3)	Brought at Fig. 3.
S3	70 vol.% FeCrSiB[2) + 30 vol.% WC-Co[4)	

[1) wt.%: 0.25 C, 0.70 Si, 1.60 Mn, 1.00 Cr, 0.70 Ni, 0.80 Mo, 0.004 B, bal. Fe (SSAB Oxelösund)
[2) wt.%: 2.07 C, 2.67 Si, 0.32 Mn, 13.72 Cr, 6.04 Ni, 3.40 B, 0.02 S, bal. Fe (Höganäs AB)
[3) disintegrator milled angular hardmetal reinforcement (mixture of WC-3Co, WC-6Co, WC-10Co, WC-15Co), 1.0 – 2.5 mm (Tallinn University of Technology)
[4) Ø2.8 mm spherical hardmetal reinforcement (WC-15Co; Wangsheng Cemented Carbide Ltd.)

For calculation of AIEW, models of plastic deformation, brittle fracture and surface fatigue were used.

Wear at Plastic Deformation (Microcutting). Eq. 1, proposed by Beckmann [2], was used for the calculation of the wear due to the horizontal component of impact velocity:

$$W_{cutting} = k_r \frac{3}{4\pi} \cdot \frac{\tau_0}{e_s} \cdot \left[6.81 \cdot \left(\frac{h_p}{R}\right)^{0.5} \cdot \frac{2\rho_2 v_0^2 cos^2\alpha}{3H_1} + 0.85 \cdot \left(\frac{h_p}{R}\right)^2 \right], \tag{1}$$

where k_r is the dimensionless coefficient (taken as $k_r = 1.45$ [1]); τ_0/e_s is the dimensionless ratio, taken from [1]; h_p is the depth of an impact crater [mm]; R is the average diameter of an erodent particle [mm]; ρ_2 is the density of the erodent [mg/mm^3]; v_0 is the impact velocity [m/s]; α is the impact angle [º]; H_1 is the average static hardness of the target material [N/mm^2].

Wear at Surface Fatigue. Wear due to the vertical component of the impact velocity by the surface fatigue mechanism was calculated by the Eq. (2), proposed by Hutchings [10]:

$$W_{fatigue} = 0.033 \cdot \frac{\alpha' \cdot \rho_1 \cdot \sqrt{\rho_2} \cdot v_0^3 \cdot sin^3\alpha}{\varepsilon_c^2 \cdot H_{dynamic}^3 / 2}, \tag{2}$$

where $\frac{\alpha'}{\varepsilon_c^2}$ is a dimensionless ratio, taken from [10]; ρ_1 is the density of the target material [mg/mm^3]; $H_{dynamic}$ is the dynamic hardness of the target material [N/mm^2]; HV1 was used for calculations [11].

Wear at Brittle Fracture. Wear in the case of the brittle materials due to the vertical component of impact velocity was calculated by the Eq. 3, proposed by Gotzmann [4]:

$$W_{brittle} = 0.75 \cdot \sqrt{3} \frac{\rho_1}{\rho_2} \left(\frac{C_r}{R}\right)^2 \cdot \left(\frac{h_p}{R}\right)^{0.5}, \tag{3}$$

where C_r – the middle length of the radial crack.

Calculation of Total Wear. The wear of a ductile target material (steel and self-fluxing alloy) was calculated as

$$W_{ductile}^{total} = W_{cutting} + W_{fatigue}. \tag{4}$$

The total wear of a brittle target material (hardmetal) was calculated as

$$W_{brittle}^{total} = \left\{ \left[W_{brittle}(H_i) + W_{fatigue}(H_1) \right] \cdot P(H_i) + W_{cutting}(H_i) \cdot [1 - P(H_i)] \right\} \times f(H_i) \cdot \frac{\Delta H}{n}, \tag{5}$$

where H_i is the average hardness of a hardmetal hardness range [N/mm^2]; $P(H_i)$ is the probability of a brittle fracture; ΔH is the entire hardness range of hardmetal reinforcement; n is the number of ranges, taken as n = 4.

The total wear of the composite material is calculated as

$$W_{total} = W_{ductile}^{total} \cdot x + W_{brittle}^{total} \cdot (1 - x), \tag{6}$$

where x – the volume proportion of matrix.

Experimental Wear Rates. The wear tests were performed according to parameters, brought in Table 1. The centrifugal type tester CAK (Fig. 2 a) was used for the low-energy wear tests and disintegrator type tester DESI (Fig. 2 b) – for the high-energy ones.

The volumetric wear rate was calculated as:

$$W_{experimental} = \frac{360 \cdot \Delta m}{M \cdot \delta \cdot \rho_1}, \tag{7}$$

where Δm is the weight loss of the target material [mg]; M is the total mass of the abrasive [kg]; δ is the target hit sector angle; $\delta = 8.5º$ in CAK and $\delta = 9.4º$ in DESI.
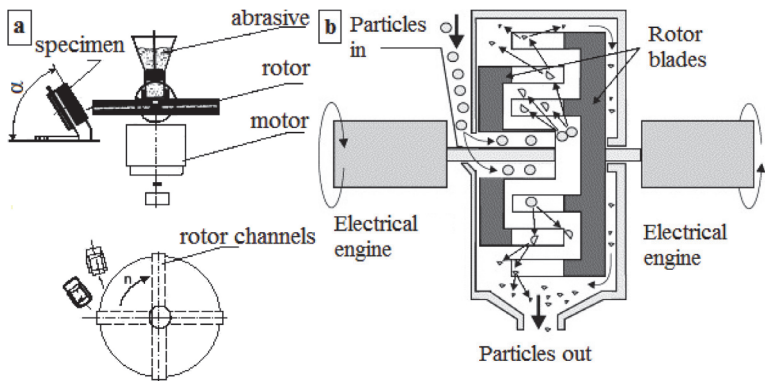
Fig. 2. Schematics of the wear testers: a – CAK; b – DESI

Comparison of Calculated and Experimental Wear Rates

The wear rates were calculated, assuming that density of the erodent $\rho_2 = 2.5$ mg/mm^3, Poisson's ratio of the erodent $\mu_2 = 0.17$, Young's modulus of the erodent $E_2 = 90$ GPa, normal force F_n was 0.19×10^{-3} N and 0.85 N at $v_0 = 40$ m/s and 0.75×10^{-3} N and 3.45 N at $v_0 = 80$ m/s respectively under low-energy and high-energy AIEW conditions. The data of the materials, necessary for calculation of wear rates, is brought in Table 3 and Fig. 3.

Table 3. The input data of the materials to be studied

Target material	τ_0/e_s	Poisson's ratio μ_1	Young's modulus E_1, $\times 10^3$ N/mm^2	Density ρ_1 [mg/mm^3]	Hardness HV1 [N/mm^2]	Fracture toughness K_{1C} [MPa·m$^{-0.5}$]
H400	0.09	0.3	185	7.85	5250	–
P1[1)]	0.19	0.26	291	7.40	6695	–
C3 matrix	0.19	0.26	291	7.40	10990	–
C3 reinforcement	0.12	0.24	430 – 650	14.1 – 15.3	16800 – 24130	10.5 – 19.5
S3 matrix	0.19	0.26	291	7.4	10460	–
S3 reinforcement	0.12	0.24	430	14.1	18100 – 24020	19.5

[1)] Taken from Fig. 3.

Under the low-energy AIEW conditions, under the oblique impact angle the difference between the experimental and the calculated wear rates varies 1.4 – 2.1 times in the case of the homogeneous materials (Hardox 400 and FeCrSiB) and 3.3 times in the case of the composite material (C3; Table 4). However, under the normal impact angle the difference between the wear rates is generally remarkably different, being eleven orders of magnitude lower in the case of the homogeneous materials and 1.4 – 3.4 times higher in the case of the composite material (C3).

Under the high-energy AIEW conditions, the calculated wear rates were twelve orders of magnitude lower in the case of the homogeneous materials and 56 – 213 times lower, in the case of the composite material (S3), to be compared with the experimental results (Table 4).

The analysis of the calculated and the experimental wear rates, as well as of calculations themselves (not shown), demonstrates that the wear values, calculated by Eq. 4, are much lower to be compared with the experimental ones. There could be different reasons for that. The applied Hutchings' model ignores the shear deformation of the material [10]. However, multiple researchers reported the formation of "lips" at the walls of the impact craters, left by the erodent particles [15,16]. According to [16], they may be easily detached by the subsequent nearby impacts. Secondly, the size and shape of the particles is not taken into account, what results in, for example, the same values of wear rates for low-energy and high-energy AIEW (Table 4). Thirdly, this model does not take into account the residual stresses in the material, what may also influence the final result, especially in the case of composite structures [17,18].
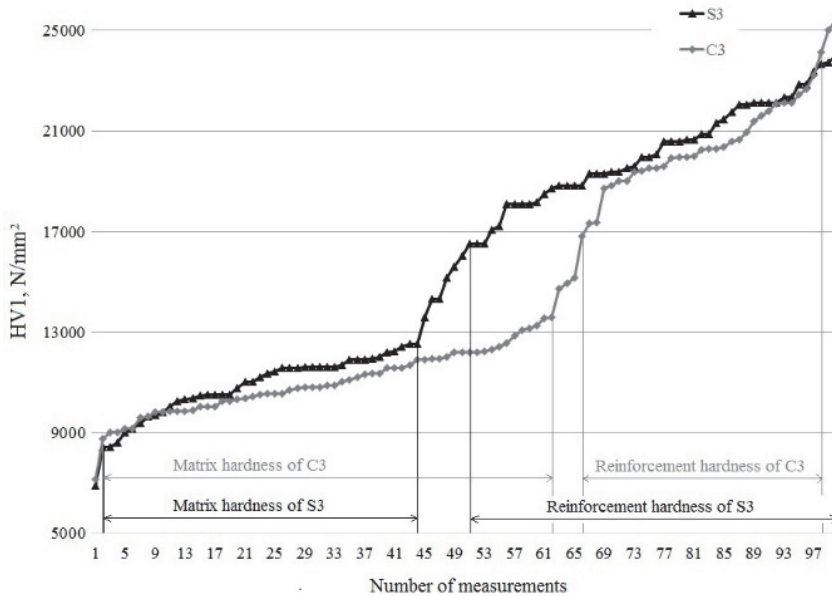
Fig. 3. Hardness distribution in C3 and S3

Table 4. Experimental wear rates, mm^3/kg

Material	Low-energy								High-energy			
	Velocity [m/s]											
	40				80				40		80	
	Impact angle [º]											
	30		90		30		90		90			
	Calc.	Exp.	Calc.	Exp.	Calc.	Exp.	Calc.	Exp.	Calc.	Exp.	Calc.	Exp.
H400	3.8	7.9	6.0×10^{-12}	3.8	21.8	37.0	4.8×10^{-11}	30.0	6.0×10^{-12}	26.1	4.8×10^{-11}	85.4
P1	4.6	3.2	2.7×10^{-12}	10.0	25.7	12.0	2.2×10^{-11}	21.5	2.7×10^{-12}	9.3	2.1×10^{-11}	29.5
C3	–	–	1.1	3.7	42.9	12.9	23.4	16.7	–	–	–	–
S3	–	–	–	–	–	–	–	–	0.4	85.2	3.2	180.7

Summary

1. A good applicability of the used mathematical models was demonstrated for the oblique impact angle abrasive impact erosion wear (AIEW) conditions. Under the normal impact angle AIEW conditions, the used mathematical models, especially the Hutching's model, proved to be unsuitable.
2. For a more accurate prediction of wear under the normal angle AIEW conditions, plastic deformation of the target material and, on the other hand, the geometry (size, angularity, etc.) of the erodent should be taken into account.

References

[1] I. Kleis, P. Kulu, Solid Particle Erosion. Occurrence, Prediction and Control, Springer-Verlag, London, 2008.

[2] G. Beckmann, I. Kleis, Abtragverschleiß von Metallen, VEB Deutcher Verlag für Grundstoffindustrie, Leipzig, 1983.

[3] G. Beckmann, J. Gotzmann, Modelling blast wear on ceramic materials, Proc. Techn. Univ. Tallinn 609 (1985) 102-109.

[4] J. Gotzmann, Modellierung des Strahlverscleißes an keramischen Werkstoffen, Schmierungstechnik, Fachzeitschrift für Tribotechnik, VEB Verlag Technik Berlin, 20 (1989) 324-329.

[5] R.R.E. Ellermaa, Erosion prediction of pure metals and carbon steels, Wear 162 (1993) 1114-1122.

[6] P. Kulu, R. Veinthal, Characterization and modelling erosion wear of powder composite materials and coatings, Int. J. Materials and Product Technology 28 (2007) 425-447.

[7] R. Veinthal, Characterization and modelling of erosion wear of powder composite materials and coatings, PhD thesis, TUT Press, Tallinn, 2005.

[8] I.M. Hutchings, Some comments on the theoretical treatment of erosive particle impacts, Proc. 5th Int. Conf. on Erosion by Liquid and Solid Impact, Cambridge, 3–6 of September 1979, paper 36.

[9] I.M. Hutchings, Tribology: Friction and Wear of Engineering Materials, Cambridge, 1992.

[10] I.M. Hutchings, A model for the erosion of metals with spherical particles at normal incidence, Wear 70 (1981) 269-281.

[11] T. Simson, R. Tarbe, M. Tarraste, M. Viljus. Abrasive impact erosion of composite Fe-based hardfacings with coarse WC-Co reinforcement. Proc. 24th IFHTSE Congress European Conf. Heat Treatment and Surface Engineering, 26–29 of June 2017, Nice, France.

[12] A.G. Evans, M.E. Gulden, M. Rosenblatt, Impact damage in brittle materials in the elastic-plastic response regime, Proc. Roy. Soc. Lond. A361 (1978) 343-365.

[13] P. Kulu, A. Surzhenkov, M. Viljus, T. Simson, R. Tarbe, M. Saarna, Wear resistance and mechanisms of composite hardfacings at abrasive impact erosion wear. J. Phys.: Conf. Ser. 843 (2017) 012060.

[14] T. Simson, P. Kulu, A. Surženkov, R. Tarbe, D. Goljandin, M. Tarraste, M. Viljus, Wear resistance of sintered composite hardfacings under different abrasive wear conditions, Materials Science (Medžiagotyra) (2017) (in press).

[15] I.M. Hutchings, R.E. Winter, J.E. Field, Solid particle erosion of metals: the removal of surface materials by spherical particles, Proc. R. Soc. Lond. A348 (1976) 379-392.

[16] M. Antonov, J. Pirso, A. Vallikivi, D. Goljandin, I. Hussainova, The effect of fine erodent retained on the surface during the erosion of metals, ceramics, plastic, rubber and hardmetal, Wear 354–355 (2016) 53-68.

[17] I. Hussainova, On micromechanical problems of erosive wear of particle reinforced composites, Proc. Estonian Acad. Sci. Eng. 11 (2005) 18-30.

[18] A. Surzhenkov, A. Vallikivi, V. Mikli, M. Viljus, T. Vilgo, P. Kulu, Wear resistant self-fluxing alloy based TiC-NiMo and Cr_2C_3-Ni hardmetal particles reinforced composite coatings, Proc. 2nd Int. Conf. Manufacturing Engineering & Management 2012, 5–7 of December 2012, Prešov, Slovakia, 33-36.

Curriculum Vitae

Personal data
Name: Taavi Simson
Date and place of birth: 24.06.1989, Tallinn, Estonia
E-mail: taavi.simson@ttu.ee

Education

Period	Institution	Education (field of study, degree)
2014 – 2018	Tallinn University of Technology	Materials Engineering, PhD
2012 – 2014	Tallinn University of Technology	Product development and production engineering, MSc
2009 – 2012	Tallinn University of Technology	Product development and production engineering, BSc
2002 – 2009	Tallinn Technical Gymnasium	Secondary education
1997 – 2002	Tallinn Arte Gymnasium	-

Language skills (native speaker, fluent, average, basic skills)

Language	Level
Estonian	Native speaker
English	Fluent
Russian	Basic skills

Professional employment

Period	Organisation	Position
10.2014 – …	Tallinn University of Technology	Early Stage Researcher
01.07.2013 – 31.08.2013	AS Norma	Trainee

Elulookirjeldus

Isiku- ja kontaktandmed
Nimi: Taavi Simson
Sünniaeg ja -koht: 24.06.1989, Tallinn, Estonia
E-mail: taavi.simson@ttu.ee

Hariduskäik

Periood	Organisatsioon	Haridus (eriala, omandatud kraad)
2014 – 2018	Tallinna Tehnikaülikool	Mehhanotehnika, PhD
2012 – 2014	Tallinna Tehnikaülikool	Tootearendus ja tootmistehnika, MSc
2009 – 2012	Tallinna Tehnikaülikool	Tootearendus ja tootmistehnika, BSc
2002 – 2009	Tallinna Tehnikagümnaasium	Keskharidus
1997 – 2002	Tallinna Arte Gümnaasium	-

Keelteoskus (emakeel, alg-, kesk- või kõrgtase)

Keel	Tase
Eesti	Emakeel
Inglise	Kõrgtase
Vene	Algtase

Teenistuskäik

Periood	Organisatsioon	Positsioon
10.2014 – …	Tallinna Tehnikaülikool	Nooremteadur
01.07.2013 – 31.08.2013	AS Norma	Praktikant